PERFORMANCE ENHANCEMENT IN COPPER TWISTED PAIR CABLE COMMUNICATIONS

Beier Li

Electrical Engineering, De Montfort University, UK,

email: p1319654x@my365.dmu.ac.uk

Wise men speak because they have something to say; Fools because they have to say something. - Plato

Acknowledgement

I would like to thank my family for all their selfish-less support and love they have given me over the years. My parents have always their faith in me, this taught me to believe in myself. My son Anji brings happiness to me everyday, he is always my energy source.

To Prof. Alistair Paul Duffy, you have been an inspiring supervisor over the three years at the De Montfort University. I have learnt so much from you, my time here has been a very amazing experience. Thanks for your supervision, enthusiasm, and for believing in me.

To my colleagues at the research group: Dr. Hugh Sasse, Dr. Parminder Singh Kang, Dr. Riyadh Mansoor, Edwin Arihilam, Florence Akinnuoye, and Katharina Seitz, working with you has been a real pleasure.

To my former supervisor Mr. Andreas Foglar of Innoroute, vielen Dank fuer deine langzeitige Unterstuetzung und Freundschaft.

To my friends Mr. David Kiddo, Mr. Dave Hass, Mr. Paul Cave, thank you for your help during my research work.

Also my friends Anney Yimeng An and Dahai Gao, thank you for your kind help at DMU.

Especially thank Professor Marc Moonen from KULeuven for his advice and guidance over the past years.

Finally to my great family and friends, including but not limited, Prof. Ji Baocheng and Mrs. Chen Zuying, Prof. Du Yubo and Mrs. Li Liping, Prof. Sheng Xigui, Prof. Zheng Wenhong and Mrs. Cao Yang, Dr. Bu Jianjun, Dr. Li Haibin, Dr. Allen Lu and Mrs. Maggie Ma, Pieter Schuddinck, Xing Lei, Sophie Vloebergh and Dr. Bruno Defraene, Dr. Kim Ngo, Song Yinan, Ma Qiang and Liu Fali, Yu Dongping, Yu Feixiong, Dr. Yun Zhou, Sijia Zhang, Wang Cheng and Ren Shizi, and my uncle Li Gui. Living overseas can be a difficult time, your in-town visit or inter-continent support have contributed to an important part of my life, which turned in my confidence to my study. Especially my uncle Xu Jiang, who made a surprise trip to Leicester with the whole family at the summer of 2014.

Abstract

The thesis focuses on the area of copper twisted pair based wireline communications. As one of the most widely deployed communication media, the copper twisted pair cable plays an important role in the communication network cabling infrastructure. This thesis looks to exploit diversity to improve twisted pair channels for data communications in two common application areas, namely Ethernet over Twisted Paris and digital subscriber line over twisted pair based telephone network.

The first part of the thesis addresses new approaches to next generation Ethernet over twisted pair cable. The coming challenge for Ethernet over twisted pair cable is to realise a higher data rate beyond the 25/40GBASE-T standard, in relatively short reach scenarios. The straight-forward approaches, such as improving cable quality and extending frequency bandwidth, are unlikely to provide significant improvement in terms of data rate. However, other system diversities, such as spectrum utilization are yet to be fully exploited, so as to meet the desired data rate performance. The current balanced transmission over the structured twisted pair cable and its parallel single-in-single-out channel model is revisited and formulated as a full-duplex multiple-in-multiple-out (MIMO) channel model. With a common ground (provided by the cable shield), the balanced transmission is con-

verted into unbalanced transmission, by replacing the differential-mode excitation with single-ended excitation. In this way, MIMO adoption may offer spectrum utilization advantages due to the doubled number of the channels. The S-parameters of the proposed MIMO channel model is obtained through the full wave electromagnetic simulation of a short CAT7A cable. The channel models are constructed from the resulting S-parameters, also the corresponding theoretical capacity is evaluated by exploiting different diversity scenarios.

With higher spectrum efficiency, the orthogonal-frequency-division-multiplexing (OFDM) modulation can significantly improve the theoretical capacity compared with single-carrier modulation, where the channel frequency selectivity is aided. The MIMO can further enhance the capacity by minimising the impact of the crosstalk. When the crosstalk is properly handled under the unbalanced transmission, this thesis shows that the theoretical capacity of the EoTP cable can reach nearly $200GBit/s$.

In order to further extend the bandwidth capability of twisted pair cables, Phantom Mode transmission is studied, aiming at creating more channels under balanced transmission operation.

The second part of the thesis focuses on the research of advanced scheduling algorithms for VDSL2 QoS enhancement. For VDSL2 broadband access networks, multi-user optimisation techniques have been developed, so as to improve the basic data rate performance.

Spectrum balancing improves the network performance by optimising users transmit power spectra as the resource allocation, to mitigate the impact from the crosstalk. Aiming at enhancing the performance for the upstream VDSL2 service, where the users QoS de-

mand is not known by all other users, a set of autonomous spectrum balancing algorithms is proposed. These optimise users transmit power spectra locally with only direct channel state information. To prevent selfish behaviour, the concept of a virtual user is introduced to represent the impact on both crosstalk interference and queueing status of other users. Moreover, novel algorithms are developed to determine the parameters and the weight of the virtual user.

Another type of resource allocation in the VDSL2 network is crosstalk cancellation by centralised signal coordination. The history of the data queue is considered as a time series, on which different smooth filter characteristics are investigated in order to investigate further performance improvement. The use of filter techniques accounts for both the instantaneous queue length and also the previous data to determine the most efficient dynamic resource allocation. With the help of this smoothed dynamic resource allocation, the network will benefit from both reduced signalling communication and improved delay performance.The proposed algorithms are verified by numerical experiments.

Acrosyms Table

ADSL	Asymmetric Digital Subscriber Line
AN	Access Node
ASB	Autonomous Spectrum Balancing
CAT7A	Catagory 7A
CO	Central Office
CPE	Customer Premises Equipment
CSI	Channel State Information
CST	Computer- Simulation Technology
DAC	Digital-to-analogue -converter
DFE	Decision- feedback- equaliser
DOCSIS	Data Over Cable Service Interface Specification
DMT	Discrete multi-tone
DRA	Dynamic resource allocation
DS	Downstream
DSB	Distributed spectrum balancing
DSL	Digital subscriber line
DSLAM	Digital Subscriber Line Access Multiplexer
DSM	Dynamic spectrum management
EOR	End-of- the-row
EoTP	Ethernet over Twisted Pair
EMC	Electromagnetic compatibility
FEXT	Far end crosstalk
FFT	Fast Fourier Transformer
FIFO	First-In-First-Out
FTTB	Fibre-to-the-building
FTTC	Fibre-to-the-cabinet
FTTN	Fibre-to-the-neighbourhood
IEEE	The Institute of Electrical and Electronics Engineers
iFFT	inverse Fast Fourier Transformer
ISI	Intersymbol interference
ISO	Internation Standard Organization
ITU-T	The ITU Telecommunication Standardization Sector
ISB	Iterative spectrum balancing
IWF	Iterative water filling

LAN	Local area network
LSOH	Low Smoke Zero Halogen
LTE	Long Term Evolution
MIMO	Multiple-In-Multiple-Out
MMSE	Minimum mean-square error
MRL-ASB	Multiple reference line autonomous spectrum balancing
MWS	Max-Weight Scheduling
NEXT	Near end crosstalk
OFDM	Orthogonal Frequency Division Multiplexing
PAM	Pulse Amplitude Modulation
PCC	Partial crosstalk cancellation
PLC	Power Line Communication
PSD	Power spectral density
PVC	Polyvinyl chloride
QAM	Quadrature ampli- tude modulation
QLD	Quadratic Lyapunov drift
QoS	Quality of Service
RLCG model	Resistance (R), inductance (L), capaci- tance (C), and conductance (G)
RT	Remote terminal
RU	Real users
S/FTP	Shielded/Foiled Twisted Pair Cable
SC	Single-carrier
SINR	Signal-to-interference-and-noise-ratio
SISO	Single-In-SIngle-Out
SMA	Simple Moving Average Filter
SVD	Singular value decomposition
TCL	Transverse conversion loss
TCTL	Transverse conversion transfer loss
TOR	Top-of-the-rack
UTP	Unshielded twisted pair cable
US	Upstream
VDSL	Very-high-bit-rate digital subscriber line
VDSL2	Very-high-bit-rate digital subscriber line 2
VNA	Vectored network analyser
VU	Virtual user
WMA	Weighted Moving Average Filter
WRS	Weighted Rate Sum
ZF	Zero-forcing

Contents

List of Figures

List of Tables

Chapter 1

Introduction

The beginning is the most important part of the work. - Plato

1.1. THE HISTORY OF COPPER TWISTED PAIR CABLE FOR COMMUNICATION NETWORKS

Copper twisted pair cable was invented by the pioneer of telecommunications, Alexander Graham Bell in 1881 [1]. Twisted pair cable consists of two identical copper wires, which are twisted together as a single circuit, also forms a balanced circuit [2]. The principle behind the twisted pair cable is the balanced signal transmission, where the two wires are excited by the signal with same amplitude but opposite phase. External noise, in the form of common mode noise, is eliminated in the balanced circuit.

One significant application of twisted pair cable is the telephone network, where the existing open-wire for the telegraph transmission is not able to provide reliable voice signal transmission, in terms of attenuation and reach. During the decades, the twisted pair cable

Table 1.1. The Evolution of the EoTP Standards

EoTP Standard	10BASE-T	100BASE-T	1000BASE-T	10GBASE-T	25/40GBASE-T
Twisted Pair Used	2	2	4	4	4
Coding	Manchester	4B/5B	PAM5	THP-PAM16	TBD
Transmit Voltage	± 2.5V	$\pm 1, 0$V	$\pm 2, \pm 1, 0$V	max$\pm$2V	TBD
Symbol Rate	10 MBd	125 MBd	125 MBd	250 MBd	TBD
Pub. Year	1990	1995	1999	2006	TBD

Table 1.2. CATx Cable Specifications

	Cat. 3	Cat. 4	Cat. 5	Cat. 5a	Cat. 6	Cat. 6a	Cat.7	Cat.7a
Frequency	16MHz	20MHz	100MHz	100MHz	250MHz	500MHz	600MHz	1600MHz
Data Rate	10Mbit/s	16Mbit/s	100Mbit/s	100Mbit/s	1Gbit/s	10Gbit/s	10Gbit/s	25/40Gbit/s
Reach	100m	100m	100m	100m	100m	55m	100m	50m
Cable Screening	none	none	none	none	none	none/foil	braiding/foil	braiding/foil
Pair Shielding	none	none	none	none	none	foil/none	foil	foil

has been developed as one of the most accessible communication cables, with a complete eco-environment for itself, including the research, the standardisation, the design and the manufacturing.

Originally invented for the voice signal band transmission, the twisted pair cable has found significance in the application of the digital signal transmission. In the early stage of the computer networks, the co-axial cable was chosen for the physical interconnections of the Ethernet networks, but soon replaced by the unshielded twisted pair based UTP cable.

The UTP cable is assembled from four standard telephone twisted pair cables, and with 8-pin RJ-45 connectors at each end [3]. UTP cable has considerable advantage over co-axial cable, in terms of size, weight and flexibility in deployment. The evolution of the EoTP standards and the corresponding footprint of the EoTP cable are concluded in Table 1.1 and Table 1.2, respectively.

Table 1.3. The xDSL Standards

	HDSL	ADSL	ADSL2	ADSL2+	VDSL	VDSL2	G.Fast
Data Rate	2.048 Mbit/s	7Mbit/s DS 800kbit/s US	12.0 Mbit/s DS 1.3 Mbit/s US	24.0 Mbit/s DS 1.4 Mbit/s US	52.0 Mbit/s DS 16 Mbit/s US	100.0 Mbit/s DS 100 Mbit/s US	500.0 Mbit/s DS 500 Mbit/s US
Reach	3.7 km	4 km	4 km	4 km	1 km	500 m	500m
Frequency	772 kHz	1104 kHz	1104 kHz	2.2 MHz	12 MHz	30 MHz	106 MHz
Pub. Year	1993	1998	2002	2008	2001	2006	2014

Not only in the local network, the twisted pair cable based telephone network is also transformed into data communication network. From the early analog modems of ITU-T V-series protocol [4], where only a few kilobit are transmitted per second, to the latest gigabit level, also known as G.Fast [5], the widespread telephone network infrastructure is used to deliver high speed Internet service. Particularly, the digital subscriber line (DSL) technology is dedicated for high speed data communication over the telephone network. Another well established network, the co-axial cable based television cable network, is also used to provide data service. These legacy infrastructure networks allowed telecom operators to quickly develop the data service business, without investing another infrastructure system. The development of the xDSL standards is summarised in Table 1.3. Note that there are many annexes of each DSL standard, therefore the data specification listed in Table 1.3 is the typical specification used in practical implementation.

In recent years, the twisted pair cable is used mostly in the edge part of the telephone network topology, as the broadband access network to connect the end user to the central office or fibre node. With the digitalised telephone and television transmission, a new type of access service known as Triple-play has been deployed, which provides high definition digital television, Internet access and telephone over a single broadband connection. For such service-oriented access network, the quality-of-service (QoS) and the quality-of-

experience are drawing more attention, rather than solely the data rate performance [6, 7].

1.2. SIGNAL TRANSMISSION IN THE TWISTED PAIR CABLES AND THE STATE OF THE ART

In this section, the current technology used for the signal transmission over the twisted pair cables are briefly introduced.

The first question to be answered is that, with the current twisted pair cable transmission, do we need it better?

Local computer network and data centres are the major cabled Ethernet application scenarios. The latest published standard of the Ethernet over twisted pair (EoTP) is the 10G BASE-T standard [8], while the ongoing standardisation procedure is finalising the 40G BASE-T [9] standard. Despite some available optical connection can reach $100Gbit/s$ or higher, the technology of a full optical network is yet immature. The EoTP system is still attractive for its advantages of low cost, flexible deployment and easy maintenance. Just the speed of EoTP should catch up with the optical systems.

For the telephone network, some ambitious operators have advertised or planned to replace the copper access network with optical access network, like fibre to the end user. Although the optical technology is ready, such complete infrastructure renewal leads to a unacceptably massive budget for both equipment and engineering. Therefore the hybrid access network with twisted pair cable connecting the end user will still serve for a foreseeable period of a few decades.

The twisted pair cables will still serve as a key element in the cable data transmission infrastructure, hence we need better technology to make better use of the twisted pair

cables.

The fundamental function of the twisted pair cables is to provide the communication channels, in which the signal will be attenuated in the channel, according to the electromagnetic characteristics of the channel, also known as the insertion loss [10]. Therefore the received signal contains the desired but attenuated signal and other noisy components.

A conductor can be excited by an incident electromagnetic field. The remote noise source generates noise into the twisted pair cable in this way, e.g., the amateur radio. Any two adjacent conductors will cause a electromagnetically coupling, if at least one of them has electric current flowing. Such coupling could be intentional or unintentional. As an example of the intentional coupling, the signal is generated from the excitation circuit and then coupled into the twisted pair cable. If there is an impedance mismatch between the excitation source and the cable, some of the transmit power will be reflexed back as the echo, also known as the return loss.

The Ethernet cable consists of four twisted pairs, while the underground telephone cable bundle at least 25 twisted pairs, or even more than one hundred pairs. These twisted pairs are compactly placed together, therefore they are electromagnetically coupled. The signal being transmitted in the cable is leaked into other cables, as received as interference, this is also known as the crosstalk in the domain of transmission line theory. The crosstalk is a major interference source for twisted pair cables, because of the strong coupling between the twisted pairs and the same frequency band as the desired signal.

With a history of over a century, the twisted pair cable itself for the telephone network has not been changed much. The early paper-wrapped low quality twisted pair is now replaced by PVC or polyethylene wrapped twisted pair. When attempting to realise

high speed data transmission, the main obstacle is the poor channel condition on the high frequencies. Due to the physical nature of the conductor material, i.e., the copper, the insertion loss and the crosstalk of the twisted pair cable is significantly degraded with the increased frequency. This phenomenon is also referred to as the channel frequency selectivity, which is a well-known performance bottleneck in many communication channels.

For the many digital communication systems, the multi-carrier orthogonal frequency-division multiplexing (OFDM) was introduced to replace the single-carrier modulation schemes, to cope the channel frequency selectivity [11–13]. Lately, based on the features of the OFDM modulation, multi-user spectrum coordination [14–16] and signal coordination [5, 17, 18] have been developed and recently standardised, the frequency efficiency can be further improved. The multi-user crosslayer design [19–21] will be powerful tool to help the QoS of the broadband access network [22–24].

The basic structure of the EoTP cable remains the original design, but evolved with more insulation layers, e.g., the pair-wise metal foil as the screening and the metallic braiding as the shield, aiming at enhancing the electromagnetic properties. The single-carrier pulse-amplitude modulation (PAM) has been the communication fundamental from the early standard, which later being evolved with expanded frequency band and increased modulation order. The same channel frequency selectivity and crosstalk problems as in the telephone networks, are seen as the bottleneck for further standard evolution [9]. Hence alternative approaches are expected, so as to further improve the performance of the EoTP transmission.

1.3. THE OBJECTIVES OF THE RESEARCH

As the raw material of the conductor in the twisted pair cables, the copper metal is a non-sustainable natural resource. Either from ore processing or old data cable recycling, the manufacturing of the twisted pair cable requires considerable energy and other resources. Furthermore, the existing cabling infrastructure of the telephone networks and the computer networks have been built with enormous effort over decades. Also, society and commerce are placing ever increasing data throughput demand on the data infrastructure. Hence there is a contention between updating the cabling to accommodate new demands or cutting demands to avoid the need for infrastructure replacement. Given that physical redesign of the cabling infrastructure is expensive, as a result, an open question is how can more data throughput be obtained for existing cabling infrastructure [25, 26]. Therefore this thesis attempts to propose novel techniques that can balance that contention. In particular it addresses the throughput increase of the Ethernet twisted pair cable and quality of experience in DSL networks. The solution adopted is to exploit diversity in coding and spectrum. To achieve this, the following objectives are set:

1. Channel remodelling for the Ethernet over twisted pair cable. (Conductor Diversity)

2. Alternative transmission techniques. (Modulation Diversity)

3. Phantom mode transmission over Ethernet cable. (Virtual Channel Diversity)

4. Smoothed Max-Weight based dynamic resource allocation in VDSL2 networks. (Data Time Series Diversity)

5. Virtual user assisted autonomous spectrum balancing in VDSL2 networks. (Virtual Network Diversity)

1.4. THESIS OVERVIEW AND CONTRIBUTIONS

An overview of the thesis and its major contributions are now given.

Some of the important concepts are introduced in the Chapter 2.

Part I of this thesis exploits the diversity in the EoTP cable. With structured EoTP cable as the study subject, the goal is to determine the theoretical capacity of the EoTP cable with alternative transmission mode and transmission techniques.

Chapter 3 reformulates the EoTP cable as a full-duplex MIMO channel model, under both balanced and unbalanced transmission mode. A short CAT7A cable is simulated with CST Microwave studio, where the insertion loss, the return loss, the crosstalk and the channel length of both balanced and unbalanced transmission mode are investigated.

The unbalanced transmission has doubled the number of the communication channels in the EoTP cable, with more smaller conductor path for the signal transmission and more crosstalk paths. The short cable shows improved insertion loss and increased crosstalk coupling, which indicates that the short cable does not necessarily provide better channel condition than the 30 meters long cable. Together with the reformulated full-duplex MIMO channel model, the cable capacity under different setups can be evaluated by accommodating more alternative transmission techniques, for instance, OFDM modulation and MIMO crosstalk cancellation.

The theoretical capacity of simulated channel models is examined in Chapter 4, where the OFDM modulation is introduced and compared with the single-carrier modulation.

The benefit of the MIMO crosstalk cancellation and the impact of the transmit power are also discussed in Chapter 4.

The multi-carrier OFDM modulation scheme has shown significantly improved capacity from the PAM of the current Ethernet standard, also strong resilience against the crosstalk and frequency selectivity. The unbalanced transmission has shown great potential with proper crosstalk cancellation. The one meter CAT7A cable can reach a theoretical capacity of nearly $200Gbit/s$, not just far beyond the current going 40G BASE-T, but also this ensures a possible future for a 100G BASE-T EoTP standard.

The phantom mode transmission and its simulation result are presented in Chapter 5, where the impact of the impedance mismatch is demonstrated in both S-parameter and the resulting theoretical capacity.

The impedance mismatch of the Phantom circuit has been indicated as the main bottleneck of the Phantom mode transmission, which causes severe crosstalk and consequently degrades the transmission capacity. This could further be used as the design criteria of Phantom circuit implementation.

The materials of the Chapter 3 and IWCS 2016 [27] and the Chapter 4 are published in IWCS 2015 [28] and Cabwire2015 [29], respectively. A more comprehensive report is in preparation as a journal paper.

Part II of this thesis develops novel scheduling algorithms for the QoS enhancement in VDSL2 networks. Generally speaking, QoS contains various technical and other commercial factors, therefore in this thesis only the delay performance is considered as the QoS performance metric. Based on the existing spectrum balancing and signal coordination of the VDSL2 networks, the goal is to reduce the signalling overhead in the centralised signal

coordination and to improve the delay performance of the autonomous spectrum balancing algorithms.

Chapter 6 introduces the transmission stability and the dynamic resource allocation of the spectrum balancing and the signal coordination in VDSL2 networks. The time-series smooth filter is applied to the dynamic resource allocation algorithm of the partial crosstalk cancellation, so as to reduce the signalling overhead and improve the delay performance, while the transmission stability is preserved.

The smoothing effect can lower the signalling demand in the dynamic resource allocation of the DSL networks, which can further practically reduce the implementation cost in PCC dynamic resource allocation. Moreover, this smooth concept could also be widely used in other network topologies in the research area of the network dynamic resource allocation.

In Chapter 7, the concept of virtual user is presented, which helps the autonomous spectrum balancing algorithm to take other users' delay performance into account, to prevent a selfish dynamic resource allocation.

The virtual user and virtual network concept enable a new class of autonomous spectrum balancing algorithms, where no QoS status information exchange is required. This is especially important for the upstream service, where the information exchanges between the CPEs are not feasible. The proposed algorithms also have very low computational complexity, then they can be implemented into the low-cost massive CPE chipsets, so as to improve both the data rate and delay performance.

A report on the result of Chapter 6 has been submitted to IEEE Communication letters, currently under review. The material of the Chapter 7 is published in IWCS 2014 [30], also

a journal paper of the same topic is in preparation.

Conclusions are drawn and interesting topics for future research are discussed in Chapter 8.

Chapter 2

Basic Concepts

In this chapter, the basic concepts underpinning the research presented in the thesis work are outlined. First, copper based communication cables are introduced. Then the network topology in typical application scenarios and its impact on the crosstalk are discussed. Finally single-carrier and multi-carrier modulation schemes are presented.

2.1. THE COMMON COPPER CABLES FOR COMMUNICATIONS

Many communication networks transmit either electrical or optical signal. The optical signal is transmitted over optical fibre cables, while the electrical signal must be transmitted over conductive medium,

2.1.1. The Structured Twisted Pair Cable for Ethernet

The twisted pair cable in the telephone network has only one twisted pair per cable, which are not covered in any form of protection. Therefore, a large amount of the twisted pairs

bundled together in the cable bundle may generate significant crosstalk and therefore interfere with each other. This section focuses on the EoTP cable.

Emerging as a cost-effective solution for LAN cabling infrastructure, the early structured EoTP cable simply assembled four individual telephone twisted pair cables with an outer layer jacket, which is also referred to as unshielded twisted pair (UTP) cable. As the main functional component of the EoTP cable, the four twisted pairs, each of which consists of two copper wires, compose the conductor paths for signal transmission. During the evolution of the Ethernet standards and the corresponding EoTP developments, other components are introduced to improve the cable performance, e.g., non-conductive protection layers, conductive shielding layers and spacing accessories.

A cross section diagram of one of the more advanced standardised EoTP cable, i.e., the S/FTP CAT7A cable, is illustrated in Fig. 2.1. The copper wire is coated with non-conductive insulation, in order to prevent direct contact between the two wires and to control the primary and secondary transmission line parameters. Then each pair is covered with metallic foil as screening, which prevents the crosstalk coupling between other pairs. Another layer of thin metal wire braiding is weaved outside the four twisted pairs as the shield, to further suppress the crosstalk emission and reduce the external interference. The outer most layer is a non-conductive and purely a physical protection jacket.

Each twisted pair consists of two identical copper wires, which are twisted together. These two wires have the same conductor length and same impedance, therefore the twisted pair forms a balanced transmission line [2, 10, 31]. The four twisted pairs usually have different twisting rates, i.e., they have different numbers of turns in a unit length, so as to avoid repeated electromagnetic field between each other. Such non-repetitive ge-

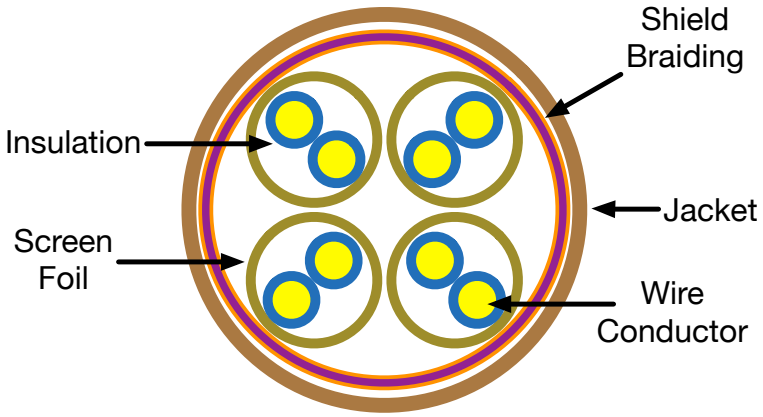

Fig. 2.1. S/FTP Cable Design

ometry is demonstrated in Fig. 2.2, where only the wires are shown.

2.1.2. Other Cables for Data Communication

Another legacy network intensively used for data access network is the service is the co-axial television cable network, with the protocol of the Data Over Cable Service Interface Specification (DOCSIS) [32, 33]. The structure of the co-axial cable, as illustrated in Fig. 2.3, significantly differs from twisted pair based cables. The signal is transmitted over a copper wire, with the metallic braiding as the ground. This forms a typical unbalanced transmission line [2, 10, 31].

Driven by the growing data transmission of triple-play, high definition video and high speed Internet, DOCSIS began to utilise higher frequency band. Then the physical nature of copper leads to frequency selectivity as well, where the previously adopted single-carrier modulation shows severe performance degradation. Aiming at Gigabit level data

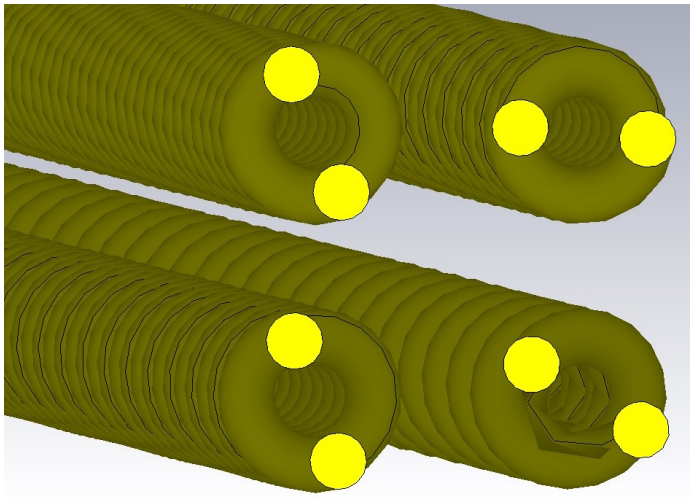

Fig. 2.2. Twisted Pair Model

rate, the latest DOCSIS 3.1 standard has replaced single-carrier from the early standard with the OFDM modulation as well, in order to realise the expectation in data rate. The downstream data rate is significantly increased from $42.88Mbit/s$ in the DOCSIS 3.0 to $10Gbit/s$ in the DOCSIS 3.1, while the upstream data rate is increased from $30.72Mbit/s$ in the DOCSIS 3.0 to $1Gbit/s$ in the DOCSIS 3.1 as well.

The twin-axial cable based Ethernet has finalised the 40GBASE-CR4 and 100GBASE-CR4/CR10 standards for the 40Gbit/s and 100Gbit/s transmission [34], which are ,essentially of multiple 10GBASE-CR lanes in parallel, i.e., the 10G Ethernet over twin-axial cable. Twin-axial cable has a very similar structure to co-axial cable, but with two copper wire conductors within the insulation. The two wires of the twin-axial cable are fed with a differential signal, the metallic braiding functions as an electromagnetic shielding layer. The twin-axial cable also adopts single-carrier PAM modulation.

Recently, power-line communication (PLC) has become as a candidate for in-house

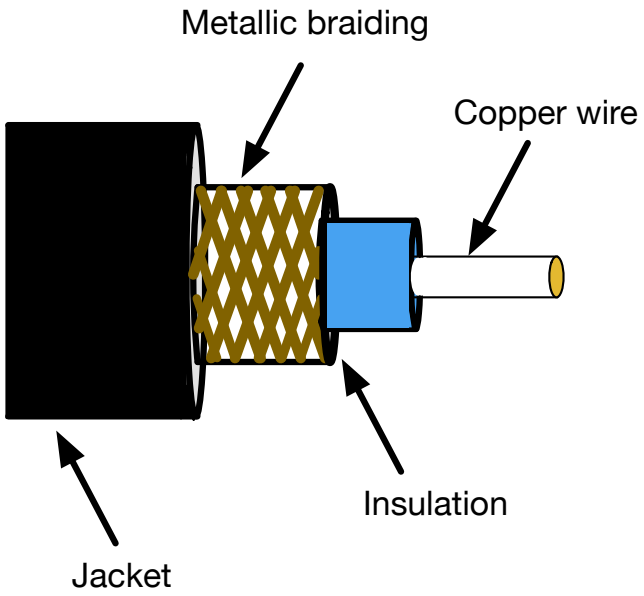

Fig. 2.3. Co-Axial Cable structure

networks [35, 36], where the data is carried by the legacy power line network. The PLC network cable is ordinary power line cable, which varies based on the specification of different countries. The modulation scheme used in the PLC network is also OFDM modulation.

2.2. TOPOLOGY AND CROSSTALK COUPLING

For wireline communication networks, the network topology determines the two ends of each transmission, where a cable connects these two ends. The geometry distribution of the cables could be sparse or compact, depending on the network topology. This then directly influences the crosstalk coupling distance of the cables. In this section two typical network topologies for the Ethernet network and the telephone network are discussed.

2.2.1. The Star Network Topology

In an Ethernet based LAN network, there are one or more computer or other devices as the end node, while one hub as the central access node [37]. The end nodes could be either wired or wireless connected to the hub. The hub can be a router or a switch, which may be connected to an upper layer switch or another parallel hub. This is considered as a star network, as illustrated in Fig. 2.4.

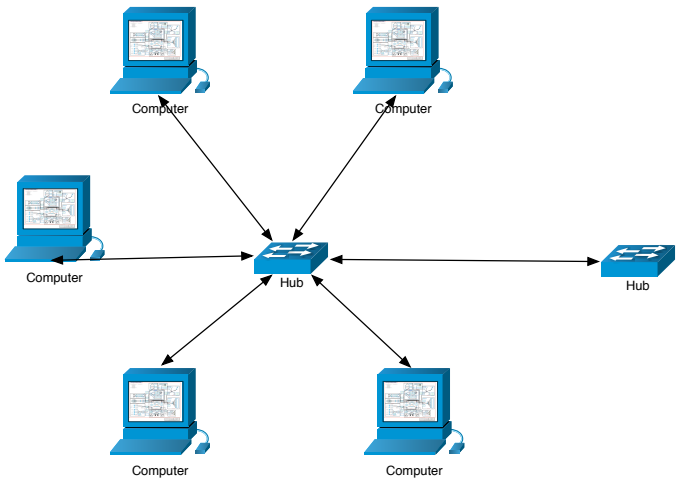

Fig. 2.4. The Star Network of LAN

The data centre is a large scale and layered LAN. The server rack, where a few servers are hosted, can be seen as the smallest LAN network on the edge of the whole network. There are two types of the cabling setting: top-of-the-rack (TOR) setting places one switch on the top of the rack, which connects all the server to the TOR switch; and the end-of-the-row (EOR) setting connects all the server in all the racks to the main switch at the end of the rack row. The TOR setting is gaining more popularity, with the advantage of easy cabling management and higher switch failure redundancy [38, 39]. The cable layout in

this TOR scenario is relatively compact at the switch side, on the other end spread down to the servers.The server to switch distance is only a few meters, due to the different server levels, the cable coupling is as short as one or two meters. Plus due to the well designed EoTP cable screen and shield, the crosstalk between EoTP cables, usually referred to as alien crosstalk, can be considered as trivial [39]. The most significant crosstalk is the coupling within the EoTP cable, among the twisted pairs, also this short coupling crosstalk will be the interest of the research in this thesis.

2.2.2. The Telephone Access Network

With the rapidly growing demand for bandwidth, much of the telephone network infrastructure, from the backhaul network and upwards to the core network, has been transformed to optical communication. While the access network part, from the access node (AN) to the customer-premises equipment (CPE), is connected by twisted pair cable.

For the long reach standards like ADSL, all the CPEs are directly connected to the CO, or to a remote terminal (RT) if there is one nearby. With the deployment of high speed but short reach VDSL and VDSL2, the AN moves even closer to the CPE, like fibre-to-the-cabinet (FTTC), fibre-to-the-neighbourhood (FTTN) and fibre-to-the-building (FTTB). While the majority of access network still runs over the underground cable bundle of the twisted pair cables, the different ANs lead to a mixed deployment topology, as demonstrated in Fig. 2.5.

In such a mixed deployment topology, each individual twisted pair cable may start and end at different locations, which is referred to as the near-far problem. In the underground cable bundle, the twisted pair cables are tidily bundled together for hundreds of meters,

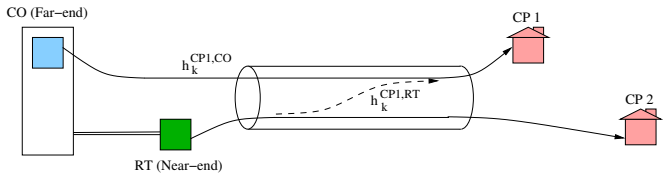

Fig. 2.5. The Mixed Deployment Topology of the xDSL Network

even over kilometres. Without any screen or shield, these twisted pair cables have strong coupling to each other, thus the resulting crosstalk severely degrades the performance of the xDSL networks.

Moreover, due to non-technical reasons, e.g., anti-monopoly regulation for telecoms, the cables in the same cable bundle might be owned by one company, but usually operated by two or more competing companies. Thus multi-user signal processing techniques can only be applied to the cables that are operated by the same company, then the resulting crosstalk from the differently coordinated cables causes more performance degradation [14, 40]. Such interference is within the same frequency band, therefore unpredictable due to the unknown multi-user technique. In the research of the xDSL network, the crosstalk generated by the twisted pair cable outside the multi-user coordinated group is defined as alien crosstalk.

2.3. DIGITAL MODULATION

From the perspective of frequency band utilisation, all the modulation techniques can be sorted into two camps, single-carrier modulation and multi-carrier modulation. The two modulation schemes are introduced in this section, then their performance for the EoTP cable will be evaluated later.

2.3.1. Pulse-Amplitude Modulation

For early narrow band or voice band communication systems, especially the analog transmission systems, the single carrier transmission has been an attractive option due to its low complexity. The AM and FM radio system are well known examples for analog modulation. Pulse-amplitude PAM modulation is one of the most used digital modulation methods, also adopted in the EoTP transmission.

PAM modulation can be understood as a digital correspondence of the analog amplitude, where the continuous carrier is replace by time-discrete pulse series, also the amplitude is quantised to a finite set of levels. In [41], for a given channel, the information bound b (in bit) can be carried on one pulse, i.e., one symbol, is calculated as follows,

$$b = \log_2(1 + SINR), \tag{2.1}$$

where SINR denotes the signal-to-interference-and-noise-ratio. With the carrier frequency f_s, the achievable data rate R of the whole transmission system is calculated as follows,

$$R = f_s \times b. \tag{2.2}$$

Intuitively, to expand the carrier frequency to transmit more symbols per second, or improve the SINR to transmit more bits per symbol can both increase the data rate. However, in reality, the channel condition is always impaired as the frequency increases. For a particular channel, the optimal carrier frequency for the PAM modulation is always a trade-off between the SINR and the frequency, rather than the highest frequency available.

2.3.2. The Orthogonal Frequency Division Multiplexing (OFDM) Modulation

As wireline communication systems switch to broadband systems, the increased channel frequency selectivity caused by the expanding transmission frequency band and the crosstalk become the major performance bottleneck. Hence, multi-carrier modulation schemes gradually emerge as powerful tools for broadband systems. Multiple carrier transmission techniques divide the broadband channel into a set of parallel narrow band flat channels (sub-carriers), then transmit over these separate channels simultaneously. as illustrated in Fig. 2.6.

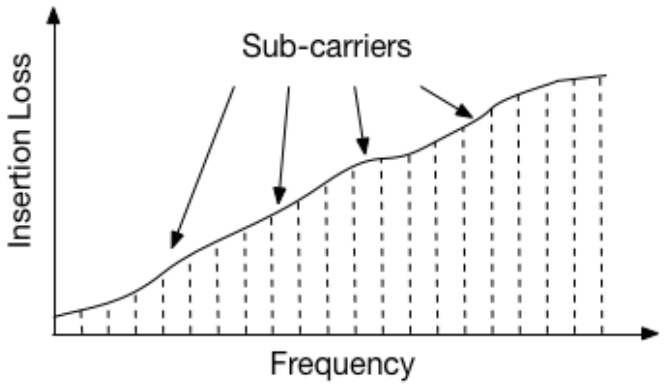

Fig. 2.6. OFDM Frequency Utilisation

A very popular multiple carrier technique in recent commercial practice is orthogonal frequency division multiplexing (OFDM), whose sub-subcarriers are orthogonal to each other [42, 43]. At the transmitter side, the transmit data is first converted to a set of parallel baseband data streams through a serial-to-parallel converter, where each of these stream corresponds to a sub-carrier, then independently modulated into quadrature amplitude modulation (QAM) symbols. So far, the data signal is still in the time domain. Then the parallel QAM symbols are fed into an inverse Fast Fourier Transformer (iFFT), whose

output is a serial signal in frequency domain, then is further converted into analogue signal by a digital-to-analogue converter (DAC). At last this transmit signal will go through the copper wire. This procedure is depicted in Fig. 2.7.

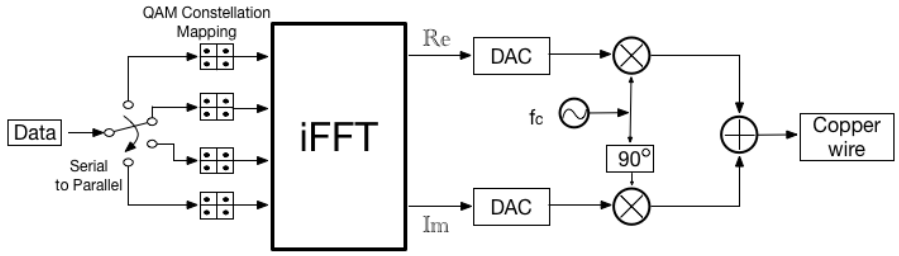

Fig. 2.7. OFDM Transmitter

At the receiver side, the received signal is converted into a digital signal through an analogue-to-digital converter (ADC), then separated into real and imaginary parts by a Fast Fourier Transformer (FFT), which converts the serial time domain signal back into parallel frequency domain QAM symbols. The the QAM symbols will be resolved into data bits, later combined in order into the received data. This procedure is depicted in Fig.2.8.

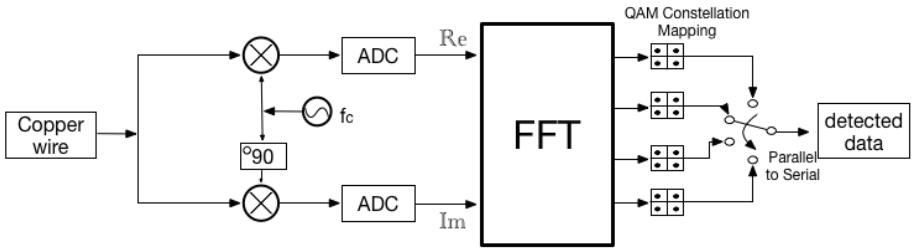

Fig. 2.8. OFDM Receiver

Mathematically, the frequency band F_{max} is divided into N sub-carriers, which is smaller or equal to the size of FFT/iFFT. Each carrier has a bandwidth of Δf, which

is chosen to be narrow enough that demonstrates a flat frequency channel condition. The symbol rate on each sub-carrier is denoted by f_s, while the corresponding symbol duration is $T = 1/f_s$ second. The bitloading b^n on sub-carrier n, i.e., the information can be carried on sub-carrier n in $bits$, is calculated as follows,

$$b^n = \log_2(1 + SINR), \tag{2.3}$$

and the achievable data rate R of the whole transmission system is calculated as follows,

$$R = f_s \sum_{n=1}^{N} b^n. \tag{2.4}$$

Compared with single carrier transmission, the performance degradation caused by the channel selectivity will be improved in OFDM, in that only the sub-carriers on the severely affected frequency will suffer performance degradation. For instance, the severe insertion loss in the high frequency part of Fig. 2.6 will not impact the separate transmission in the low frequency part. In the receiver design of the single carrier transmission, usually a time domain filter is adopted for the channel equalisation. Such a time domain filter invloves a large number of filter taps, which means high complexity, power consumption and processing delay. At the OFDM receiver side, the output of the FFT is parallel QAM symbols, which is low symbol rate frequency domain signal in the form of complex number. The channel equalisation can be easily implemented by multiplication of the QAM symbol with the inverse of the sub-carrier channel estimate.

2.4. SUMMARY

This chapter has introduced the basic concepts for the research work of the thesis. The EoTP cable and other copper based communication cables were introduced. Then the star network topology and telephone network topology and their impact on the crosstalk were discussed. Also, single-carrier and multi-carrier modulation schemes were presented.

Chapter 3

The Channel Model of The EoTP Cable

The sciences do not try to explain, they hardly even try to interpret, they mainly make models. By a model is meant a mathematical construct which, with the addition of certain verbal interpretations, describes observed phenomena. The justification of such a mathematical construct is solely and precisely that it is expected to work. - Johann Von Neumann

3.1. INTRODUCTION

At the time of writing, the early $10Mbit/s$ Ethernet over twisted pair cable has been upgraded to $10Gbit/s$: one thousand times faster. Meanwhile, the 40G BASE-T standard is being finalised by the IEEE 802.3 study group [44]. Thus the research goal here is to investigate the possibility of even higher data rate over the EoTP cable, namely $100Gbit/s$ or higher.

Since the introduction of the structured twisted pair cable as the foundation for the

Ethernet in the early 1980s, the same channel model has been used in all the work related to EoTP, e.g., the cable design and standard development. From the perspective of the "classic" communication theory, the EoTP cable provides four parallel SISO channels, where the crosstalk is seen as static noise and time-invariant. Also, the channel condition is determined by the carrier frequency of the single-carrier modulation.

From Table 1.1 and Table 1.2, the development of the EoTP standards can be catagorised as three straight-forward approaches:

- Higher cable quality
- Expanding the frequency bandwidth
- Increasing the PAM modulation order

In [9], the channel condition requirement of a 30 meter long CAT7A cable is specified, whose Shannon capacity is estimated for below $80Gbit/s$, over the four parallel SISO channel model. With this theoretical capacity, the expected $40Gbit/s$ transmission will be feasible with a considerable margin.

During the development of the 40G BASE-T, the straight-forward approaches are going close to the physical property bound of the EoTP cable. As specified in [9], the frequency has more than tripled from the 500MHz of the CAT6A to the 1600MHz of the CAT7A. Due to the physical nature of the conductor material, the copper, the insertion loss and the crosstalk level rapidly increase at Giga Hertz frequency. Restricted by the size and the cost of the EoTP cable, there is very little space for a further separation to reduce the crosstalk. Higher order PAM modulation requires better channel SINR, which is very challenging at such high frequency. Therefore, with the current transmission technique

establishment under this degraded channel condition, very dim possibility is seen for a future 100G BASE-T.

In this chapter, the EoTP cable and its channel are revisited, then the parallel SISO channel model is re-formulated into a full-duplex MIMO channel model. Under balanced transmission, the MIMO channel model is of 4×4 dimension, where both detailed near-end and far-end crosstalk coefficients are included. Then through the mixed-mode signal analysis, the signal is split into differential-mode signal and common-mode signal, then analysed in single-ended excitation on each wire. The metallic shield of the CAT7A cable is used as ground for the eight wires. The wire-level single-ended excitation is further developed into an unbalanced transmission mode, in which the number of the MIMO channels is doubled.

With the 30 meter long CAT7A cable specification in [9] as reference channel, a one meter long CAT7A cable is modelled and simulated. The numerical S-parameter from the simulation is used to characterise the balanced and unbalanced transmission, which is further used in the next chapter to evaluate the theoretical capacity of the EoTP cable.

In Sec. 3.2, the significance of short cable for the intra-rack connectivity is discussed. In Sec. 3.3 the EoTP channel is revisited and remodelled as a full-duplex MIMO channel. Sec. 3.4 provides a mixed-mode point of view of the EoTP signal transmission. Then the EoTP cable is further extended into unbalanced transmission mode in Sec. 3.5. The simulation methodology and results are given in Sec. 3.6.

3.2. THE INTRA-RACK CONNECTIVITY OVER COPPER

The general computer network topology was discussed in Sec. 2.2.1. Throughout the Part of the thesis, the research focuses on the micro-level network within the server rack.

Compared to the rapidly emerged wireless Ethernet in the home and office areas, data centre networks (DCN) and high performance computer (HPC) network still rely on the high throughput and the high reliability of the cable infrastructure [39, 45–55]. The HPC systems have usually very high density of the computing nodes, thus the HPC networks consist of chip-to-chip and board-to-board networks as the edge connectivity. As high-end computer systems, HPC networks have very rigorous delay and throughput specifications, therefore many HPC networks are customised or self-built networks with non-standard components [39, 52, 56].

With the trend of cloud computing and cloud storage [38], the data centres, as the fundamental element of such infrastructure, will be constantly upgraded to meet an ever growing demand. Then for the DCN, not only the performance, but also the deployment cost and maintenance cost are important factors in the DCN designing and planing. In the pyramidal structure of a state-of-the-art data centre, typically a few thousands of servers, as the basic functional node, are installed into a few hundreds server racks, regardless to the network routing optimisation [46,50,54,55,57,58]. Each server is usually connected to more than one routers [50], therefore there are more such edge connection between server and router installed than other aggregation connections. This further makes the cost of the edge connection a relatively large part in the total network expenditure, which includes the purchase, the installation and the maintenance [46, 50, 54, 55, 58].

The most popular technology for the edge connection in the DCN is 10G Ethernet

[50,54,58], which is offered with three cabling options: twisted pair cable, twinaxial cable and optical fiber. For the same length, the EoTP cable implementation costs in the region of 25% of the twin-axial cable or optical fiber cable [54, 58]. Although in [9], the 40G BASE-T is specified up to 30 meters as a typical reach, the intra-rack connectivity distance between the server and TOR router is restricted by the size the to the rack dimension to a few meters [59]. The silicon implementation of EoTP is considerably cheaper than the other options as well, which makes the corresponding network equipments, e.g., network adaptors, router and switches, more economical. Moreover, the EoTP cable is favoured in practical deployment for the easy bending and customised cable lengths, which results in a much lower maintenance cost. In this way, EoTP is a cost-effective solution for the intra-rack connectivity.

The aggregation connections between the racks require much higher throughput than the edge connection, which carry the aggregated data from multiple edge connections, even the 40G BASE-T can barely satisfy this scenario. Also the distance between such routers are longer than the intra-rack connectivity, which cover the dimension of a data centre [46, 57]. In such scenario, Ethernet over optical fibre is a better choice.

In this thesis, a one meter cable is modelled as an exemplar case for the short reach study. The insertion loss, return loss and crosstalk coupling level of such short EoTP cable have not been studied, to the best of our knowledge. The 30 meter cable channel model specified in [9] is used as a reference, to demonstrate the properties of the short reach cable.

3.3. THE MIMO CHANNEL MODELLING OF THE BALANCED TRANSMISSION

In the current EoTP standards, the twisted pairs are excited in differential mode. The two wires of each pair are fed with the voltage signals with same amplitude and different signs at the transmitter, then the voltage difference between the two wires at the receiver is taken as the output signal [2, 10, 31, 37]. Combining the balanced line and the differential signal, the signal transmission over each twisted pair is a *balanced transmission*. Moreover, at any point outside a twisted pair, the emitted signal from these two wires should also be of the same amplitude and different signs, so the resulting interference is also minimised.

The four twisted pairs in a EoTP cable form four parallel direct channels, who interfere each other with crosstalk channels. The actual received signal includes the desired signal, which is degraded by the insertion loss, the reflected signal, which is the transmit signal at the same side reduced by the return loss, the crosstalk and the external noise. As a point-to-point transmission, EoTP transmission is full duplex, in that the transmitter and receiver of each twisted pair are located at the same end of each pair, which working simultaneously over the same frequency band. The crosstalk received from the transmitters on the other end is defined as the far end crosstalk (FEXT), while the crosstalk received from the transmitters on the same end is defined as the near end crosstalk (NEXT). Therefore the EoTP cable can be seen as a multi-user interference-limited communication system with four single-in-single-out (SISO) channels, as demonstrated in Fig. 3.1.

In transmission line theory [2, 10, 31], the EoTP cable can be modelled as an 8-port network, as illustrated in Fig. 3.2.

From another point of view, at each end of the EoTP cable the transmit and received

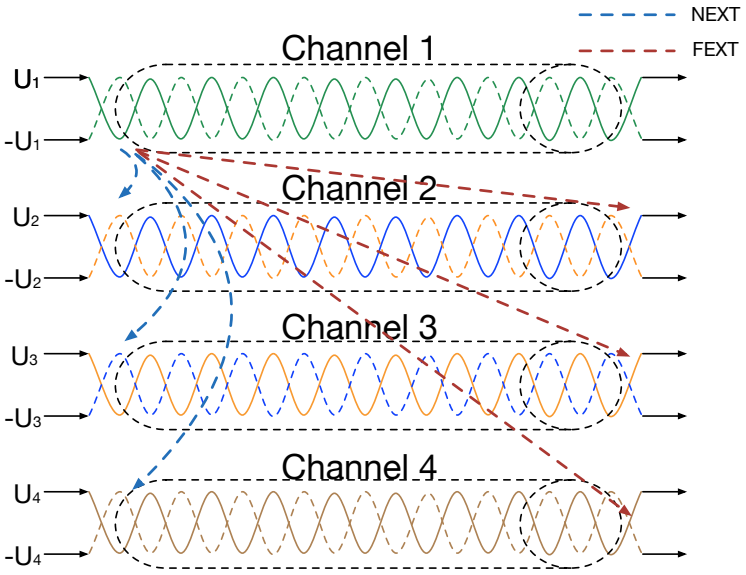

Fig. 3.1. The Four Channels in EoTP Cable

signal of the four SISO channel cans conveniently be processed in a coordinated fashion, so as to implement variety of MIMO techniques for performance enhancement. With the knowledge of the transfer function of any two ports of the network, the EoTP cable can be modelled as a 4×4 MIMO system. Assuming the transmission direction from port 1 to port 4 as downstream (DS), e.g., from the switch to the server, also the other direction as upstream (US), the MIMO channel model of the EoTP cable DS is given by matrix Eq. (3.1):

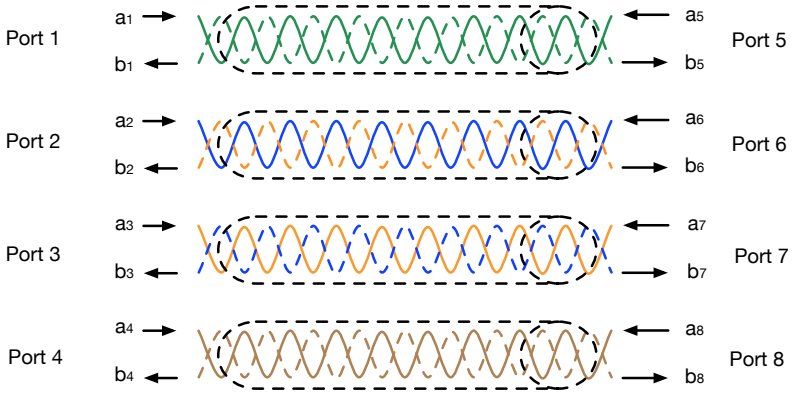

Fig. 3.2. 8-port Network Model of the EoTP Cable

$$\begin{bmatrix} b_5 \\ b_6 \\ b_7 \\ b_8 \end{bmatrix} = \begin{bmatrix} h_{5,1} & h_{5,2} & h_{5,3} & h_{5,4} \\ h_{6,1} & h_{6,2} & h_{6,3} & h_{6,4} \\ h_{7,2} & h_{7,2} & h_{7,3} & h_{7,3} \\ h_{8,1} & h_{8,2} & h_{8,3} & h_{8,4} \end{bmatrix} \begin{bmatrix} a_1 \\ a_2 \\ a_3 \\ a_4 \end{bmatrix} + \begin{bmatrix} h_{5,5} & h_{5,6} & h_{5,7} & h_{5,8} \\ h_{6,5} & h_{6,6} & h_{6,7} & h_{6,8} \\ h_{7,5} & h_{7,6} & h_{7,7} & h_{7,8} \\ h_{8,5} & h_{8,6} & h_{8,7} & h_{8,8} \end{bmatrix} \begin{bmatrix} a_5 \\ a_6 \\ a_7 \\ a_8 \end{bmatrix} + \begin{bmatrix} z_5 \\ z_6 \\ z_7 \\ z_8 \end{bmatrix}, \quad (3.1)$$

or compact as in Eq. (3.2),

$$\vec{b}_{DS} = H_{DS}\vec{a}_{DS} + H_{US}\vec{a}_{US} + \vec{z}, \quad (3.2)$$

where the vector $\vec{b}_{DS} = [b_5, b_6, b_7, b_8]^T$ denotes the received differential signal of channel 1 to 4 at port 5 to 8. The vectors $\vec{a}_{DS}$, $\vec{a}_{US}$ and $\vec{z}$ with the same structure as $\vec{b}_{DS}$ denote the transmit signal vectors for DS and US, and the external noise vector, respectively. H_{DS} and H_{US} are 4×4 channel coefficient matrices for DS and US, respectively. The diagonal elements of H_{DS} are the insertion loss coefficient of the direct channel, where

the off-diagonal elements of H_{DS} are the FEXT coefficient. The diagonal elements of H_{US} are the return loss coefficient, where the off-diagonal elements of H_{US} are the NEXT coefficient. A precise model for the alien crosstalk for EoTP cable, i.e., the crosstalk from other EoTP cables, is still an open issue, therefore the alien crosstalk is considered as a component in external noise.

Similarly, the MIMO channel model of the EoTP cable US is given by Eq. (3.3):

$$\begin{bmatrix} b_1 \\ b_2 \\ b_3 \\ b_4 \end{bmatrix} = \begin{bmatrix} h_{1,5} & h_{1,6} & h_{1,7} & h_{1,8} \\ h_{2,5} & h_{2,6} & h_{2,7} & h_{2,8} \\ h_{3,5} & h_{3,6} & h_{3,7} & h_{3,8} \\ h_{4,5} & h_{4,6} & h_{4,7} & h_{4,8} \end{bmatrix} \begin{bmatrix} a_5 \\ a_6 \\ a_7 \\ a_8 \end{bmatrix} + \begin{bmatrix} h_{1,1} & h_{1,2} & h_{1,3} & h_{1,4} \\ h_{2,1} & h_{2,2} & h_{2,3} & h_{2,4} \\ h_{3,1} & h_{3,2} & h_{3,3} & h_{3,4} \\ h_{4,1} & h_{4,2} & h_{4,3} & h_{4,4} \end{bmatrix} \begin{bmatrix} a_1 \\ a_2 \\ a_3 \\ a_4 \end{bmatrix} + \begin{bmatrix} z_1 \\ z_2 \\ z_3 \\ z_4 \end{bmatrix}, \quad (3.3)$$

or compact as in Eq. (3.4),

$$\vec{b}_{US} = H_{US}\vec{a}_{US} + H_{DS}\vec{a}_{DS} + \vec{z}. \quad (3.4)$$

With any MIMO realisation, after obtaining the parameters for the channel coefficient matrices H_{DS} and H_{US}, the transmit vectors $\vec{a}_{DS}$ and $\vec{a}_{US}$, and the external noise $\vec{z}$, the total data rate of the MIMO EoTP can be calculated by the equation Eq. (3.4). Also, this channel model can be easily extended to an OFDM-MIMO model, where the spectrum efficiency can be further improved by OFDM modulation.

3.4. MIXED-MODE SIGNAL ANALYSIS

Firstly the EoTP cable is studied from a mixed-mode signal point of view. For the simplest ideal balanced transmission model with two parallel and identical conductors, any received external interference will be removed as common-mode signal [2, 10, 31, 60]. Conductor-wise, the CAT7A EoTP cable has four twisted pairs, four pair-screens and one metallic shield. For each twisted pair, the external interference includes the crosstalk from other pairs and external interference through the shield. Traditionally, the EoTP is analysed as an 8-port network, where each twisted pair is modelled as a two-port network, as illustrated in Fig. 3.2. Due to the compact size of the EoTP cable, the spacing between the two wires of the same twisted pair is not electronically small enough to receive the identical crosstalk from other pairs. Moreover, at different locations of the cable, the wires have different geometry distributions. This further leads to different mutual inductance (L_m) and capacitance (C_m).

In the real-world EoTP cable, the energy going into the wire and travelling towards the other end of the wire is composed of both the desired differential-mode signal and the received non-ideal common-mode signal from other wires. From the mixed-mode signal point of view, each wire of the EoTP cable can be seen as two individual single-ended transmission lines , the differential-mode excitation source and the common-mode excitation source. At the other end of the transmission line, the received energy of these two transmissions contains the differential-mode signal from the same wire and the differential-mode signal and the common-mode signal from other wires.

In order to study the differential-mode signal and the common-mode signal separately, a common ground is required for all the wires in the circuit model. In practice, even

without the presence of a drain wire, the metallic shield can serve well as the common ground for all the wires. Then the EoTP cable can be modelled as a multiple conductor transmission systems, where the conductor paths are parallel to each other and share a common ground [61]. Such a system can be seen as a cascade of a series of small cable segments, each of which can be modelled by a resistance (R), inductance (L), capacitance (C), and conductance (G) RLCG model. The RLCG model of a EoTP cable segment is depicted in Fig. 3.3.

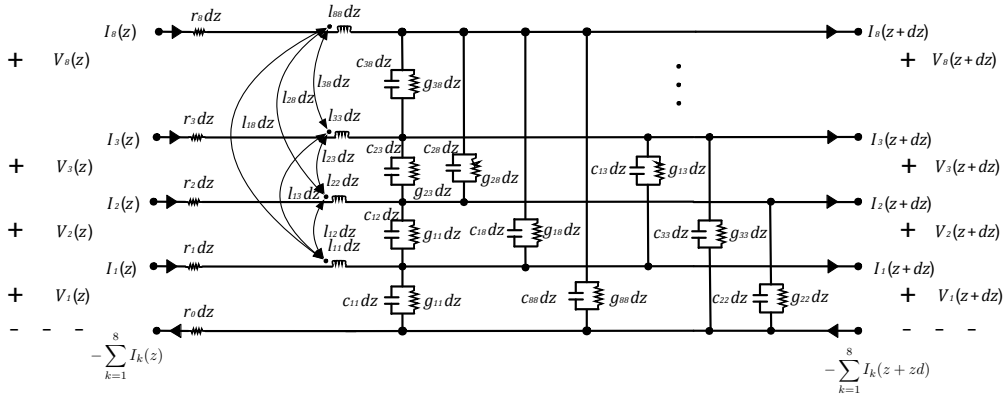

Fig. 3.3. The RLCG Model of the EoTP Cable Segment

Theoretically, with the given material physical properties and the conductor geometry distribution, the RLCG parameters of each cable segment can be calculated, also further used to produce the transfer functions. By cascading the segments, the transfer function of the whole cable can be obtained [61]. However in most of the practical system, the almost infinitely fine segmentation and the variation in conductor geometry distribution lead to a unsolvable computation-intensive problem, which prohibit the use of this method to analyse the EoTP cable.

In the 8-port network Fig. 3.2, the transmit signal a_n and received signal b_n at port n

are composed of both the differential-mode signal and the common-mode signal, denoted by a_{dn}, a_{cn},b_{dn} and b_{cn}, respectively. The mixed-mode signal S-parameters of the EoTP cable is defined as follows Eq.(3.5),

$$\begin{bmatrix} b_{d1} \\ \vdots \\ b_{d8} \\ b_{c1} \\ \vdots \\ b_{c8} \end{bmatrix} = \begin{bmatrix} \begin{bmatrix} S_{dd1,1} & S_{dd1,2} & \cdots & S_{dd1,8} \\ S_{dd2,1} & S_{dd2,2} & \cdots & S_{dd2,8} \\ \vdots & \vdots & \ddots & \vdots \\ S_{dd8,1} & S_{dd86,2} & \cdots & S_{dd8,8} \end{bmatrix} \begin{bmatrix} S_{dc1,1} & S_{dc1,2} & \cdots & S_{dc1,8} \\ S_{dc2,1} & S_{dc2,2} & \cdots & S_{dc2,8} \\ \vdots & \vdots & \ddots & \vdots \\ S_{dc8,1} & S_{dc8,2} & \cdots & S_{dc8,8} \end{bmatrix} \\ \begin{bmatrix} S_{cd1,1} & S_{cd1,2} & \cdots & S_{cd1,8} \\ S_{cd2,1} & S_{cd2,2} & \cdots & S_{cd2,8} \\ \vdots & \vdots & \ddots & \vdots \\ S_{cd8,1} & S_{cd8,2} & \cdots & S_{cd8,8} \end{bmatrix} \begin{bmatrix} S_{cc1,1} & S_{cc1,2} & \cdots & S_{cc1,8} \\ S_{cc2,1} & S_{cc2,2} & \cdots & S_{cc2,8} \\ \vdots & \vdots & \ddots & \vdots \\ S_{cc8,1} & S_{cc8,2} & \cdots & S_{cc8,8} \end{bmatrix} \end{bmatrix} \begin{bmatrix} a_{d1} \\ \vdots \\ a_{d8} \\ a_{c1} \\ \vdots \\ a_{c8} \end{bmatrix} \tag{3.5}$$

.

The mixed-mode S-parameter matrix in Eq. 3.1 can be divided into four sub-matrices, which consists of S_{dd} sub-matrix for differential-mode S-parameters, S_{dc} sub-matrix for common-mode to differential-mode conversion S-parameters, S_{cd} sub-matrix for differential-mode to common-mode conversion S-parameters and S_{cc} sub-matrix for common-mode S-parameters. For these sub-matrices, the diagonal elements represent the direct signal or its echo, while all the off-diagonal elements represent the coupling between the wires. Note that there is no reflected signal component other than the echo at any port, otherwise errors will be included [60].

In the real cable, the spacing between the copper wires will cause considerable coupling between them. Also in the cable specification, the common-mode coupling is rela-

tively tolerated, as long as they are well balanced, i.e., the common-mode coupling signal can be largely removed in the differential signalling output. Moreover, in an arbitrary segment of the cable the coupling from on disturbing wire into the two wires of the same twisted pair will rarely be identical, due to the twisting nature, as shown in Fig. 2.2. Then this unbalance in common-mode signal causes non-zero crosstalk.

In practical cabling system installations, the common-mode balance parameters, i.e., the transverse conversion loss (TCL) and transverse conversion transfer loss (TCTL) [9,62, 63], is usually used as a diagnosis tool to examine the channel performance of the installed cable. Despite the difficult direct measurement of the common-mode balance parameters, it can be derived from the relatively easily measured single-ended S-parameters of each wire through the single-ended to mixed-mode conversion technique [60].

3.5. THE MIMO CHANNEL MODEL OF THE UNBALANCED TRANSMISSION

With a common ground for all the wires of the EoTP cable, single-ended measurement can be obtained by a vector network analyser (VNA). The corresponding model is expanded from the 8-port network for differential-mode signal driven EoTP to a 16-port network with single-ended excitation, as illustrated in Fig. 3.4.

Instead of differential signals, if the eight single-ended excitation sources are fed with individual signal streams, the EoTP cable becomes an eight-channel communication system in each direction. The common-mode interference will not be cancelled, while the wires will interfere with each other via crosstalk. The signal flow diagram of such a unbalanced EoTP transmission is demonstrated in Fig. 3.5.

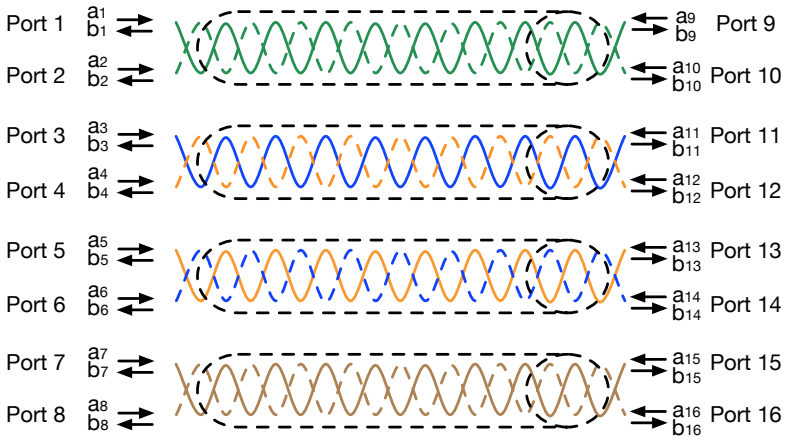

Fig. 3.4. 16-port Network Model of the EoTP Cable

Compared with each single channel in the balanced EoTP transmission, each channel in the unbalanced transmission will incur predictably increased crosstalk and degraded insertion loss. Given the same total transmit power to drive the EoTP cable, the transmit power into each channel (each wire) of the the unbalanced transmission is reduced to half of that of the balanced transmission. Moreover, the crosstalk in the unbalanced transmission is from seven disturber wires, rather than the three disturber pairs in the balanced transmission. Intuitively, the two wires in the same twisted pair are twisted closely to each other, where the coupling of such two wires (intra-pair crosstalk) is expected higher than the coupling between the pairs (inter-pair crosstalk). With all these factors, the unbalanced EoTP cable is considered as an interference-limited system.

If the transmit signal or/and the received signal of the multiple transceivers can be coordinated, the interference or the crosstalk can be well addressed by MIMO techniques, then the capacity of the whole system largely depends on the number of the communication channels [64, 65]. By introducing such unbalanced transmission, the EoTP cable

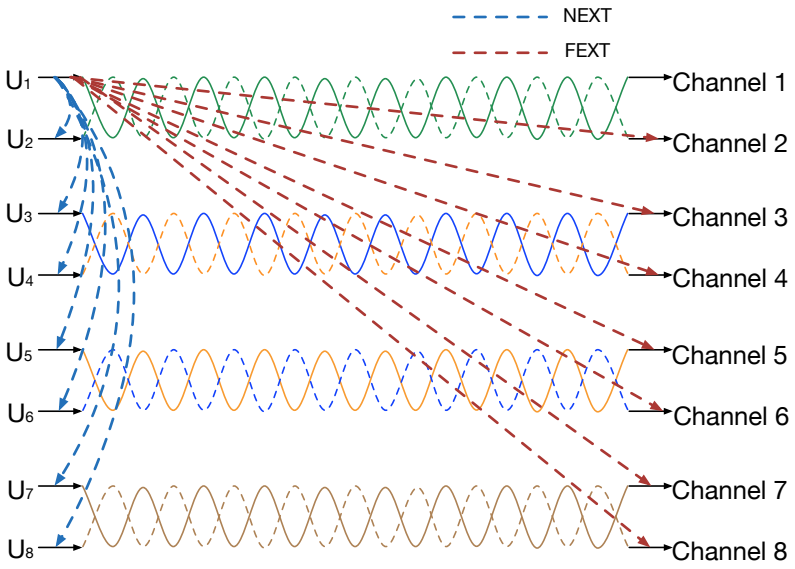

Fig. 3.5. The Unbalanced Transmission in EoTP Cable

could further exploit MIMO diversity through the doubled number of channels. Many practical and commercial MIMO applications and systems have already shown significant performance improvement from the increased number of the channels, e.g., the multiple antenna configuration of the wireless LAN IEEE 802.11n [66] and the LTE [67]. Therefore with the aid of MIMO technique to reduce the impact of the crosstalk between the wires, the increased number of channels has the potential to significantly enhance the total capacity of the EoTP cable.

The MIMO channel model for the unbalanced transmission is similar to the balanced transmission in Eq. (3.2), but the length of the vectors are extended to eight, also the channel matrices H_{DS} and H_{US} are of the dimension of 8×8. As an example, the downstream

MIMO channel model of the unbalanced transmission of EoTP cable is defined as follows,

$$\begin{bmatrix} b_9 \\ b_{10} \\ \vdots \\ b_{16} \end{bmatrix} = \begin{bmatrix} h_{9,1} & h_{9,2} & \cdots & h_{9,8} \\ h_{10,1} & h_{10,2} & \cdots & h_{10,8} \\ \vdots & \vdots & \ddots & \vdots \\ h_{16,1} & h_{16,2} & \cdots & h_{16,8} \end{bmatrix} \begin{bmatrix} a_1 \\ a_2 \\ \vdots \\ a_8 \end{bmatrix} + \begin{bmatrix} h_{9,9} & h_{9,10} & \cdots & h_{9,16} \\ h_{10,9} & h_{10,10} & \cdots & h_{10,16} \\ \vdots & \vdots & \ddots & \vdots \\ h_{16,9} & h_{16,10} & \cdots & h_{16,16} \end{bmatrix} \begin{bmatrix} a_9 \\ a_{10} \\ \vdots \\ a_{16} \end{bmatrix} + \begin{bmatrix} z_9 \\ z_{10} \\ \vdots \\ z_{16} \end{bmatrix}. \tag{3.6}$$

Both the balanced and unbalanced MIMO channel model will be characterised by a realistic CAT7A cable simulation as given in the next section.

3.6. SIMULATION RESULT OF S-PARAMETERS

3.6.1. Simulation Software and Cable Specification

The simulation software is Computer Simulation Technology (CST) Microwave Studio, which is an accurate 3D electromagnetic simulation and analysis tool [68]. The CST software is running on a workstation with a quad-core Intel i5-2400 CPU at 3.1GHz, and 12 Gbit RAM. The CST software meshes the model into small mesh cells, excites the model at predefined ports, then calculate the electro-magnetic sub-problem in each mesh cell.

The cable specification of a one meter long CAT7A screened S/FTP cable is then modelled in the CST software. The conductor, i.e., the wire, is 22 AWG solid copper, with a diameter of 0.64 ± 0.008mm. The conductor is covered by a layer of FR-4 as insulation, the thickness of which is 0.4 mm. The total diameter of the insulated wire is 1.45 ± 0.1mm.

The four twisted pairs are twisted with different twisting rate, namely 65.2, 64.8, 56.2 and 51.7 turns per meter, respectively. Each pair is wrapped with a $65\mu m$ thick aluminium foil, to provide an individual screen against the electro magnetic coupling between the pairs.

The outer layer of the cable has a metal braiding covering the four pairs, for the purpose of external interference rejection. The braiding is woven by tinned copper wire with a diameter of 0.12 mm, which covers 40% of the cylinder outside the four pairs. For unbalanced transmission, all the eight wires are connected to this braid as the common ground. In the end, there is a layer of non-conductive Low Smoke Zero Halogen (LSOH) as the protection jacket.

Originally the cable was designed for a maximum frequency of 1200 MHz, however in the simulation software we specify the frequency up to 1700 MHz, allowing consideration of the frequency of 1600 MHz specified in [9]. Then the cable model was meshed into approximately 2.58 million mesh cells. The cable model and its meshing result are displayed in Fig. 3.6. Note that the braid and jacket is configured as invisible, for the consideration of visual clarity.

The port and wire labelling for the balanced and unbalanced transmission is the same as shown in Fig. 3.2 and Fig. 3.4, respectively.

3.6.2. Insertion Loss and Return Loss Performance

The direct channel simulation result is presented in Fig.3.7, i.e., the insertion loss and the return loss, for both balanced and unbalanced transmission of the one meter cable, also with the 30 meter cable studied in ISO standard [9] as a reference. The S-parameters of

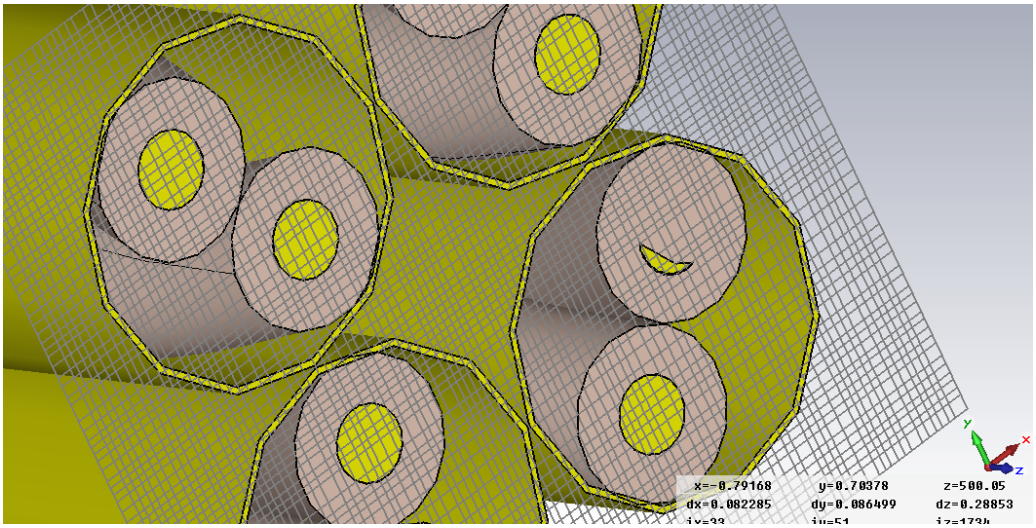

Fig. 3.6. The Meshing of the Cable Model

the 30 meter reference cable is generated by the worst case scenario specified in [9]. Due to the limitation of space, not result from all the wires and pairs are displayed here.

First of all, the simulated curves of the one meter cable are not ideally smooth, but periodically rippled by slightly more than $100MHz$, as observed from Fig.3.7. This is caused by the dielectric reflection, which can also be observed in all the following simulations.

The lowest insertion loss comes from the one meter balanced transmission, while the 30 meter cable shows a much higher insertion loss, which is increasing with the frequency. For the unbalanced transmission, the insertion loss performance is slightly higher than the balanced transmission, only degrades for over 10 dB gap after 1400 MHz.

The return loss performance of the balanced transmission is plotted in Fig.3.8, where we can see that the one meter cable has a similar return loss as the 30 meter cable. From Fig.3.9, we can see that the return loss performance of the unbalanced transmission is even lower than the balanced transmission in most of the frequency range. Note that although

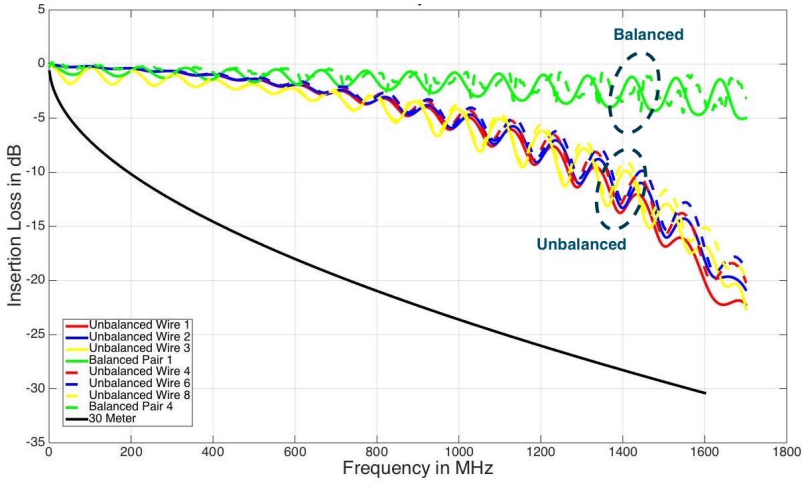

Fig. 3.7. The Insertion Loss Performance

the return loss looks like a major disturbance source, in practice the return loss can be largely removed by very simple echo cancellation circuit, e.g., the echo cancellation is implemented as $-55dB$ for 10GBASE-T [8].

This part of simulation result shows that both balanced and unbalanced transmission have better insertion loss with respect to the 30 meter cable, and satisfactory return loss.

3.6.3. Crosstalk Performance

Firstly, the FEXT channel of unbalanced transmission was investigated. The FEXT simulation result of wire 1 and wire 2 is shown in Fig.3.10. Due to the limited space, other wires with similar results are not shown here. The two curves on the top are the intra-pair FEXT of pair 1, i.e., between wire 1 and wire 2. Clearly, these intra-pair FEXT is higher than other inter-pair FEXT received by wire 1 from the other wires. The reason is that, for the unbalanced transmission, the intra-pair crosstalk is between two closely twisted wires while the inter-pair crosstalk is reduced through two screening layers between the twisted

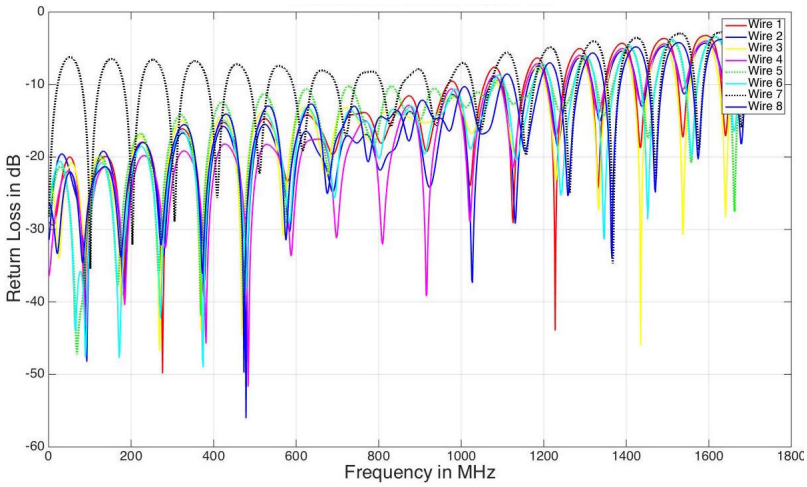

Fig. 3.8. The Return Loss of Balanced Transmission

pairs. This observation confirms the prediction in the previous section, that the intra-pair crosstalk is stronger than the inter-pair crosstalk.

In Fig.3.11, a comprehensive comparison between the intra-pair, inter-pair FEXT of unbalanced transmission and the FEXT in balanced transmission is presented. The FEXT is the coupling from one port to another port at opposite ends of the cable. Therefore the FEXT signal will experience the propagation loss along the cable. The dependency of the FEXT on the cable length can be observed from the fact that the FEXT of the 30 meter cable is significantly lower than that of the one meter cable in both balanced and unbalanced transmission. Moreover, this indicates that the channel condition of a short cable is not necessarily better than a longer cable, especially in the TOR scenarios.

The FEXT of the balanced transmission is lower than the the intra-pair FEXT and higher than the inter-pair FEXT of the unbalanced transmission. Clearly the screening of each twisted pair and the differential-mode transmission helps the balanced transmission to reduce the FEXT level, with respect to the intra-pair FEXT of the unbalanced transmission.

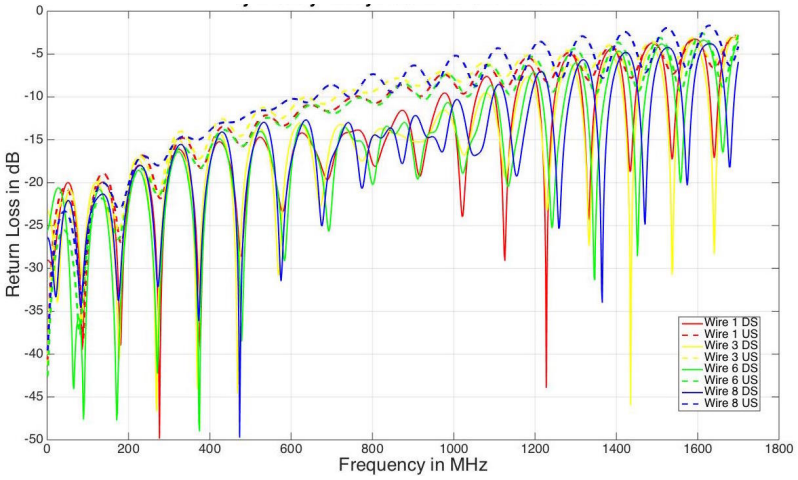

Fig. 3.9. The Return Loss of Unbalanced Transmission

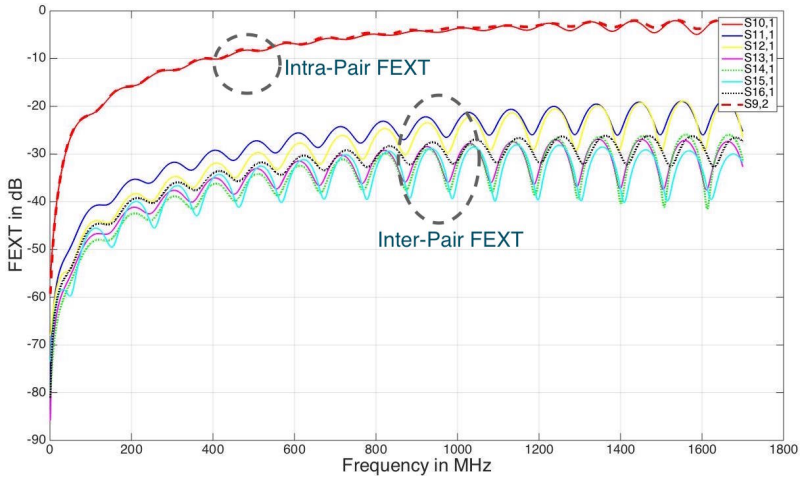

Fig. 3.10. The FEXT of the Unbalanced Transmission

On the other hand, the double-sized conductor of the balanced transmission leads to higher FEXT than the inter-pair FEXT of the unbalanced transmission. Generally speaking, for the balanced transmission the common-mode coupling within the twisted pair is more dominant than the coupling between the twisted pairs.

The simulation results of the NEXT are formulated similar to the FEXT simulation

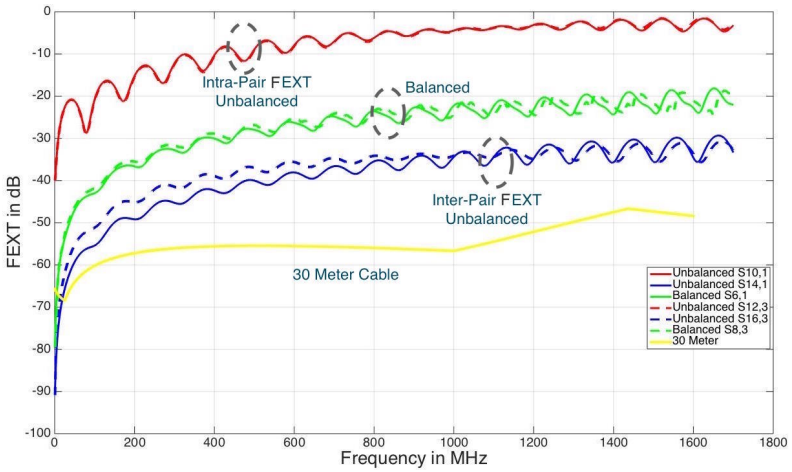

Fig. 3.11. The FEXT Performance Comparison

results, where Fig.3.12 demonstrates the the NEXT performance, while Fig.3.13 shows a comprehensive comparison of the balanced and the unbalanced transmission. Similar observation from the FEXT performance can be obtained from the NEXT as well. This includes the strong intra-pair NEXT, the NEXT dependency of the cable length and the balanced NEXT between the intra-pair and the inter-pair NEXT of the unbalanced transmission.

3.6.4. The Channel Length of the EoTP Cable

The actual signal into the channels is always a series of modulated pulses, which are generated by the DAC. The non-ideal pulse will always have resonance as signal spreading in the physical channel, which turns the unwanted energy residual into an interference for the subsequent signal pulses. This is also known as intersymbol interference (ISI). The longer the signal stays in the channel, the more subsequent will be corrupted by the ISI. The channel length can be measured in absolute time dimension, or relatively represented

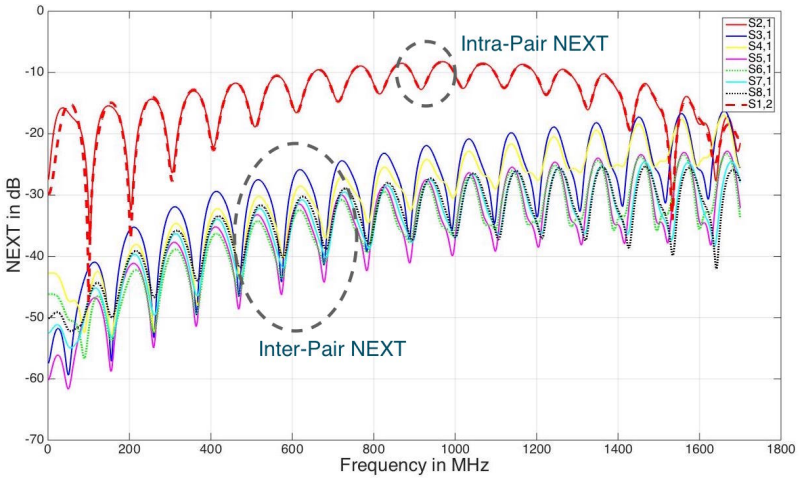

Fig. 3.12. The NEXT of the Unbalanced Transmission

by how many pulse durations, according to the signal frequency.

With the increasing frequency used in the EoTP, the interval between the signal symbols is even smaller than before. The pulse duration is $2 \times 10^{-9}s$ for $500MHz$ and $6.25 \times 10^{-10}s$ for $1600MHz$. Usually the impact of the ISI is minimised by match filter or error correcting codes, both of which will be challenging in the implementation at such high frequency. The problem of the ISI is addressed in OFDM transmission by a cyclic prefix, however, this additive redundancy impacts the frequency efficiency.

Here, the signal spreading in the EoTP cable is studied as the normalised signal pulse amplitude in the time domain. The near-end signal observations of Pair 1 of the balanced transmission and Wire 1 of the unbalanced transmission are demonstrated in Fig.3.14 and Fig. 3.15, f. The noticeable signal are observed in three time-windows. The first time-window occurs at $2.5 \times 10^{-9}s$, approximately, which includes the excitation signal "iI" with the largest amplitude, the immediate reflection signal and the NEXT to other conductors. In the second time-window, the echo, i.e., the reflected excitation signal from

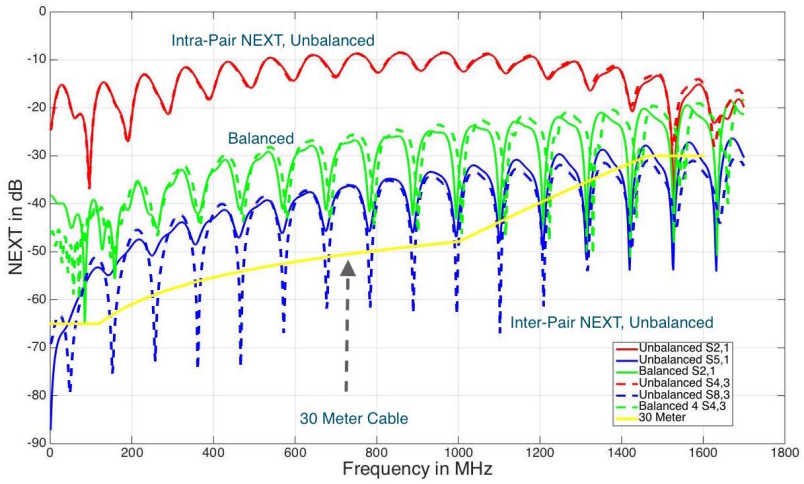

Fig. 3.13. The NEXT Performance Comparison

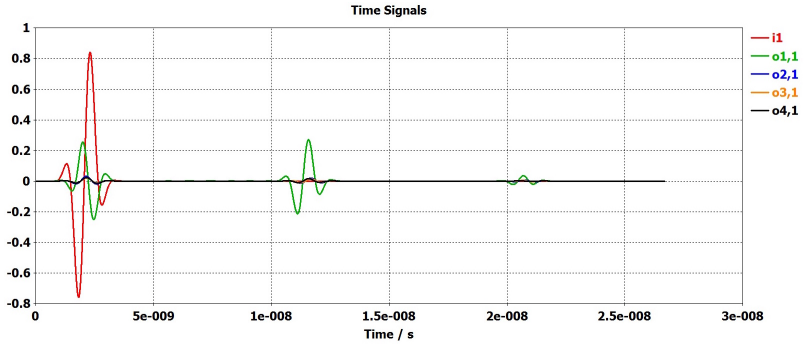

Fig. 3.14. The Signal Spreading of Pair 1 in the Near-end

the other end of the conductor, is dominant in both figures, while the strong intra-pair NEXT "$o2,1$" of the unbalanced transmission can be clearly observed in Fig. 3.15. The last time-window observation is composed with insignificant signals, which are attenuated to a negligible level.

The far-end signal observations are more of interest, as they are the direct cause of the ISI. Similarly, the far-end signal observations of Pair 1 of the balanced transmission and Wire 1 of the unbalanced transmission are demonstrated in Fig. 3.16 and Fig. 3.17,

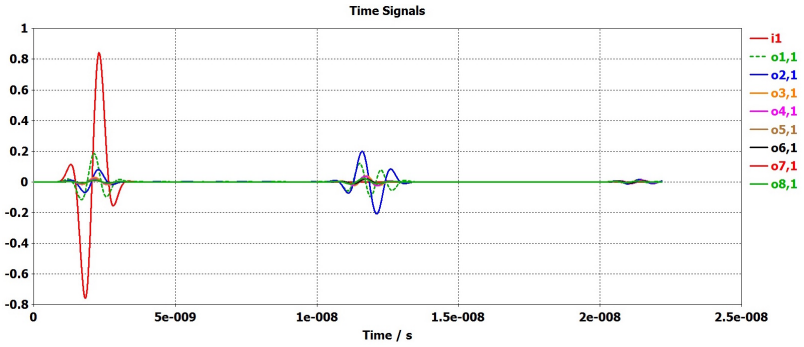

Fig. 3.15. The Signal Spreading of Wire 1 in the Near-end

respectively. The far-end signal of the balanced transmission are observed in three time-windows, while only two time-windows for the unbalanced transmission, while the signals in the third time-window of the balanced transmission is faded to negligible level as well. In Fig. 3.17, a very strong intra-pair FEXT curve "*o10,1*" is observed as well.

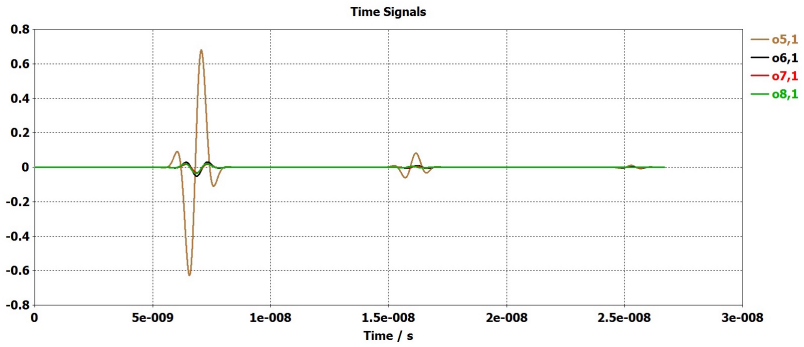

Fig. 3.16. The Signal Spreading of Pair 1 in the Far-end

Apart from the FEXT to other conductors, the curve "*o5,1*" in Fig. 3.16 and the curve "*o9,1*" in Fig. 3.17 represent the direct channel signal, which represents the desired received signal in the first time-window but ISI signal in the second time-window. The ISI signal arrives approximately $1 \times 10^{-8}s$ after its original transmit signal, therefore it will interfere with the received signal transmitted $1 \times 10^{-8}s$ later. Generally speaking, the

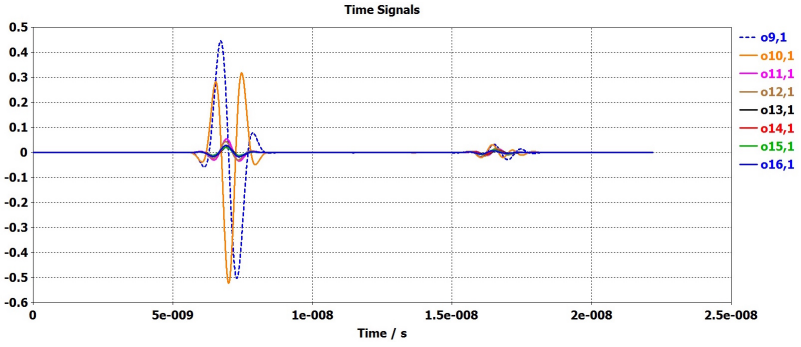

Fig. 3.17. The Signal Spreading of Wire 1 in the Far-end

EoTP can be considered as an one-tap filter channel with a fixed delay, which is simpler than most of the complicated wireless channels.

The delay of the ISI signal is $1 \times 10^{-8}s$, which corresponds to 5 or 16 pulse durations, for $500MHz$ and $1600MHz$, respectively. The signal is observed for the one meter cable, while the travel time of the signal is proportional to the length of the conductor.

Considering the $1600MHz$ frequency for the 40G BASE-T, each PAM signal pulse carries a symbol, then the fifteenth symbol thereafter will be impacted by the ISI from the current symbol in the simulated EoTP cable. For the OFDM transmission, one symbol consists a large number of pulses. The prefix is used in OFDM symbol construction as an ISI prevention method, where the end part of the symbol is repeated and padded as the header of the symbol. As the guard interval, the length of the prefix should be no shorter than the channel length, which is sixteen pulses here. The prefix will be further discussed in the next section.

Moreover, the amplitude of the near-end signals are similar for both balanced and unbalanced transmission. However, when comparing the signal amplitude of the direct channel received signal and the ISI signal, the amplitude is reduced from over 0.4 to lower

than 0.05 for the unbalanced transmission, and from over 0.6 to about 0.1 for the balanced transmission. This indicates that the ISI interference causes less signal degradation per channel in the unbalanced transmission.

3.7. SUMMARY

In this chapter, the channel model of the EoTP cable was revisited from a multi-user communication point of view. Firstly a full-duplex MIMO channel model for EoTP cable was developed. Then the EoTP cable was studied from a mixed-mode signal analysis point of view, by observing the single-ended excitation S-parameters. Furthermore, the unbalanced transmission over the EoTP cable was proposed, where the metallic shield was used as the common ground for the eight wires, so as to increase the number of channels in the MIMO channel model. A one meter long CAT7A cable was modelled in CST Microwave Studio and simulated for both balanced and unbalanced transmission. Also, a 30 meter long CAT7A cable based of the ISO standard specification was used as a reference for comparison. From the simulation result, the one meter long CAT7A cable showed better insertion loss and stronger crosstalk in both balanced and unbalanced transmission, with respect to the 30 meter long cable, also the resulting capacity is to be examined in the next chapter. The channel length was studied as well, that the impact of the ISI in EoTP cable was generally less than in the wireless channels.

The channel models studied and simulated in this chapter will be evaluated for their theoretical capacity in the next chapter.

Chapter 4

The EoTP Capacity with Alternative Transmission Techniques

A good decision is based on knowledge and not on numbers. - Plato

4.1. INTRODUCTION

From the observation of the simulation result in the last chapter, the insertion loss and the crosstalk level increases rapidly with increasing frequency, even for short cables. For such a frequency selective channel condition, the SINR in the GHz frequency range could be unsatisfactory for higher order PAM modulations. Hence alternative transmission techniques are considered here, which aim to improve the frequency efficient of the given channel condition.

The period of the EoTP development is also a golden age for computer science, electronic and communication technology, while new communication theory concepts and new

transmission techniques have also been developed for broadband data communications, e.g., OFDM modulation [11, 42, 43, 69] and MIMO techniques [64, 65, 70–72]. These technology advances are enabling the convenient and reliable information technology infrastructure of the world. The most seen bottlenecks in the communication channels are the frequency selectivity problem and the crosstalk or the inter-channel interference problem. Particularly, the multi-carrier OFDM modulation and the MIMO based multi-user signal coordination technique have shown significant performance boost in many high speed data communication system.

For instance, OFDM has been applied in xDSL networks [5, 13, 73], in PLC networks [35, 36], in wireless LAN [66], and in "Digital Video Broadcasting - Terrestrial (DVB-T) [74] and Digital audio broadcasting (DAB) systems [75]. Recently,OFDM has been discussed and considered as the modulation method for the next generation $100G/200G/400G$ long reach Ethernet over optical fibre [76, 77], which commits to realise ultra high speed data transmission over frequency selective optical channels.

Furthermore, MIMO and OFDM together are considered as a very important tool to transmit very high speed data under very complex channel conditions, e.g., both the latest wireless LAN IEEE 802.11n [66] and the the fourth generation mobile communication, the Long Term Evolution (LTE) standard [67] use more than one antennas on each terminal with OFDM transmission.

In the previous chapter, new channel models of the EoTP cable were proposed, which are used here as the foundation to accommodate the alternative transmission techniques. This chapter examines the theoretical capacity of the EoTP cable by applying alternative transmission techniques, i.e., the multi-carrier OFDM modulation, and the MIMO

crosstalk cancellation effectiveness, to the new channel models.

Unlike theoretical studies, the design of any practical communication system,or even every engineering problem, is always a trade-off between performance and resources, or in other words, how to efficiently utilise the given resource, under realistic restrictions. The channel condition defines the theoretical capacity of the system by the Shannon formula, which should not be exceeded in the system design. The actually realised performance depends on a variety of implementation factors, such as transmit power, modulation configuration, external noise, etc. The specified operating performance is always lower than the theoretical capacity of the communication system, so as to ensure the realised performance is guaranteed with a margin. Therefore, the theoretical capacity of the system serves as an important guide for the system design.

In this chapter, the theoretical capacity over the simulated CAT7A cable channels is examined from different perspectives, i.e., balanced/unbalanced transmission mode, single-carrier/multi-carrier modulation and the benefit resulting MIMO implementation, and the transmit power. As the final part of the study, the comparison of diversities is discussed, so as to evaluate the potential of the EoTP cable.

The simulation result from the previous section provides three EoTP channel models to investigate in this section, which are:

- *Balanced Cable Model* is the channel data from the simulated one meter CAT7A cable in balanced transmission mode, which consists of four parallel channels.

- *Unbalanced Cable Model* is the channel data from the simulated one meter CAT7A cable in unbalanced transmission mode, which consists of eight parallel channels.

- *Reference Cable Model* is the channel data from the simulated 30 meters CAT7A cable based on the ISO document [9], which consists of four parallel channels.

The performance comparison of single-carrier modulation and OFDM modulation over the EoTP cable is presented in Sec. 4.2. Then MIMO crosstalk cancellation effectiveness is discussed in Sec. 4.3. The impact of transmit power on the theoretical capacity is demonstrated in Sec. 4.4.

4.2. SINGLE-CARRIER VS MULTIPLE-CARRIER MODULATION

Nowadays, the frequency range used in communication systems is much wider than before, where channel frequency selectivity is commonly seen in these systems. Single-carrier PAM modulation has been used in the EoTP transmission with a long history, while other emerging wireline/wireless communication systems are adopting multi-carrier modulation, especially OFDM modulation. In many practical high speed communication systems, OFDM has shown considerable improvement in frequency efficiency.

In this section, the theoretical capacity of the EoTP cable single-carrier (SC) modulation and multi-carrier modulation is evaluated. The channel coding is not considered in this study, because the channel coding gain strongly depends on the code design, which may vary significantly with the implementation detail. For both modulation schemes, some common configuration parameters from 10G BASE-T standard are used as a guidance to evaluate the 40G BASE-T standard [9], and these parameters are used here: the transmit power of $3dBm$, the external noise level of $-150dBm/Hz$, the return loss cancellation C_{Echo} of $55dB$, the NEXT cancellation C_{NEXT} of $28dB$ and the FEXT cancellation C_{FEXT} of $14dB$. The transmit power is assumed to be equally distributed to all the

channels.

The SC capacity is calculated as the information theory bound at a particular frequency, which is defined by the Shannon Theory [41], then multiplied by this frequency. The information theory bound B, in the unit of bit, is defined as follows,

$$B = \log_2(1 + SINR), \tag{4.1}$$

where the SINR is the signal-to-interference-and-noise ratio. The received signal is the transmit signal degraded by the insertion loss, while the interference includes the return loss, the NEXT and the FEXT. As a study of the theoretical capacity, the information bound is computed as a continuous value, not rounded down to the nearest integer, which is usually required for the practical implementation.

OFDM modulation divides the whole frequency band into a number of sub-carriers, which are considered as flat narrow-band. The sub-carrier with large insertion or/and strong crosstalk can carry less information, while the remaining sub-carrier can still provide good channel condition and SINR, in this way the impact of the frequency selectivity is reduced. The parallel information streams from the sub-carriers are assembled into serial OFDM symbols, with the help of the Fast-Fourier-Transform (FFT). The in-depth introduction of the OFDM modulation has been presented in various paper [11, 43, 69], therefore omitted here. The capacity of the OFDM modulated EoTP channel is calculated as the sum of the information theory bound at each sub-carrier, each of which is computed by Eq. 2.3, then multiplied by the symbol rate. The input signal from each sub-carrier into the FFT is already integral, thus not only the continuous capacity, also the discrete capacity is calculated for the OFDM modulation.

One critical configuration parameter in the OFDM modulation is the sub-carrier width and the corresponding number of sub-carriers. In order to achieve the frequency flatness in the sub-carrier, the sub-carrier width should be sufficiently small. If a small width of the sub-carrier leads to a large number of the sub-carriers, which further causes implementation difficulty. For the VDSL2 networks, the total frequency is $0.138 - 30MHz$, and the sub-carrier width is $4.3125kHz$, giving over 3000 sub-carriers depends on the profile. The DOCSIS 3.1 standard has a maximum frequency of $1218MHz$, and the sub-carrier width is $25/50kHz$, giving $7600/3800$ sub-carriers. Comparing the frequency selectivity of the EoTP observed in the channel simulation and the VDSL2 channel in [73] and the DOCSIS channel in [33], the insertion loss fluctuation over the frequency of the EoTP cable is not so severe, therefore the sub-carrier width of the EoTP OFDM modulation is relaxed to $200kHz$, while the total number of the sub-carriers is 8000. This also defines the length of the OFDM symbol to be 8000 OFDM samples (pulses). Then the EoTP OFDM modulation can be implemented though a 8192 point FFT. The DOCSIS 3.1 standard has specified a similar number of $7600/3800$ sub-carriers, therefore such sized FFT will be commercialised with an affordable hardware solution. The $3dB$ transmit power will be equally distributed to the 8000 sub-carriers of each channel, this leads to $-95dBm/Hz$ and $-98dBm/Hz$ power spectral density (PSD) for the balanced and unbalanced transmission, respectively.

For instance, the single-carrier capacity of reference cable without crosstalk cancellation and the OFDM capacity (in bit/s) of unbalanced cable with crosstalk cancellation is calculated as below Eq. (4.2) and Eq. (4.3), respectively:

Table 4.1. The Theoretical Capacity of the EoTP Channel Models

	No Crosstalk Cancellation		With Crosstalk Cancellation		
	SC	OFDM (Continuous)	SC	OFDM (Continuous)	OFDM (Discrete)
Unbalanced Cable DS	10.903	25.451	37.805	76.299	69.830
Unbalanced Cable US	10.600	24.528	37.630	76.265	69.762
Balanced Cable DS	32.150	44.341	64.760	77.330	74.200
Balanced Cable US	34.6838	45.552	65.061	77.652	74.267
Reference Cable	27.8759	49.845	47.696	74.574	71.385

$$Capacity_{SC} = \sum_{Channel=1}^{4} f \times \log_2 \left(1 + \frac{P_{\text{insertion loss}}}{\sum_{\text{other channels}}(P_{\text{crosstalk}}) + P_{\text{return loss}}}\right), \quad (4.2)$$

$$Capacity_{OFDM} = \sum_{Channel=1}^{8} f_s \times \sum_{\text{All sub-carriers}} \log_2 \left(1 + \frac{P_{\text{insertion loss}}}{\sum_{\text{other channels}}(P_{\text{crosstalk}} - C_{FEXT}/C_{NEXT}) + P_{\text{return loss}} - C_{Echo}}\right), \quad (4.3)$$

where $P_{\text{insertion loss}}$ denotes total transmit power for SC modulation and per sub-carrier transmit power for OFDM modulation, respectively. $P_{\text{crosstalk}}$ and $P_{\text{return loss}}$ denote the crosstalk signal power level and the return loss power level, respectively.

The theoretical capacity of the three channel models with the SC and OFDM modulation described above is presented in Table 4.1, the unit is $Gbit/s$. The theoretical capacity with only return loss cancellation but no NEXT or FEXT cancellation is also included. The Reference cable model is symmetric for DS and US, thus only one result listed here.

First of all, the OFDM modulation has considerably outperformed the SC modulation

in all the scenario listed in Table 4.1. Applying no crosstalk cancellation, the three channel models fail to reach the capacity of 40Gbit/s with the SC modulation, while the OFDM modulation helps the balanced channel model and the reference cable model to achieve a capacity over 40Gbit/s, that enhances the capacity of the unbalanced channel model by a factor of 2.5. The robustness of the OFDM modulation under severe channel condition is well demonstrated here.

From Fig. 3.7, the balanced channel model shows a relatively flat insertion loss, where the reference cable models has a fast descending slope over the frequency. In Fig. 3.11 and Fig. 3.13, both channel models have similar FEXT and NEXT curves with a nearly constant gap. Therefore the capacity of the SC reference cable model is more influenced by the frequency selectivity of the insertion loss. When this frequency selectivity is helped by the OFDM modulation, the capacity of the reference cable model is more enhanced, as the balanced channel model suffers more crosstalk than the reference cable model.

When the channel condition is aided by the crosstalk cancellation, the SC capacity of the balanced channel model and the unbalanced cable model is hugely increased, over 260% for the unbalanced channel model, over 90% for the balanced channel model and over 70% for the reference cable model. Again the significance of the crosstalk impact to the short cable is demonstrated here. Also, the OFDM modulation further improves the capacity, so as to help the three channel models to reach a similar capacity.

Discussed in the previous section, the cyclic prefix of the OFDM modulation will be a redundant part of the transmit signal as a prevention of the ISI, where considered as performance loss in the capacity. For the 30 meter cable, the cyclic prefix needs to be at least $30 \times 16 = 480$ OFDM samples, so as to remove the impact of ISI. This means that

the OFDM modulation will lose about $\frac{480}{8000+480} \simeq 6\%$ of the capacity. This is still lower than the typical cyclic prefix of 10% or even 15% in the wireless communication systems. With this much capacity loss, the theoretical capacity of the OFDM modulation is still better than that of the SC modulation.

Then the key observation from Table 4.1 is the enhanced theoretical capacity of the OFDM modulation, with respect to the current SC modulation.

Not only, is it worth considering other benefits of the OFDM modulation. For example, one attractive advantage of the OFDM modulation is to allow convenient frequency-domain channel equalisation, while the time domain channel equalisation of the SC modulation schemes leads to very high computational complexity.

The main issues of the OFDM modulation, e.g., the doppler shift sensitivity, the frequency synchronisation and the peak-to-average-power ratio (PAPR) problem, have more impact for the wireless/mobile communications system, while these issues are relatively easier to address in the wireline communication with time-invariant channel and relaxed transceiver design restrictions.

The unbalanced channel models have not shown particularly desirable theoretical capacity, due to the increased crosstalk from the increased crosstalk sources. The potential of the extra channels of the unbalanced channel model and the crosstalk cancellation is discussed in the following part as an enhancement to the effectiveness of the MIMO implementation.

4.3. THE CROSSTALK CANCELLATION THROUGH MIMO

As one of the revolutionary concepts invented in the field of the communication theory, the multiple-inpu-multiple-output (MIMO) technique has been rapidly applied to many state-of-the-art communication system, so as to boost the capacity of the systems. There has been some early research work on incorporating the MIMO technique into the EoTP system [78, 79]. Due to the immaturity of the MIMO itself and the underdeveloped MIMO implementation solution at that stage, the current EoTP standards have not yet introduced MIMO technique into practice.

The natural advantages of the EoTP system to adopt MIMO include the same transceiver chip to handle all the channels at each end of the transmission, the relatively time-invariant channel (compared with wireless channels) to provide reliable channel state information. The full-duplex MIMO channel model for the balanced and the unbalanced channel models have been introduced in Sec. 3.3 and Sec. 3.5. Not only with the current SC modulation, MIMO technique can also be applied with the OFDM modulation [80].

The goal of adopting MIMO is to multiply the capacity of the EoTP cable. Ideally, the theoretical capacity of the MIMO system can be achieved by performing singular value decomposition (SVD) precoding at both the transmitter and the receiver [81], also allocating the transmit power in a water-filling fashion [41]. This is also equivalent to an interference-free transmission.

The practical expectation from MIMO is to mitigate the interference within the cable, i.e. the return loss, the NEXT and the FEXT. In the 10G BASE-T standard [8], a set of parameters are specified for the cancellation, which are the return loss cancellation $CR = 55dB$, the NEXT cancellation $CN = 28dB$ and the FEXT cancellation

$CF = 14dB$. Generally speaking, the return loss and the NEXT cancellation can be realised with analogue circuit with considerable performance, plus the digital signal processing to achieve higher performance. The FEXT cancellation mostly depends on digital signal processing. A few candidate techniques are available for FEXT cancellation, which are linear/non-linear precoding at the transmitter, decision feedback equaliser (DFE), minimum mean-square error (MMSE) detection at the receiver.

To design a specific MIMO implementation for the EoTP channel models with desirable performance will be another complete piece of research work, which involves algorithm selection, parameter definition and tuning, etc. Therefore the study here focuses on the potential of the EoTP channel models with benefit from a virtual MIMO implementation. In other words, the area of interest of this study is to investigate the theoretical capacity enhancement of the MIMO efficiency, where the MIMO is interpreted as the crosstalk cancellation performance. By investigating the relationship between the potential capacity and the crosstalk cancellation performance, a guideline for the design of the MIMO implementation can be obtained.

The two types of the crosstalk, namely the near-end crosstalk NEXT and the far-end crosstalk FEXT, result in capacity loss with the unequal levels. In Fig. 4.1, the FEXT cancellation is considered as a constant $CF = 14$, as specified in 10G BASE-T [8]. Then the OFDM theoretical capacity is plotted as a function of the NEXT cancellation, between $0dB$ and $100dB$, where the theoretical capacity is calculated with CN of $1dB$ step. At the beginning, the three channel models start with slightly different theoretical capacities, which increases rapidly with the NEXT cancellation. After the NEXT cancellation reaching about $35dB$, the theoretical capacity is stabilised with little improvement.

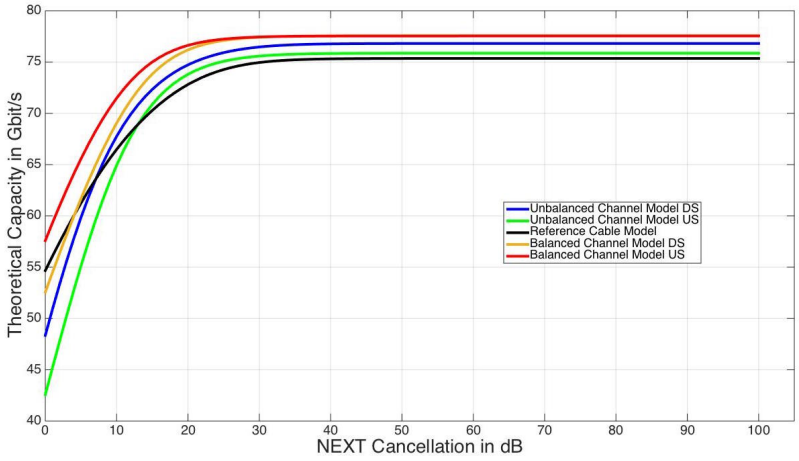

Fig. 4.1. The OFDM Theoretical Capacity Versus the NEXT Cancellation

As specified in 10G BASE-T [8], the NEXT cancellation is considered as a constant $CN = 28$. In Fig. 4.2, the OFDM theoretical capacity is plotted as a function of the FEXT cancellation, between $0dB$ and $100dB$, where the theoretical capacity is calculated with CF of $1dB$ step. Here the behaviour of the FEXT cancellation is not the same as the NEXT cancellation. The reference cable models starts with acceptable theoretical capacity, which shows limited improvement with increased NEXT cancellation. The other two channel models have relatively low capacity at first, where the capacity is significantly improved with NEXT cancellation. The unbalanced channel models shows dramatic capacity boost with more FEXT cancellation, also reaches over $160Gbits/s$. The stable level are approached at $40dB$ for the balanced channel model and $50dB$ for the unbalanced channel model.

From Fig. 4.1 and Fig. 4.2, a ”ceiling” of the OFDM theoretical capacity is observed, when keeping one of the FEXT or the NEXT cancellation as per the 10G BASE-T standard, and increasing the other one. With the current $28dB$ NEXT cancellation, a large

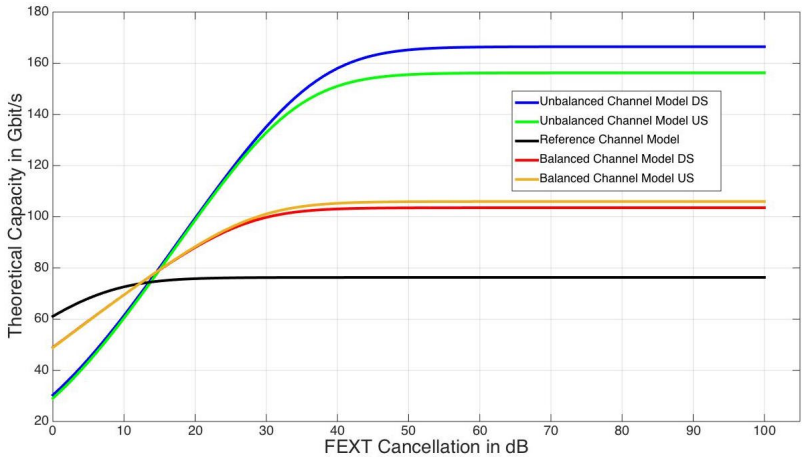

Fig. 4.2. The OFDM Theoretical Capacity Versus the FEXT Cancellation

proportion of the NEXT cancellation improvement can be obtained for both three channel models. The FEXT shows a mild impact on the reference channel model, the unbalanced and the balanced channel model are very beneficial from the FEXT cancellation. The theoretical capacity of the SC modulation is more degraded by the crosstalk, where the effectiveness of the crosstalk cancellation should be similar, therefore the discussion on the SC modulation is omitted in this part.

Taking another view on this problem, assuming either the FEXT or the NEXT was mostly removed, the relation between theoretical capacity and the residual of the other crosstalk also shows the potential of the channel models with the crosstalk cancellation. In Fig. 4.3, the FEXT cancellation is set to $50dB$ as a FEXT-free scenario, at which the capacity reaches the ceiling in Fig. 4.2, then the theoretical capacity is plotted for both OFDM and SC modulations with the NEXT cancellation as variable. Considering the clarity of the graph, only the DS data is plotted. The OFDM modulation again outperforms the SC modulation for all three channel models. The reference cable model has

the least impact from the FEXT, also similar maximum capacity with only $14dB$ FEXT cancellation in Fig. 4.2. The balanced channel models shows over $100Gbit/s$ capacity for both OFDM and SC modulations, where the gap between the two modulation options is smaller than the other two models. The unbalanced channel models shows great potential and sensitivity against the FEXT. With the standard specified $28dB$ NEXT cancellation, a good FEXT cancellation can boost the capacity to roughly $120Gbit/s$ and $160Gbit/s$ for the SC modulation and the OFDM modulation, respectively. When both FEXT and NEXT largely removed, the unbalanced channel model can ultimately reach a theoretical capacity of almost $200Gbit/s$ with OFDM modulation.

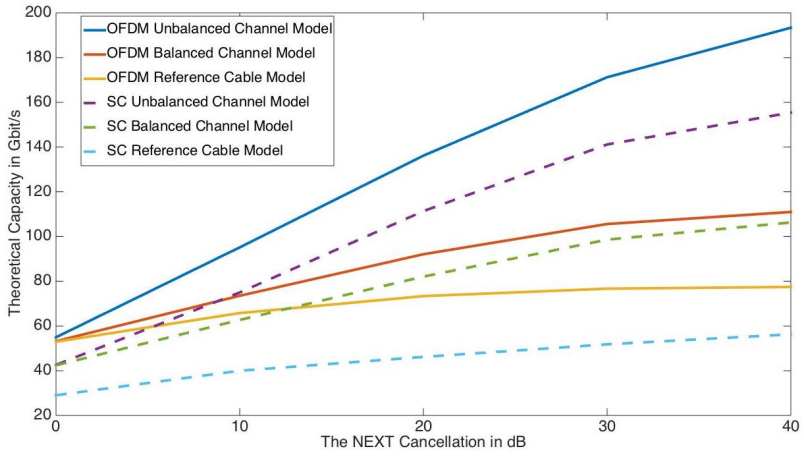

Fig. 4.3. The FEXT-free Theoretical Capacity Versus the NEXT Cancellation

Similarly, in Fig. 4.4, the NEXT cancellation is set to $40dB$, while the FEXT cancellation is the variable. The observation is basically identical to that of Fig. 4.3 for the balanced channel model and the reference cable model. However, with the standard specified $14dB$ of FEXT cancellation, the achieved capacity of the three models is lower than that of Fig. 4.3. For the unbalanced channel model, although the the theoretical capacity

reach the same level as in Fig. 4.3 in the end, the growth speed is much slower with the increasing NEXT cancellation.

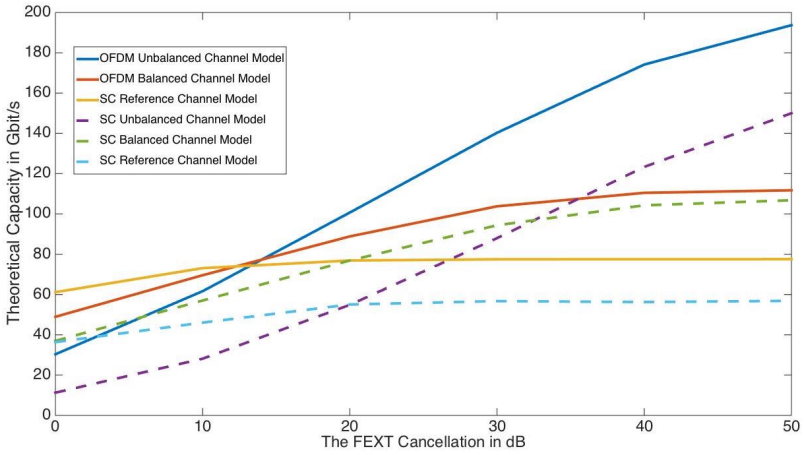

Fig. 4.4. The NEXT-free Theoretical Capacity Versus the FEXT Cancellation

4.4. THE IMPACT OF THE TRANSMIT POWER

From the Shannon formula, Eq. (4.1), for a given channel, the capacity is a non-decreasing function of the transmit power. Also, due to the nonlinearity of the logarithm function, the growth of the channel capacity gradually starts with a slope and eventually stops at the maximum channel capacity, with respective to the transmit power.

In a realistic communication system, there are various factors to restrict the transmit power into the channel. For instance, the power supply, battery life, the front-end amplifier and electromagnetic compatibility (EMC) requirement. In the system design, the transmit power is thus usually a trade-off between the low transmit power and the desired performance metric.

In order to determine the optimal transmit power range for the EoTP transmission, the

relation between the transmit power and capacity is investigated in this section. The experiment setting is identical to the specification of 10G BASE-T, i.e., the external noise level of $-150dBm/Hz$, the return loss cancellation of $55dB$, the NEXT cancellation of $28dB$ and the FEXT cancellation of $14dB$. The three channel models as in the previous sections are investigated here. Without losing generality, only OFDM modulation is considered. The transmit power ranges from $-20dB$ to $30dB$, then the corresponding theoretical capacity is demonstrated in Fig. 4.5.

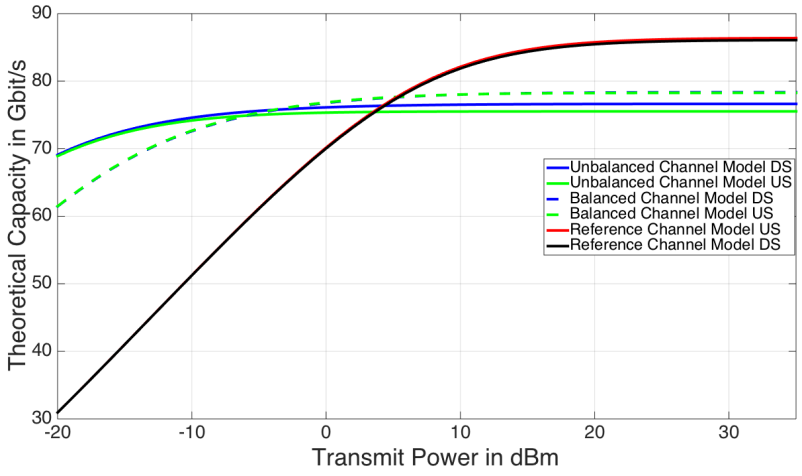

Fig. 4.5. The EoTP Theoretical Capacity Versus the Transmit Power

In Fig. 4.5, the stable transmit power level for the three channel models are approximately $0dBm$ for the unbalanced channel model, $5dBm$ for the balanced channel model and $15dBm$ for the reference channel model. They approach most of their maximum capacity at least $5dB$ below the stable transmit power level. With a $3-5dBm$ transmit power, all three channel models have satisfactory capacity of over $70Gbit/s$. Hence this $3-5dBm$ is suggested as the transmit power upper bound for the EoTP transmission, or could be even lower for the short distance transmission.

The reference channel model (the 30 meter cable) is observed to be more sensitive to the transmit power, compared with both channel models of the short cable. The reason is that the insertion loss of the reference channel model is much higher than the other two channel models, also the resulting SINR falls mostly in the slope region of the logarithm.

From the conclusion of the previous sections, the theoretical capacity of the balanced and unbalanced channel model is more limited by crosstalk, especially the unbalanced channel model. Therefore the unbalanced channel model shows the best capacity with low transmit power, while the other two gradually takes over. In the end, the reference channel model slightly outperform the other two with less crosstalk and relatively stronger desired signal by increased transmit power. In future short distance EoTP, e.g., within a few meters, as may be expected in data centres, the transmit power should be considered to reduce from the $3dBm$ of the 10G BASE-T standard.

4.5. SUMMARY

Throughout the study of the theoretical capacity in this section, the following key observations are obtained:

1. OFDM modulation outperforms the current SC modulation in terms of the theoretical capacity of the channel models, especially the frequency selectivity of the reference cable model is well managed.

2. The channel improvement from the MIMO implementation results in a significant boost to the theoretical capacity, such that the EoTP cable could reach a theoretical capacity of almost $200Gbit/s$. With such a theoretical capacity, a future short reach

EoTP transmission of $100Gbit/s$ might be expected.

3. The balanced and unbalanced channel models, i.e., the short cable model, are crosstalk-limited. If the crosstalk is not properly handled, the performance of the short cable is not necessarily better than the 30 meter cable.

4. The unbalanced channel model shows great potential, together with OFDM modulation and MIMO, it reaches the highest theoretical capacity in the study. Its main bottleneck is the FEXT.

5. The reference channel model is more sensitive to the transmit power, because of the relatively higher insertion loss than the other two channel models.

6. Due to the high crosstalk level and the relatively low insertion loss, the transmit power for future short distance EoTP transmission should be considered to be reduced from the $3dBm$ of the 10G BASE-T standard.

With these key observations, the potential of the balanced and unbalanced channel models are thoroughly studied with different perspectives. The single carrier PAM modulation and multi-carrier OFDM modulation are compared, where OFDM shows considerable capacity enhancement under the EoTP cable frequency-selective channel. The Effectiveness of MIMO crosstalk cancellation is evaluated as well. The crosstalk limited balanced and unbalanced channel models are more beneficial than the reference channel model, moreover, the theoretical capacity can be significantly improved towards $200Gbit/s$. The impact of the transmit power is examined, that for the short distance EoTP transmission the transmit power can be reduced.

Chapter 5

Phantom Mode Transmission

5.1. INTRODUCTION

The number of physical channels over EoTP cable has been extended from 4 to 8 by adopting unbalanced transmission. Thanks to the multi-conductor line nature of the EoTP cable, not only physical channesl can be created, but also virtual channels can be created through phantom mode transmission.

In a transmission line system with multiple balanced lines, the phantom mode transmission transmits the (phantom) balanced signal over a pair of balanced lines. Such excitation circuit is defined as phantom circuit. Combinatorially, a system with n balanced lines can construct up to $2n-1$ channels. Since the phantom signal fed into each balanced line is identical to the two conductors, the balanced transmission within each balanced line is preserved.

The concept of the phantom mode transmission was invented and applied in the early age of telecommunication, however it soon dropped out of usage due to the high crosstalk

and severe performance degraded by the impedance mismatch. Phantom mode transmission is currently used as DC power supply method for professional condenser microphone [82].

Recently, phantom mode transmission has found new application in the area of VDSL2 networks, in [83–86]. This application takes the advantage of multiple telephone cables to the same VDSL2 user. For instance, if two pairs of telephone cables (quad cable) serve the same household, the two pairs can provide two parallel channel and one phantom channel. This could also be extended to more than two cables, depends on the available cable configuration. The technical novelty behind the phantom mode transmission re-adoption is the extra impedance compensation circuit [87], with DSP based crosstalk cancellation (vectored VDSL2). The trade-off is that the phantom mode gain exceeds the negative impact of the increased crosstalk. As a result, a considerable data rate performance improvement has been demonstrated in the VDSL2 networks by Huawei and Alcatel-Lucent [88, 89].

In this chapter, the phantom mode transmission over EoTP cable is discussed. For simplicity, no impedance matching compensation circuit is considered. Only one level phantom mode is studied, where the twisted pairs are used just for one phantom channel, which results in two extra phantom channels. The insertion loss and the crosstalk impact of the phantom channels are examined through the similar CST cable modelling and simulation in the previous chapters.

The concept and design of the phantom mode transmission over EoTP cable is introduced in Sec.5.2. The channel models simulation result and the corresponding theoretical capacity are presented in Sec.5.3.

5.2. PHANTOM MODE TRANSMISSION OVER EOTP CABLE

The EoTP cable is constructed with four twisted pairs as four balanced lines, forming four parallel channels. With the co-located transceiver of the four twisted pairs, the phantom mode transmission can be conveniently implemented by simply feeding the phantom signal. Aiming at investigating the potential of the phantom mode transmission over the existing EoTP infrastructure, extra transceiver component circuit or hardware structure modification is not considered here. Hence there is no impedance matching circuit, also phantom signal excitation source is directly attached to the twisted pairs.

When each two twisted pairs are used as one conductor, three phantom channels can be generated. If all the three phantom channels are configured, each twisted pair will be excited by the original balanced signal and two phantom signals, coupled with two phantom channels. For better understanding the interaction between the phantom channels and the original balanced channels, only two orthogonal phantom channels are configured. In this way, the signal over each twisted pair will be its own balanced signal and one phantom signal. The circuit diagram of the phantom circuit on the EoTP cable is demonstrated in Fig. 5.1.

The twisted pairs of the EoTP cable have different twisting rates, therefore the impedance and other EMC parameters of the twisted pairs are not identical to each other. This also results in variation of insertion loss and crosstalk between the twisted pairs, as seen in the simulation result in Sec. 3.6. Hence, the phantom channels of the EoTP cable are operated over flawed balanced lines.

In principle, each single twisted pair is designed to be a balanced line. However, due to manufacturing imperfection and other practical restrains, the two conductors of the twisted

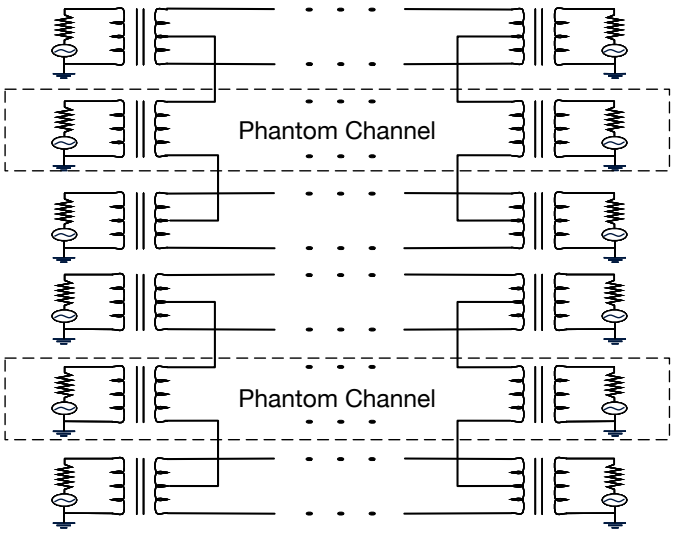

Fig. 5.1. The Circuit Diagram of the Phantom Mode Transmission Over EoTP Cable

pair can not be ideally balanced, therefore there is always an impedance mismatch between them. The imbalance between the two conductor is further altered by the phantom circuit, intuitively, not improved. Moreover, the impact of the phantom circuit is also increased by the very closed coupling distance, due to the compact size of the EoTP cable. The resulting crosstalk performance is of research interest here, which is investigated through simulation in the next section.

With these two phantom channels, there are two phantom ports at each end of the EoTP cable, defined as in Fig. 5.2. On the top of the existing crosstalk between the balanced channels, the phantom channel to balanced channel and the phantom channel to phantom channel crosstalk are introduced. Note that, these newly introduced phantom crosstalk is not linearly added to the existing balanced transmission, as the phantom circuit may alter the coupling between the balanced channels as well.

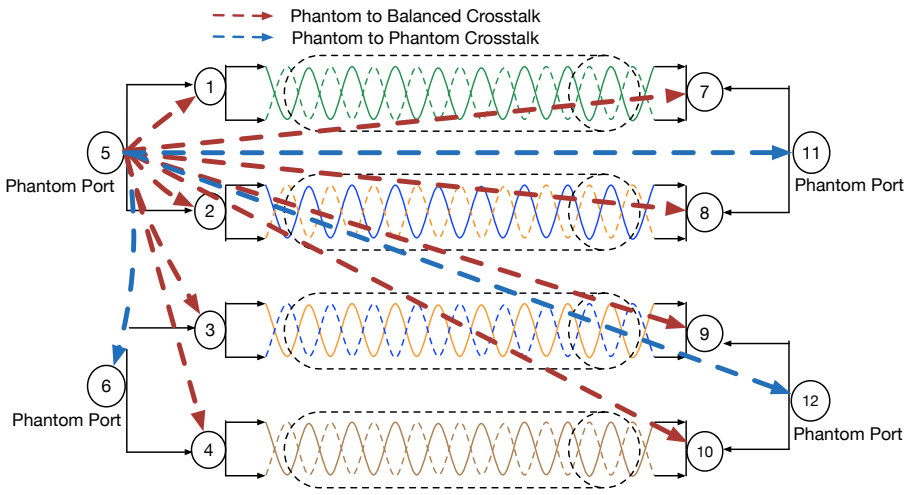

Fig. 5.2. The Crosstalk of the Phantom Mode Transmission Over EoTP Cable

The phantom mode transmission over EoTP cable forms a 6×6 MIMO system, which can be characterised by extending the channel model of the balanced transmission Eq. (3.1) and Eq. (3.3). The channel performance and the theoretical capacity of the phantom mode transmission will be studied in the next section.

5.3. SIMULATION RESULT

5.3.1. Insertion Loss and Return Loss Performance

The simulation method and cable specification of the phantom mode transmission channel is similar to the simulation in Sec. 3.6.1, where two phantom ports are added to each end of the one meter CAT7A cable. The impedance of the phantom port is 50ω, while the impedance of the balanced port is 100ω.

Note that the port in the software modelling is a virtual element without occupying any space, which is connected to the circuit by wires without occupying any space. Therefore

the attaching tip of the wire to the circuit may cause further imperfection, depending on the chosen point on the circuit.

The downstream and upstream insertion loss of the phantom mode transmission over EoTP cable is illustrated in Fig. 5.3 and Fig. 5.4, respectively. The port $5, 6, 11, 12$ are phantom ports, as defined in Fig. 5.2, then the corresponding S-parameters are the insertion loss of the phantom channels, where the rest are the insertion loss of the balanced channels.

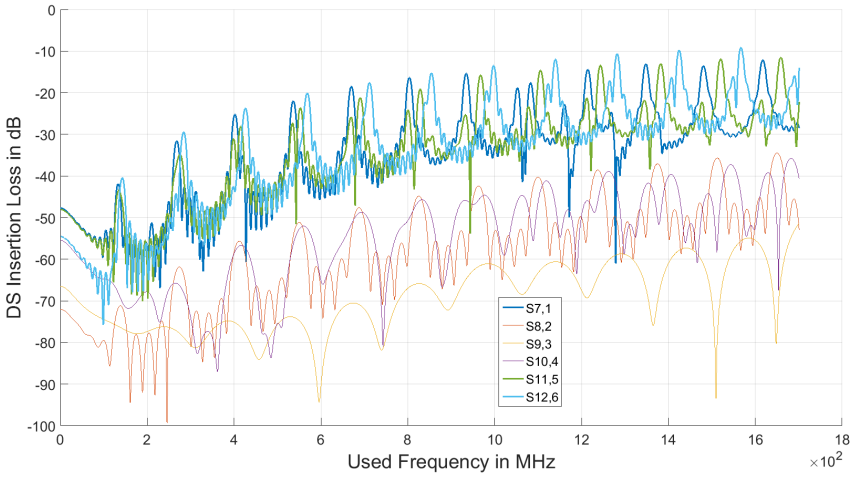

Fig. 5.3. The Downstream Insertion Loss of the Phantom Mode Transmission Over EoTP Cable

Compared with the balanced or unbalanced transmission over the same cable, the insertion loss is significantly degraded for all the channels in phantom mode. Intuitively, the desired signal will be severely attenuated and a very poor data rate is to be expected. Another distinct observation is that the insertion loss of the low frequency is worse than that of the high frequency. These facts are caused by the hugely changed circuit structure of the EoTP cable.

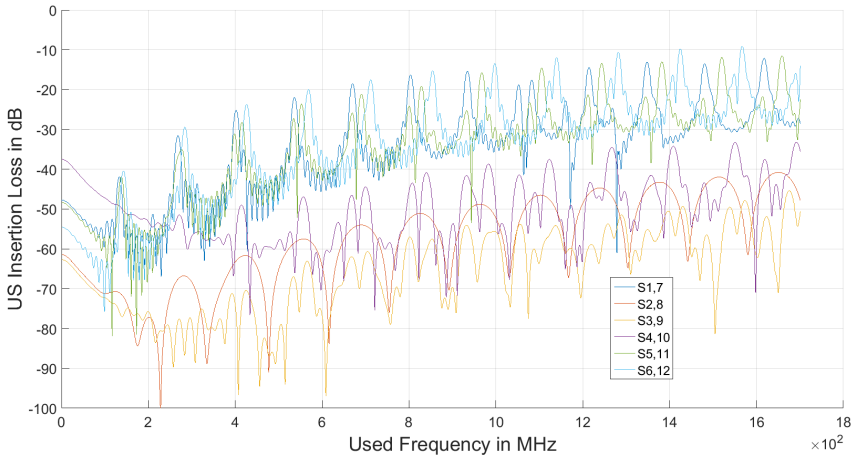

Fig. 5.4. The Upstream Insertion Loss of the Phantom Mode Transmission Over EoTP Cable

The phantom channels have shown lower insertion loss than most of the balanced channels, which means that the imbalance of the twisted pairs are further enlarged by the phantom circuit.

The return loss of the phantom mode transmission over EoTP cable is presented in Fig. 5.5. The return loss of all the channels are close to $0dB$, which means most of the transmit power is reflected back at the excitation source. This indicates a very severe impedance mismatch. The return loss unacceptably exceeds the CAT7A specification, defined in [3], which will generate enormous interference to the signal transmission.

5.3.2. Crosstalk Performance

The S-parameter of the balanced port 1 and 2 is demonstrated in Fig. 5.6 and Fig. 5.7, respectively. Under the impact of phantom circuit configuration, the insertion loss is at very similar level as the crosstalk, the crosstalk interference will hence be more damaging than the balanced and unbalanced transmission.

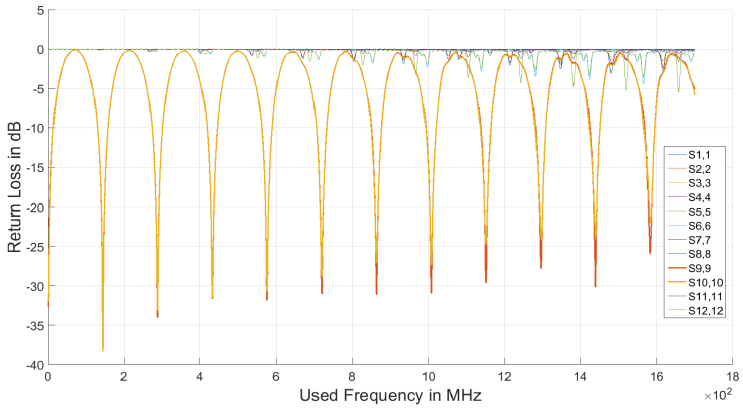

Fig. 5.5. The Return Loss of the Phantom Mode Transmission Over EoTP Cable

The two ports have a common observation that the crosstalk channel, for both NEXT and FEXT, within the phantom circuit coupled ports, i.e., the port $1, 2, 5, 6, 7, 8, 11, 12$, are stronger than that of the other ports which are not coupled by the phantom circuit. The difference between these two groups is roughly $20dB$. So similar to the inter-pair and intra-pair crosstalk phenomenon in the unbalanced transmission, there is an inter-phantom and intra-phantom phenomenon in the phantom mode transmission.on the impedance match of the intra-phantom circuits.

If the twisted pair is used in more than one phantom channel, the crosstalk coupling will be obviously increased, as more of the relatively strong intra-phantom crosstalk will be introduced. Also, the design of the impedance matching compensation circuit should focus on the intra-phantom impedance matching.

in Fig. 5.8 and Fig. 5.9, the S-parameter of the phantom port 5 and 6 is displayed, respectively. Like the balanced ports, the insertion loss curves of the phantom ports are blended in the crosstalk curves. The difference between the inter-phantom and intra-

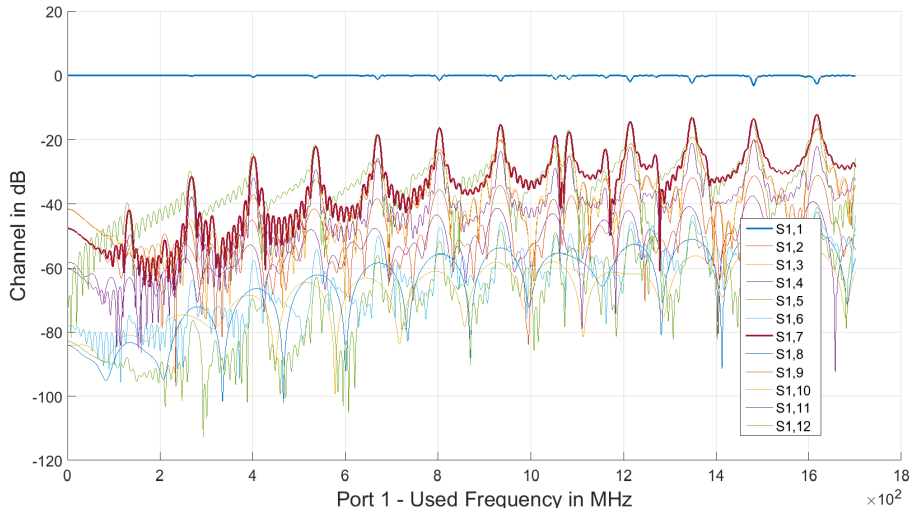

Fig. 5.6. The Port 1 S-parameter of the Phantom Mode Transmission Over EoTP Cable

phantom crosstalk is observed as well.

Generally speaking, the channel characteristics of the phantom channel and the balanced channel are similar, due to the strong intra-phantom coupling.

The other ports have similar results, therefore omitted here.

5.3.3. The Theoretical Capacity

The channel S-parameter obtained from the simulation is used to construct the numerical MIMO channel for the phantom mode transmission. As a fair comparison, the theoretical capacity is evaluated using the same specification as the 10G BASE-T, which include the external noise level of $-150dBm/Hz$, the return loss cancellation of $55dB$, the NEXT cancellation of $28dB$, the FEXT cancellation of $14dB$ and the transmit power of $3dBm$ for the six channels on each side.

With these parameters, the theoretical capacity is calculate with the same method

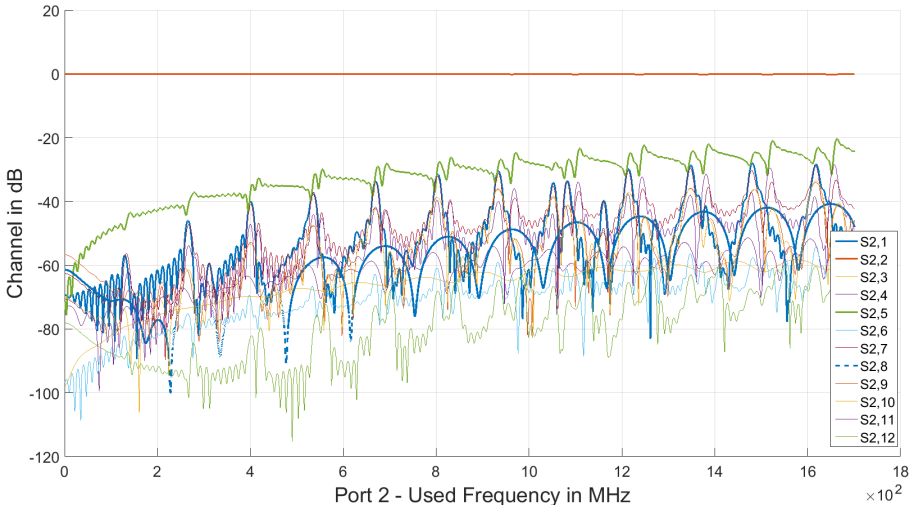

Fig. 5.7. The Port 2 S-parameter of the Phantom Mode Transmission Over EoTP Cable

as in [9], where all balanced channels and phantom channels are used in each direction. The resulting theoretical capacity for the downstream and upstream transmission is $15.7332 Gbit/s$ and $15.3359 Gbit/s$, respectively. Under balanced transmission, the theoretical capacity of the 30 meter long CAT7A cable can is $85 Gbit/s$. On the opposite of the expectation of improved performance, the capacity of the phantom mode transmission is far from satisfactory.

This capacity is a reflection of the severely degraded insertion loss and the elevated return loss and crosstalk level. Not only do the extra phantom channels not provide extra capacity increase, but the balanced channels of each single twisted pair is also damaged. Clearly, the impedance mismatch introduced by the phantom circuit is the main cause of this performance collapse.

The impedance match issue is also the main technical concern of the VDSL2 phantom mode transmission [83, 87]. Hence the potential of the phantom mode transmission

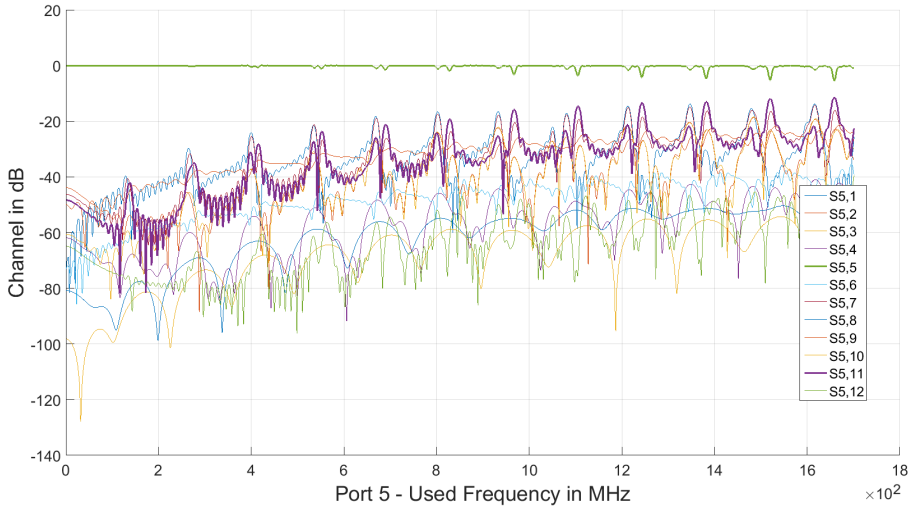

Fig. 5.8. The Port 5 S-parameter of the Phantom Mode Transmission Over EoTP Cable

over EoTP cable, as the virtual channel diversity to exploit, should be properly investigated if the impedance match is addressed. Moreover, this will require further structure modification on the existing hardware, which can be an interesting research topic for the future.

The conclusion in the part of research is that due to the impedance mismatch problem, the direct attached phantom circuit to the EoTP cable cannot improve the capacity through the created phantom channels. Furthermore, it can even severely degrade the balanced transmission channels of the twisted pairs.

5.4. SUMMARY

In this chapter, the phantom mode transmission over EoTP cable was studied. To avoid hardware modification, direct attached phantom circuit was proposed, which forms two phantom channels. Each twisted pair was only used by one phantom circuit, thus the

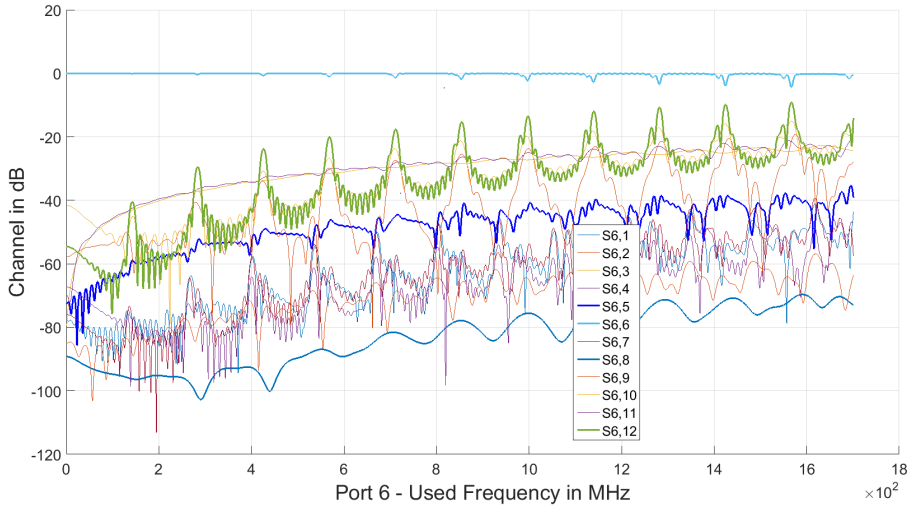

Fig. 5.9. The Port 6 S-parameter of the Phantom Mode Transmission Over EoTP Cable

phantom channel were orthogonal to each other. With the new phantom channels, the EoTP MIMO channel was extended to a dimension of 6×6. However, the channel simulation showed severely degraded insertion loss and the elevated return loss and crosstalk level, due to the impedance mismatch introduced by the phantom circuit. The resulting capacity was hugely decreased, opposite to the expectation of improved performance. The impedance match could be a critical issue for the performance of the phantom mode transmission.

Chapter 6

Smoothed Scheduling Algorithms in VDSL2 Networks

The course of true love never did run smooth. - William Shakespeare [1] [2]

6.1. INTRODUCTION

Digital subscriber line (DSL) is the predominant wireline broadband access technology, which is also widely deployed over the existing twisted pair cable based telephone network infrastructure [12, 13]. The performance of DSL networks is, however, severely degraded by crosstalk, i.e., the electromagnetic coupling between copper lines in the same cable binder. The presence of crosstalk couples the data transmission of the individual DSL lines, thus transforms the DSL access network into a challenging interfering multi-

[1] Part of work in this Chapter was developed in KULeuven, under the supervision of Professor Marc Moonen.

[2] For the full content of this chapter, please contact the author.

user transmission environment. By coordinating the allocation of physical layer resources to the interfering DSL lines, i.e., DSL modems or users, the impact of crosstalk can be mitigated and the users data rate performance can be spectacularly increased [90, 91]. More specifically, dynamic spectrum management (DSM) techniques have been developed to mitigate the crosstalk problem through spectrum coordination [14–16, 40, 92, 93], or through signal coordination [5, 17, 18, 94]. Recent application of these techniques in practical prototypes has demonstrated a huge potential, enabling data rates of up to 300 Megabits per second over just two DSL copper pairs [5]. Spectrum coordination, also known as spectrum balancing, optimises the transmit spectra of interfering DSL users, so as to effectively minimise the impact of the crosstalk. Alternatively, signal coordination removes the impact of crosstalk by using joint signal processing on co-located transmitted or received DSL signals.

Considerable research on crosstalk mitigation techniques has been devoted to the maximisation of physical layer transmit rates. Next to these standard objectives, other Quality of Service (QoS) objectives should also be considered. For instance, delay performance is a very important objective for different broadband scenarios: the impact of transmission delay on delay-sensitive applications in next generation access networks, e.g., IPTV and online gaming, is studied in [95, 96].

Existing DSL physical layer optimisation (DSM) techniques generate a static resource allocation, for instance, statically allocating transmit power and/or computational complexity to the individual users. These techniques focus on basic physical layer metrics, such as transmit rates and transmit power for the individual users. One shortcoming of such static allocation is that users are assumed to have an infinite data workload. This is

however not true in practice, where users indeed have a finite data workload, i.e., the data that user is about to transmit. Furthermore, when a user has no data to transmit, it should be allocated with as few resources as possible. A static system model does not allow the study of network throughput statically and of delay performance. A general dynamic resource allocation (DRA) framework for the layered network system model has been studied, where all the network node are extended with finite data queues [19, 20, 97, 98]. The basic Max-Weight Scheduling (MWS) algorithm has also been introduced to the DSM techniques, which aims at improving the QoS performance and preventing transmission stall in the DSL networks [23, 24].

Consider an N user interference-limited and time-slotted one-hop network instead of a general network, which could well represent N 4G phones in the same cell, or N VDSL2 users in the same cable bundle. Two open issues emerge when MWS is implemented in a practical system. Firstly, the DRA is realised through frequent hardware re-configuration, which requires either a signalling channel or signalling overhead. Secondly,limited to the transmission stability, the delay performance, i.e., the average queue lengths, is not optimised by MWS.

Motivated by the these open issues of signalling overhead and delay performance, this chapter proposes a smoothed MWS, with the guaranteed transmission stability of MWS ,with shorter queue lengths and a smoother DRA behaviour. Theoretically, fluctuation in the input of a queueing system amplifies the variation in the output, therefore degrades the performance [99]. With the help of the time series smooth filtering on queue length history, the queue length of the previous time slot(s) is taken into account, so as to smooth the weight in DRA.

Chapter 7

Virtual User Assisted Autonomous Spectrum Balancing for VDSL2 Networks

[1] [2]

This chapter presents a set of virtual user assisted autonomous spectrum balancing for VDSL2 networks, which can improve the data rate and QoS performance simultaneously in an autonomous and low-complexity fashion. The existing autonomous SB algorithms are reviewed in Sec.7.1. Then the proposed algorithms are presented in Sec. 7.2. The stability proof of the proposed algorithms is given in Sec. 7.3. Finally the simulation result demonstrate the performance of the proposed algorithms in Sec. 7.4.

[1] Part of work in this Chapter was developed in KULeuven, under the supervision of Professor Marc Moonen.

[2] For the full content of this chapter, please contact the author.

Chapter 8

Conclusions and Future Work

I think and think for months and years. Ninety-nine times the conclusion is false. The hundredth time I am right. - Albert Einstein

The goal of this thesis was to improve the performance of the twisted pair based network, including to investigate the potential of the Ethernet over twisted pair cable and to enhance the quality of service in the DSL networks, by exploiting conductor diversity, modulation diversity, virtual channel diversity, data time series diversity and virtual network diversity. This chapter summarises the key results of the thesis and suggests topics for future work.

8.1. CONCLUSION OF THE THESIS

The copper twisted pair cable has been one of the most common physical communication media, widely used as in the structured Ethernet cable and in the massive cable bundles of the telephone networks.

Part I of this thesis investigated the potential of the Ethernet over twisted pair cable for the next generation Ethernet transmission. The goal is to achieve higher spectrum efficiency over the existing EoTP cabling infrastructure, also investigate the possibility of next generation EoTP transmission beyond the 40G BASE-T standard. The EoTP evolution was previously realised through straight-forward and mostly incremented approaches, which are no more feasible due to the severe frequency selectivity of a twisted pair channel.

The current channel models represents the EoTP cable as four parallel SISO channels. Chapter 3 revisited the structure of the EoTP cable, then re-formulated the EoTP cable as an 4×4 MIMO full-duplex channel model for the balanced transmission. As a diversity mechanism in conductor structure, unbalanced transmission with single-ended excitation was proposed and modelled as an 8×8 MIMO full-duplex channel model for. These advanced channel models are capable of accommodating other performance promising transmission techniques. A one meter long CAT7A cable was simulated, so as to evaluate the direct channel performance and crosstalk coupling level for both balanced and unbalanced transmission. The one meter cable showed as more crosstalk dominant with respect to the reference 30 meter long cable, with both decreased insertion loss and increased crosstalk. The breakdown of the unbalanced transmission also revealed the difference between the intra-pair crosstalk and the inter-pair crosstalk.

Chapter 4 took the S-parameters from the channel simulation in Chapter 3, to construct three realistic channel model, so as to evaluate the theoretical capacity of the EoTP cable under alternative transmission techniques. The multi-carrier OFDM modulation scheme considerably outperformed the inherited single carrier PAM modulation, thank to its im-

proved frequency efficiency in frequency selective channel. As a further step, the possible MIMO crosstalk cancellation also demonstrated significantly theoretical capacity enhancement, which was more spectacular for the crosstalk dominant one meter cable with over $100Gbit/s$ capacity. Benefitted from the increased number of the channels, the unbalanced channel model could achieve a theoretical capacity of nearly $200Gbit/s$. The impact of transmit power for the OFDM based EoTP transmission was discussed through numerical simulation of the theoretical capacity. Not only increasing the transmit power barely improves the theoretical capacity, a reduced transmit power can also achieve satisfactory result.

Chapter 5 initiated the channel performance study of phantom mode transmission over the EoTP cable. A direct attached phantom circuit was proposed to create two orthogonal phantom channels, which do not share any twisted pair in their phantom circuits. For simplicity, the impedance compensation circuit was not considered here. By this configuration, the coupling of the phantom circuit could be exhibited clearer. In the channel simulation, the phantom channel and the existing balanced channel showed degraded insertion loss and severely elevating return loss. The crosstalk was also increased, what the intra-phantom crosstalk was stronger than the inter-phantom crosstalk. The poor channel performance was caused by the direct attach phantom circuit, which introduced large amount of undesired coupling between the conductors. Despite two extra phantom channels, the resulting capacity is much declined, due to the poor channel performance.

Part I of the thesis exploited the conductor structure diversity, modulation diversity and the virtual channel diversity of the EoTP cable, then the proposed unbalanced transmission, OFDM modulation and MIMO crosstalk cancellation can realise an over $100Gbit/s$

theoretical capacity. The research result can serve well as the theoretical guideline for the OFDM based next generation Ethernet over twisted pair cable.

Part II of this thesis developed advanced dynamic resource allocation algorithms for the signal coordination and spectrum balancing in the VDSL2 networks.The goal is based on the existing dynamic resource allocation algorithms, which focuses on the transmission stability as the basic metric, to improve the delay performance in general, to reduce the signalling communication demand of the centralised signal coordination and to realise autonomous spectrum balancing for VDSL2.

Chapter 6 proposed smoothing the Max-Weight scheduling in dynamic resource allocation by time series smooth filters can be used to improve the delay performance and reduce the signalling communication demand. Two typical smooth filters, namely simple moving average filter and weighted moving average filter, were evaluated which are both able to smooth the dynamic resource allocation and preserve the transmission stability. Through theoretical analysis, the smoothed MWS was proven to guarantee the transmission stability, regardless of the parameter of the smooth filter. In the simulation, the signalling communication demand was declined and the stability remained intact.

Chapter 7 developed a set of autonomous spectrum balancing algorithms have been proposed to improve the users experience of VDSL2 upstream service. With the consideration of no information exchange between the users in the upstream service, the users transmit power spectra is optimise locally in a virtual network with MWS algorithm. A simple method to define the strongest and the weakest virtual users of the virtual network was proposed, which reflects the impact of the crosstalk and the queueing status of other real users. This small sized virtual network also ensured a low computational complex-

ity. Three algorithms, denoted by VASB-(1-3), to update the virtual queue length were presented, which locally determine the weight of the virtual users in the virtual network, so as to represent the queueing status of the other real users. A theoretical framework of MWS stability with general sub-optimal resource allocation was developed, then applied to analyse the stable condition of virtual network in VASB- (1-3). Finally the performance enhancement from the autonomous resource allocation was discussed, also the minimum throughput region with minimum transmit power was proposed. The proposed algorithms were numerically validated through simulation.

The algorithms proposed in the Part II of this thesis well addressed the issues of the signalling communication demand in the dynamic resource allocation of signal coordination and spectrum balancing. With the transmission stability preserved, the smoothed MWS can reduce the variation in the dynamic resource allocation for the centralised signal coordination, that the virtual network realises a local transmit spectra optimisation of the upstream VDSL2 users. The research result can be incorporated into the current G.Fast, so as to enhance the quality of user experience on the top of the improved data rate.

The objectives of the research in Sec. 1.3 are achieved. The balanced and unbalanced full-duplex MIMO channel models were developed in Chapter 3, as the conductor diversity, which helped to accommodate OFDM modulation and MIMO crosstalk cancellation, as the modulation diversity. The significantly improved theoretical capacity was shown in Chapter 4. The phantom mode transmission, as the virtual channel diversity, was investigated in Chapter 5. The smoothed dynamic resource allocation was discussed in Chapter 6, as the data time series diversity, which can reduce signalling overhead and meanwhile preserve the transmission stability. In Chapter 7, the virtual network diversity was im-

plemented as the virtual user assisted autonomous spectrum balancing algorithms, where the delay performance of the upstream VDSL2 networks was improved in an autonomous fashion.

8.2. FUTURE RESEARCH

This thesis is only the first step in developing a practical EoTP system over $100Gbit/s$. Many interesting questions remain unanswered, which form the basis for future research. Some interesting, unexplored topics are listed here.

TOR Scenario EoTP Channel Model Simulation

Focus on the channel performance in the short reach scenario, an one meter CAT7A cable cable was simulated as an example. The Top-of-the-rack (TOR) scenario requires much shorter reach than the minimum reach of 30 meters specified for 40G BASE-T. This application scenario could be further studied with more comprehensive simulations. Not only with variable cable length, but also bending should be considered in the simulation.

Alien crosstalk is not discussed in this thesis. As described in the network topology, the alien crosstalk may vary significantly due to the layout of the cables. Although the metallic shield provides extra protection against alien crosstalk, how much interference exactly can alien crosstalk cause is yet to be discussed. When only considering the TOR scenario, the impact of the alien crosstalk between multiple EoTP cables could be characterised with simulations. A few typical layout examples can provide sufficient insight of the alien crosstalk in the TOR scenario.

With more simulations of the different cabling scenarios and alien crosstalk scenar-

ios, the obtained channel parameters can be used to generate a more general or empirical channel models, validate the proposed transmission schemes or modulation methods.

Optimised OFDM Modulation

The OFDM modulation in this thesis is set to have flat transmit power spectra, which means the transmit power is equally distributed to all the sub-carriers. Attenuated by the frequency selectivity of the channel, the same transmit power on different sub-carriers will have different outcome in the SINR, thus obviously not optimal. This subject has been well studied in [43, 69], that for the single user frequency selective channel the optimal transmit power allocation is obtained by water-filling. The optimal transmission and optimal capacity in the multi-user interference channel is still one open important open issue in information theory. For the general network models or some wireless communication network models, there are some very basic sub-optimal solutions, but the applicability is very limited.

Both based on twisted pair cables, the DSL channel and EoTP channel share certainly some similarity. The multi-carrier transmit power allocation has been well addressed in the DSL networks, later introduced in Part II of the thesis. Especially, the OSB algorithm is able to find the optimal transmit power allocation of the DSL channel, with the specific characteristics of the DSL channel. Then other near-optimal algorithms, like IWF, ISB, are also developed. With the help of these optimising techniques, it is very possible that the performance could be improved through transmit power optimisation, so as to further increase the spectrum efficiency.

Closed-loop MIMO Implementation Design of EoTP Transmission

The effectiveness of MIMO crosstalk cancellation has been evaluated in this thesis. As wireline communication channel, the channel of the EoTP should be considered as time invariant, also relatively convenient for an accurate channel measurement. Then the most suitable MIMO implementation is the closed-loop MIMO for EoTP transmission.

In follow up research, the MIMO implementation in other practical communication system should be reviewed, then determine the general structure of a potential MIMO system for EoTP cable, including the algorithm, the channel coding, the signal processing methods and so on. Also, the required computational complexity, the power consumption and the manufacturing cost are important factors to consider. The goal is to achieve a trade-off among all the factors, to design a MIMO solution for EoTP transmission with both considerable performance boost and reasonable cost.

Impedance Matching in Phantom Mode Transmission

Although the phantom mode transmission studied in this thesis did not provide satisfactory result, it however exposes the sever impact of the impedance mismatch in EoTP cable, which could be an useful guideline for all the EoTP cable researches. It is still very interesting to design a suitable impedance matching circuit to compensate the extra phantom circuits to the twisted pairs, so as to create extra communication channels without harming the existing channels. Alternatively, other transmission suitable for such specific channel condition could be considered as well. Not limited to orthogonal phantom channels, the impedance matching circuit should be able to adjust the impedance even for the phantom channels to share twisted pair channels. In this way, the created phantom channel can con-

tribute more to the transmission throughput and interfere less with the other twisted pair channels.

Chapter 9

List of Reference

9.1. REFERENCES

[1] Alexander Graham Bell, "Telephone-circuit," July 19 1881, US Patent 244,426.

[2] F.A. Benson and T.M. Benson, *Fields, Waves and Transmission Lines*, Springer, 1991.

[3] ISO/IEC, "Information technology - Generic cabling for customer premises ," *ISO/IEC 11801:2010*, 2010.

[4] ITU-T, "Data communication over the telephone network," 2000.

[5] G ITU-T, "G.9701 : Fast access to subscriber terminals (g.fast) - physical layer specificationg.9701 : Fast access to subscriber terminals (g.fast) - physical layer specification," Feb. 2015.

[6] J. Frnda, M. Voznak, P. Fazio, and J. Rozhon, "Network performance qos estima-

tion," in *Telecommunications and Signal Processing (TSP), 2015 38th International Conference on*, July 2015, pp. 1–5.

[7] L. Sevcik, M. Voznak, and J. Frnda, "Qoe prediction model for multimedia services in ip network applying queuing policy," in *Performance Evaluation of Computer and Telecommunication Systems (SPECTS 2014), International Symposium on*, July 2014, pp. 593–598.

[8] IEEE, "Approved ieee draft amendment of: Ieee standard for information technology telecommunications and information exchange between systems local and metropolitan area networks specific requirements part 3: Carrier sense multiple access with collision detection (csma/cd) access method and physical layer specifications: Amendment: Physical layer and management parameters for 10 gb/s operation, type 10gbase-t," *IEEE Std P802.3an/D4.0*, 2006.

[9] ISO/IEC/TR 11801-9901 Ed. 1.0, Information Technology, "Guidance for balanced cabling in support of at least 40 Gbit/s data transmission ," *ISO/IEC JTC 1/SC 25 BPUB 2014-10*, 2014.

[10] David Keun Cheng, *Field and wave electromagnetics*, vol. 2, Addison-wesley New York, 1989.

[11] Stephen B Weinstein, "The history of orthogonal frequency-division multiplexing [history of communications]," *Communications Magazine, IEEE*, vol. 47, no. 11, pp. 26–35, 2009.

[12] Thomas Starr, John M Cioffi, and Peter J Silverman, *Understanding digital subscriber line technology*, Prentice Hall PTR, 1999.

[13] ITU-T, "Ansi t1.413 network and customer installation interfaces — asymmetric digital subscriber line (adsl) metallic interface," 1998.

[14] R. Cendrillon, Jianwei Huang, Mung Chiang, and M. Moonen, "Autonomous Spectrum Balancing for Digital Subscriber Lines," *IEEE Transactions on Signal Processing*, vol. 55, no. 8, pp. 4241 –4257, August 2007.

[15] Wei Yu, G. Ginis, and J.M. Cioffi, "Distributed multiuser power control for digital subscriber lines," *IEEE Journal on Selected Areas in Communications*, vol. 20, no. 5, pp. 1105 –1115, June 2002.

[16] R. Cendrillon, Wei Yu, M. Moonen, J. Verlinden, and T. Bostoen, "Optimal multiuser spectrum balancing for digital subscriber lines," *IEEE Transactions on Communications*, vol. 54, no. 5, pp. 922–933, May 2006.

[17] R. Cendrillon, G. Ginis, M. Moonen, and K. van Acker, "Partial crosstalk precompensation in downstream vdsl," *Elsevier Signal Processing, Special Issue on Signal Processing in Communications*, vol. 84, no. 11, pp. 2005–2019, November 2004.

[18] R. Cendrillon, M. Moonen, K. Ginis, G.and van Acker, T. Bostoen, and P. Vandaele, "Partial crosstalk cancellation for upstream vdsl," *EURASIP Journal on Applied Signal Processing*, vol. 2004, no. October, pp. 1520–1535, 2004.

[19] L. Georgiadis, M. J. Neely, and L. Tassiulas, *Resource allocation and cross-layer control in wireless networks,*, vol. 1, 2006.

[20] L. Tassiulas and A. Ephremides, "Dynamic server allocation to parallel queues with randomly varying connectivity," *IEEE Transactions on Information Theory*, vol. 39, no. 2, pp. 466–478, March 1993.

[21] M.J. Neely, E. Modiano, and C.E. Rohrs, "Dynamic power allocation and routing for time-varying wireless networks," *Selected Areas in Communications, IEEE Journal on*, vol. 23, no. 1, pp. 89 – 103, January 2005.

[22] B. Li, P. Tsiaflakis, M. Moonen, J. Maes, and M. Guenach, "Dynamic resource allocation based crosstalk cancellation in DSL networks," *IEEE Global Telecommunications Conference(Globecom)*, December 2010.

[23] B. Li, P. Tsiaflakis, M. Moonen, J. Maes, and M. Guenach, "Dynamic partial crosstalk cancellation resource allocation algorithms for dsl access networks," *EURASIP J. Adv. Sig. Proc.*, vol. 2012, pp. 150, 2012.

[24] P. Tsiaflakis, Y. Yi, M. Chiang, and M. Moonen, "Throughput and delay of DSL dynamic spectrum management with dynamic arrivals," *IEEE Global Telecommunications Conference(Globecom)*, December 2008.

[25] R. Cendrillon, L. Fang, J. Chou, G. Long, and D. Wei, "Challenges and solutions in vectored dsl," in *International Conference on Access Networks*, November 2009.

[26] R. Zidane, S. Huberman, C. Leung, and Tho Le-Ngoc, "Vectored DSL: benefits and challenges for service providers," *Communications Magazine, IEEE*, vol. 51, no. 2, pp. 152–157, February 2013.

[27] B. Li and A. Duffy, "Unbalanced Transmission Channel Model Simulation For CAT7A Ethernet Cable," in *the Proceeding of International Wire & Cable Symposium (IWCS) 2016*, 2015.

[28] B. Li and A. Duffy, "OFDM Based Ethernet Transmission over Copper Cables," in *the Proceeding of International Wire & Cable Symposium (IWCS) 2015*, 2015.

[29] B. Li and A. Duffy, "Unbalanced Transmission Channel Model Simulation For CAT7A," in *the Proceeding of Cabwire 2015, 2015*, 2015.

[30] B. Li and A. Duffy, "Virtual User Assisted Autonomous Spectrum Balancing for VDSL2 Based Triple Play Upstream," in *the Proceeding of International Wire & Cable Symposium (IWCS) 2014*, 2014.

[31] Farhad Rachidi and Sergey Tkachenko, *Electromagnetic field interaction with transmission lines: from classical theory to HF radiation effects*, vol. 5, WIT press, 2008.

[32] "Data-Over-Cable Service Interface Specifications DOC- SIS 3.0 MAC and Upper Layer Protocols Interface Specification CM-SP-MULPIv3.1-I03-140610," 2012.

[33] "Data-Over-Cable Service Interface Specifications DOC- SIS 3.1 MAC and Upper Layer Protocols Interface Specification CM-SP-MULPIv3.1-I03-140610," 2014.

[34] IEEE, "IEEE Standard for Information technology– Local and metropolitan area networks– Specific requirements– Part 3: CSMA/CD Access Method and Physical Layer Specifications Amendment 4: Media Access Control Parameters, Physical Layers, and Management Parameters for 40 Gb/s and 100 Gb/s Operation,"

IEEE Std 802.3ba-2010 (Amendment to IEEE Standard 802.3-2008), pp. 1–457, June 2010.

[35] IEEE, "IEEE Standard for Broadband over Power Line Networks: Medium Access Control and Physical Layer Specifications," *IEEE Std 1901*, pp. 1–1586, Dec 2010.

[36] Hendrik C Ferreira, Henricus M Grove, Olaf Hooijen, and AJ Han Vinck, *Power line communication*, Wiley Online Library, 2001.

[37] IEEE, "IEEE Standard 802.3," *IEEE Standard For Ethernet*, 2012.

[38] Caesar Wu and Rajkumar Buyya, *Cloud Data Centers and Cost Modeling: A Complete Guide To Planning, Designing and Building a Cloud Data Center*, Morgan Kaufmann, 2015.

[39] Nathan Farrington, George Porter, Sivasankar Radhakrishnan, Hamid Hajabdolali Bazzaz, Vikram Subramanya, Yeshaiahu Fainman, George Papen, and Amin Vahdat, "Helios: a hybrid electrical/optical switch architecture for modular data centers," *ACM SIGCOMM Computer Communication Review*, vol. 41, no. 4, pp. 339–350, 2011.

[40] C. Leung, S. Huberman, and Tho Le-Ngoc, "Autonomous Spectrum Balancing Using Multiple Reference Lines for Digital Subscriber Lines," in *Global Telecommunications Conference (GLOBECOM 2010), 2010 IEEE*, dec. 2010, pp. 1 –6.

[41] Thomas M Cover and Joy A Thomas, *Elements of information theory*, John Wiley & Sons, 2012.

[42] Lajos L Hanzo, Matthias Münster, Byungcho Choi, and Thomas Keller, *OFDM and MC-CDMA for broadband multi-user communications, WLANs and broadcasting*, John Wiley & Sons, 2005.

[43] Richard van Nee and Ramjee Prasad, *OFDM for wireless multimedia communications*, Artech House, Inc., 2000.

[44] IEEE 802.3 Study Group, "http://www.ieee802.org/3/," 2015.

[45] S. Yan, S. Peng, Y. Yan, B. R. Rofoee, Y. Shu, E. Hugues-Salas, G. Zervas, D. Simeonidou, M. Svaluto Moreolo, J. M. Fbrega, L. Nadal, Y. Yoshida, P. J. Argibay-Losada, K. Kitayama, M. Nishihara, R. Okabe, T. Tanaka, T. Takahara, J. C. Rasmussen, C. Kottke, M. Schlosser, F. Jimenez Arribas, and V. Lpez, "100g beyond ethernet transport for inter- and intra-dcn communication with solutions and optical enabling technologies in the ict strauss project," in *Networks and Communications (EuCNC), 2015 European Conference on*, June 2015, pp. 350–354.

[46] Y. Cheng, M. Fiorani, L. Wosinska, and J. Chen, "Reliable and cost efficient passive optical interconnects for data centers," *IEEE Communications Letters*, vol. 19, no. 11, pp. 1913–1916, Nov 2015.

[47] C. Jayalath, J. Stephen, and P. Eugster, "Universal cross-cloud communication," *IEEE Transactions on Cloud Computing*, vol. 2, no. 2, pp. 103–116, April 2014.

[48] B. Andrus, O. M. Poncea, J. J. Vegas Olmos, and I. Tafur Monroy, "Performance evaluation of two highly interconnected data center networks," in *2015 17th In-*

ternational Conference on Transparent Optical Networks (ICTON), July 2015, pp. 1–4.

[49] D. Li, H. Zhao, M. Xu, and X. Fu, "Revisiting the design of mega data centers: Considering heterogeneity among containers," *IEEE/ACM Transactions on Networking*, vol. 22, no. 5, pp. 1503–1515, Oct 2014.

[50] D. Li and J. Wu, "On data center network architectures for interconnecting dual-port servers," *IEEE Transactions on Computers*, vol. 64, no. 11, pp. 3210–3222, Nov 2015.

[51] Daniel Law, Dan Dove, John D'Ambrosia, Marek Hajduczenia, Mark Laubach, and Steve Carlson, "Evolution of Ethernet standards in the IEEE 802.3 working group," *Communications Magazine, IEEE*, vol. 51, no. 8, pp. 88–96, 2013.

[52] J. Wang, S. Basu, C. McArdle, and L. P. Barry, "Large-scale hybrid electronic/optical switching networks for datacenters and hpc systems," in *Cloud Networking (CloudNet), 2015 IEEE 4th International Conference on*, Oct 2015, pp. 87–93.

[53] C. L. Schow, "Next generation data centres: How will optics be employed?," in *Optical Communication (ECOC), 2015 European Conference on*, Sept 2015, pp. 1–3.

[54] Yuxin Cheng, Matteo Fiorani, Lena Wosinska, and Jiajia Chen, "Reliability analysis of interconnects at edge tier in datacenters," in *Transparent Optical Networks (ICTON), 2015 17th International Conference on*, July 2015, pp. 1–1.

[55] S. Das and S. Sahni, "Network topology optimization for data aggregation," in *Cluster, Cloud and Grid Computing (CCGrid), 2014 14th IEEE/ACM International Symposium on*, May 2014, pp. 493–501.

[56] Nikolaos Bamiedakis, Jian Chen, Petter Westbergh, Johan S Gustavsson, Anders Larsson, Richard V Penty, and Ian H White, "40 Gb/s Data Transmission Over a 1-m-Long Multimode Polymer Spiral Waveguide for Board-Level Optical Interconnects," *Journal of Lightwave Technology*, vol. 33, no. 4, pp. 882–888, 2015.

[57] M. Fiorani, S. Aleksic, P. Monti, J. Chen, M. Casoni, and L. Wosinska, "Energy efficiency of an integrated intra-data-center and core network with edge caching," *IEEE/OSA Journal of Optical Communications and Networking*, vol. 6, no. 4, pp. 421–432, April 2014.

[58] J. Taylor, "Facebook's data center infrastructure: Open compute, disaggregated rack, and beyond," in *Optical Fiber Communications Conference and Exhibition (OFC), 2015*, March 2015, pp. 1–1.

[59] T. Gao, E. Kumar, M. Sahini, C. Ingalz, A. Heydari, Wendy Lu, and Xiaogang Sun, "Innovative server rack design with bottom located cooling unit," in *2016 15th IEEE Intersociety Conference on Thermal and Thermomechanical Phenomena in Electronic Systems (ITherm)*, May 2016, pp. 1172–1181.

[60] Vitaliy Zhurbenko, *Advanced Microwave Circuits and Systems*, Sciyo, 2010.

[61] Clayton R Paul, *Analysis of multiconductor transmission lines*, John Wiley & Sons, 2008.

[62] Telecommunications Industry Association, "Ansi/tia-568-c.2, balanced twisted-pair telecommunication cabling and components standard," 2014.

[63] Telecommunications Industry Association, "Ansi/tia-1005 industrial cabling standard," 2012.

[64] Lizhong Zheng and David NC Tse, "Diversity and multiplexing: a fundamental tradeoff in multiple-antenna channels," *Information Theory, IEEE Transactions on*, vol. 49, no. 5, pp. 1073–1096, 2003.

[65] J Nicholas Laneman, David NC Tse, and Gregory W Wornell, "Cooperative diversity in wireless networks: Efficient protocols and outage behavior," *Information Theory, IEEE Transactions on*, vol. 50, no. 12, pp. 3062–3080, 2004.

[66] IEEE, "IEEE standard for wireless lan," *IEEE Standard 802.11*, 2012.

[67] Basic Transmission Scheme, "LTE: the evolution of mobile broadband," *IEEE Communications magazine*, vol. 45, 2009.

[68] Computer Simulation Technology AG (CST), "Cst studio suite," 2016.

[69] Cheong Yui Wong, Roger S Cheng, K Ben Lataief, and Ross D Murch, "Multiuser OFDM with adaptive subcarrier, bit, and power allocation," *Selected Areas in Communications, IEEE Journal on*, vol. 17, no. 10, pp. 1747–1758, 1999.

[70] G. Caire and S. Shamai, "On the achievable throughput of a multiantenna gaussian broadcast channel," *Information Theory, IEEE Transactions on*, vol. 49, no. 7, pp. 1691–1706, July 2003.

[71] A Nosratinia, T.E. Hunter, and A Hedayat, "Cooperative communication in wireless networks," *Communications Magazine, IEEE*, vol. 42, no. 10, pp. 74–80, Oct 2004.

[72] Q.H. Spencer, AL. Swindlehurst, and M. Haardt, "Zero-forcing methods for downlink spatial multiplexing in multiuser mimo channels," *Signal Processing, IEEE Transactions on*, vol. 52, no. 2, pp. 461–471, Feb 2004.

[73] G ITU-T, "993.2: Very high speed digital subscriber line transceivers 2 (VDSL2)," 2011.

[74] ETSI, "Digital Video Broadcasting (DVB); Framing structure, channel coding and modulation for digital terrestrial television," *ETSI Standard: EN 300 744 V1.5.1*, 2016.

[75] ETSI, "Digital Audio Broadcasting (DAB); Guide to DAB standards; Guidelines and Bibliography," *ETSI TR 101 495 V1.4.1*, 2012.

[76] "IEEE P802.3bs 400 Gb/s Ethernet Task Force," *http://www.ieee802.org/3/bs/index.html.*, 2016.

[77] J. Wei, Q. Cheng, R. V. Penty, I. H. White, and D. G. Cunningham, "400 gigabit ethernet using advanced modulation formats: Performance, complexity, and power dissipation," *IEEE Communications Magazine*, vol. 53, no. 2, pp. 182–189, Feb 2015.

[78] J. M. Fadlullah, A. Enteshari, and M. Kavehrad, "Channel equalization for multigigabit ethernet over copper," in *Electrical and Computer Engineering, 2009. CCECE '09. Canadian Conference on*, May 2009, pp. 49–53.

[79] J. Chen, Y. Gu, and K. K. Parhi, "Novel fext cancellation and equalization for high speed ethernet transmission," *IEEE Transactions on Circuits and Systems I: Regular Papers*, vol. 56, no. 6, pp. 1272–1285, June 2009.

[80] H. Bolcskei, D. Gesbert, and A. J. Paulraj, "On the capacity of ofdm-based spatial multiplexing systems," *IEEE Transactions on Communications*, vol. 50, no. 2, pp. 225–234, Feb 2002.

[81] A Goldsmith, S.A Jafar, N. Jindal, and S. Vishwanath, "Capacity limits of MIMO channels," *Selected Areas in Communications, IEEE Journal on*, vol. 21, no. 5, pp. 684–702, June 2003.

[82] John M Woram, *The recording studio handbook*, Sagamore Publishing Company, 1976.

[83] W. Foubert, C. Neus, L. Van Biesen, and Y. Rolain, "Exploiting the Phantom-Mode Signal in DSL Applications," *IEEE Transactions on Instrumentation and Measurement*, vol. 61, no. 4, pp. 896–902, April 2012.

[84] T. Magesacher, D. Statovci, T. Nordstrm, and E. Riegler, "Performance analysis of vectored wireline systems embracing channel uncertainty," in *2013 IEEE International Conference on Communications (ICC)*, June 2013, pp. 3986–3990.

[85] C. Neus, W. Foubert, L. Van Biesen, Y. Rolain, P. Boets, and J. Maes, "Binder identification by means of phantom measurements," *IEEE Transactions on Instrumentation and Measurement*, vol. 60, no. 6, pp. 1967–1975, June 2011.

[86] R. Santos, C. Sales, M. Lima, C. Rodrigues, A. Araujo, W. C. Gomes, A. Fertner, and J. C. W. A. Costa, "Binder identification using pattern recognition on phantom measurements," *IEEE Transactions on Instrumentation and Measurement*, vol. 65, no. 3, pp. 522–534, March 2016.

[87] John M Cioffi, Bin Lee, Wonjong Rhee, and Georgios Ginis, "Phantom use in dsl systems," Aug. 10 2010, US Patent 7,773,497.

[88] HUAWEI Ltd., "Huawei demonstrates 700mb bonded dsl broadband technology," *http://www.ispreview.co.uk/story/2010/09/23/huawei-demonstrates-700mb-bonded-dsl-broadband-technology.html*, 2010.

[89] Michael Peeters and Stefaan Vanhastel, "The copper phantom, copper's renewed power is no figment of the imagination," *http://www.ospmag.com/issue/article/The-Copper-Phantom*, 2010.

[90] G. Ginis and J.M. Cioffi, "Vectored transmission for digital subscriber line systems," *Selected Areas in Communications, IEEE Journal on*, vol. 20, no. 5, pp. 1085 –1104, jun 2002.

[91] Bin Lee, J.M. Cioffi, S. Jagannathan, and M. Mohseni, "Gigabit DSL," *Communications, IEEE Transactions on*, vol. 55, no. 9, pp. 1689–1692, Sept 2007.

[92] R. Cendrillon and M. Moonen, "Iterative spectrum balancing for digital subscriber lines," in *IEEE International Conference on Communications (ICC)*, May 2005, vol. 3, pp. 1937 – 1941 Vol. 3.

[93] Wei Yu and R. Lui, "Dual methods for nonconvex spectrum optimization of multi-carrier systems," *IEEE Transactions on Communications*, vol. 54, no. 7, pp. 1310 –1322, July 2006.

[94] P. K. Pandey, M. Moonen, and L. Deneire, "MMSE-Based Partial Crosstalk Cancellation for Upstream VDSL," in *IEEE International Conference on Communications (ICC)*, May 2010, pp. 1 –5.

[95] Enrique Areizaga, Andreas Foglar, Antonio J. Elizondo, and Frank Geilhardt, "Enabling broadband as commodity within access networks: A qos recipe," *Lecture Notes of the Institute for Computer Sciences, Social Informatics and Telecommunications Engineering*, vol. 6, 2009.

[96] Andreas Foglar and Raphael Polig, "Planets qos solution," *http://www.medea-planets.eu/QoSsolution.php?page=home*, 2007.

[97] M.J. Neely, "Delay-based network utility maximization," in *INFOCOM, 2010 Proceedings IEEE*, March 2010, pp. 1–9.

[98] Mung Chiang, S.H. Low, AR. Calderbank, and J.C. Doyle, "Layering as optimization decomposition: A mathematical theory of network architectures," *Proceedings of the IEEE*, vol. 95, no. 1, pp. 255–312, Jan 2007.

[99] S. Asmussen, *Applied Probability and Queues*, Springer, New York, 2000.

[100] J. Cioffi, M. Brady, V. Pourahmad, S. Jagannathan, W. Lee, Y. Kim, C. Chen, K. Seong, D. Yu, M. Ouzzif, H. Mariotte, R. Tarafi, G. Ginis, B. Lee, T. Chung,

P. Silverman, and Assia Inc, "Vectored dsls with dsm: The road to ubiquitous gigabit dsls," 2008.

[101] J. Vangorp, P. Tsiaflakis, M. Moonen, J. Verlinden, and G. Ysebaert, "Dual decomposition approach to partial crosstalk cancelation in a multiuser dmt-xdsl environment," *EURASIP Journal on Advances in Signal Processing*, 2007.

[102] P. Tsiaflakis, J. Vangorp, M. Moonen, J. Verlinden, and K. Van Acker, "An efficient search algorithm for the lagrange multipliers of optimal spectrum balancing in multi-user xdsl systems," in *IEEE International Conference on Acoustics, Speech and Signal Processing (ICASSP)*, May 2006, vol. 4, pp. IV–IV.

[103] Tomasz Rolski, "Queues with non-stationary input stream: Ross's conjecture," *Advances in applied Probability*, pp. 603–618, 1981.

[104] Arie Hordijk, "Comparison of queues with different discrete-time arrival processes," *Probab. Eng. Inf. Sci.*, vol. 15, no. 1, pp. 1–14, Jan. 2001.

[105] R. G. Brown, *Smoothing, Forecasting and Prediction of Discrete Time Series*, Prentice-Hall, 1963.

[106] J. Papandriopoulos and J.S. Evans, "Low-Complexity Distributed Algorithms for Spectrum Balancing in Multi-User DSL Networks," in *Communications, 2006. ICC '06. IEEE International Conference on*, june 2006, vol. 7, pp. 3270 –3275.

[107] P. Tsiaflakis, M. Diehl, and M. Moonen, "Distributed spectrum management algorithms for multiuser dsl networks," *IEEE Transactions on Signal Processing*, vol. 56, no. 10, pp. 4825–4843, October 2008.

[108] T. Rahrer, R. Fiandra, and R. Wright, "Triple-play Services Quality of Experience (QoE) Requirements," *DSL Forum TR-126*, December 2006.

[109] F.P. Kelly, P.B. Key, and S. Zachary, "Distributed admission control," *Selected Areas in Communications, IEEE Journal on*, vol. 18, no. 12, pp. 2617 –2628, dec. 2000.

[110] S.S. Kunniyur and R. Srikant, "An adaptive virtual queue (AVQ) algorithm for active queue management," *Networking, IEEE/ACM Transactions on*, vol. 12, no. 2, pp. 286 – 299, april 2004.

[111] A. Lakshmikantha, C.L. Beck, and R. Srikant, "Robustness of real and virtual queue-based active queue management schemes," *Networking, IEEE/ACM Transactions on*, vol. 13, no. 1, pp. 81 – 93, feb. 2005.

[112] A. Nasipuri and S.R. Das, "Multichannel CSMA with signal power-based channel selection for multihop wireless networks," in *Vehicular Technology Conference, 2000. IEEE VTS-Fall VTC 2000. 52nd*, 2000, vol. 1, pp. 211 –218 vol.1.

Chapter 10

List of Publication

Published

1. Virtual User Assisted Autonomous Spectrum Balancing for VDSL2 Based Triple Play Upstream, *Published at the Proceeding of International Wire & Cable Symposium (IWCS) 2014, 2014.*

2. OFDM Based Ethernet Transmission over Copper Cables, *Published at the Proceeding of International Wire & Cable Symposium (IWCS) 2015, 2015.*

3. Unbalanced Transmission Channel Model Simulation For CAT7A, *Published at the Proceeding of Cabwire 2015,*

4. Unbalanced Transmission Channel Model Simulation For CAT7A Cable, *Published at the Proceeding of International Wire & Cable Symposium (IWCS) 2016, 2016.*

In Preparation

1. Performance Improved MAX-WEIGHT Scheduling, *Submitted to IEEE Communication Letters.*

2. Copper Beyond 100Gb/s, Exploiting the Diversities in the Ethernet over Twisted Pair Cable, *Journal paper in preparation.*

3. MIMO Channel Simulation For a Short CAT7A Ethernet Cable, *Conference Paper in Preparation.*

4. Virtual User Assisted Autonomous Spectrum Balancing for VDSL2 Based Triple Play Upstream, *Journal paper in preparation.*

Appedix

Proof of Theorem 1

Consider a network with N users, MWS is a throughput optimal. For an optimal resource allocation, suppose there is a mean arrival rate vector $\vec{\Lambda}$, which is strictly interior to the optimal rate region $\mathcal{R}$, while another vector $\vec{\epsilon} = [\epsilon^1, \epsilon^2, ..., \epsilon^n]^T$ with arbitrary small positive numbers, that satisfies $\vec{\Lambda} + \vec{\epsilon} \in \mathcal{R}$, the transmission stability of the optimal resource allocation is concluded as the following:

For a VDSL2 network with MWS, any arrival process with the mean arrival rate vector $\vec{\Lambda} = [\lambda^1, \lambda^2, ..., \lambda^n]^T$ can always be stabilised, therefore the system delay is upper bounded:

$$\frac{1}{T}\sum_{\tau=0}^{T-1}\sum_{n=1}^{N} Q^n(\tau) \leq \frac{1}{2\epsilon_{min}}[B + \sum_{n=1}^{N}(Q^n(0))^2], \tag{10.1}$$

where $\epsilon_{min} = min(\epsilon^1, \epsilon^2, ..., \epsilon^n)$, constant $B = N(\omega^2 + (R^{\max})^2)$, then $\vec{Q}(0)$ is the initial queue lengths of the users.

From time slot 0 to T, the users' data queues are updated by equation (6.7) at each time

slot. One variable, the arrival process $A(\vec{t})$ is stabilisable if its expectation $\vec{\Lambda}$ falls within the throughput region $\vec{\Lambda}^{TP}$. The other variable $Q(\vec{t})$ is determined as the resulting data rate of the dynamic resource allocation at each time slot. The network transmission stability defined in (6.8) will be proved through the derivation of a negative quadratic Lyapunov drift [19]. Firstly, user n's *quadratic Lyapunov drift* (QLD) between two consecutive time slots is defined as follows:

$$\Delta(\vec{Q}(t)) = \mathbb{E}[\sum_{n=1}^{N}(Q^n(t+1))^2) - \sum_{n=1}^{N}(Q^n(t))^2|\vec{Q}(t)]. \tag{10.2}$$

Consider the two possibilities for the queue update (6.7):

$$\textit{if} \quad Q^n(t) - R^n(t) \leq 0; \quad \textit{then} \quad Q^n(t+1) = A^n(t). \tag{10.3}$$

$$\textit{or, if} \quad Q^n(t) - R^n(t) > 0; \tag{10.4}$$

$$\textit{then} \quad Q^n(t+1) = Q^n(t) - R^n(t) + A^n(t). \tag{10.5}$$

As a best case, if (10.3) happens at all time slots, then the stability is obvious. Focusing on the worst case of (10.4) for all time slots, then the QLD can be expanded as follows:

$$\begin{aligned}\Delta(\vec{Q}(t)) \quad = \quad & \sum_{n=1}^{N}\mathbb{E}[(A^n(t))^2 + (R^n(t))^2|\vec{Q}(t)] \\ & + \sum_{n=1}^{N} 2Q^n(t)\mathbb{E}[(A^n(t) - R^n(t))|\vec{Q}(t)] \\ & - \sum_{n=1}^{N} 2\mathbb{E}[(A^n(t)R^n(t))|\vec{Q}(t)]. \end{aligned} \tag{10.6}$$

$A^n(t)$ is bounded by ω^n, and $R^n(t)$ is limited by $R^n_{\max}$, then the first item on the RHS of (10.6) is clearly bounded by the following:

$$\sum_{n=1}^{N} \mathbb{E}[(A^n(t))^2 + (R^n(t))^2 | \vec{Q}(t)] \leq \sum_{n=1}^{N} ((\omega^n)^2 + (R^n_{max})^2). \tag{10.7}$$

For later simplicity, we denote B to the constant on the RHS of (6.18). Moreover, $A^n(t)$ is an independent random process from $Q^n(t)$, therefore the term $\mathbb{E}[(A^n(t)|\vec{Q}(t)]$ can be replaced by λ^n. $R^n(t)$ is deterministic when $\vec{Q}(t)$ is given, therefore the term $\mathbb{E}[R^n(t)|\vec{Q}(t)]$ can be replaced by $R^n(t)$. The following inequality can be obtained from (10.6):

$$\begin{aligned} \Delta(\vec{Q}(t)) \quad \leq \quad & \sum_{n=1}^{N} 2Q^n(t)\lambda^n - \sum_{n=1}^{N} 2Q^n(t)R^n(t) \\ & + B - \sum_{n=1}^{N} 2\mathbb{E}[(A^n(t)R^n(t))|\vec{Q}(t)]. \end{aligned} \tag{10.8}$$

The last term of (10.8) is negative at the greater side of the inequality, therefore ignored. For an arbitrary stabilisable $\vec{\Lambda} \in \vec{\Lambda}^{TP}$, there exists an arbitrarily small positive vector $\vec{\epsilon} = [\epsilon^1, \epsilon^2, ..., \epsilon^n]^T$, and an intermediate vector $\vec{\tilde{\Lambda}} = [\tilde{\lambda}^1, \tilde{\lambda}^2, ..., \tilde{\lambda}^n]^T = [(\lambda^1 + \epsilon^1), (\lambda^2 + \epsilon^2), ..., (\lambda^n + \epsilon^n)]^T$, which satisfies $\vec{\tilde{\Lambda}} \in \vec{\Lambda}^{TP}$, then the MWS scheduling result Eq. (6.10) satisfies the follows:

$$\sum_{n=1}^{N} Q^n(t)R^n(t) \geq \sum_{n=1}^{N} Q^n(t)\tilde{\lambda}^n. \tag{10.9}$$

The second term on the RHS of Eq. (10.6) is negative, thus can be replaced by the

smaller term on the RHS of (10.9, which gives follows::

$$\Delta(\vec{Q}(t)) \;\leq\; \sum_{n=1}^{N} 2Q^n(t)(\lambda^n - \tilde{\lambda}^n) + B - \sum_{n=1}^{N} 2\mathbb{E}[(A^n(t)R^n(t))|\vec{Q}(t)]. \quad (10.10)$$

The last term of (10.10) is negative at the greater side of the inequality, therefore is ingored. By the definition of $\vec{\tilde{\Lambda}}$, Eq. (10.10) can be simplified as follows:

$$\Delta(\vec{Q}(t)) \;\leq\; B - \sum_{n=1}^{N} 2Q^n(t)\epsilon^n. \quad (10.11)$$

Defining a constant $\epsilon^\star = min\{\epsilon^1, \epsilon^2, ..., \epsilon^n\}$ to substitute ϵ^n in the RHS of Eq. (10.11), which results in a smaller negative terms in the greater side of the inequality, then the inequality (6.22) still holds. The expectation of $\Delta(\vec{Q}(t))$ can be taken over the distribution of $\vec{Q(t)}$, giving:

$$\mathbb{E}[\sum_{n=1}^{N}(Q^n(t+1))^2 - (Q_n(t))^2)] \leq B - \sum_{n=1}^{N} 2Q^n(t)\epsilon^\star. \quad (10.12)$$

Since Eq. (10.12) is valid for all time slots, it is summed over all time slots $t \in \{0, 2, ..., T\}$ and divided the sum by T, to give:

$$\frac{1}{T}\sum_{n=1}^{N}(Q^n(T))^2 - (Q^n(0))^2) \leq B - \frac{2\epsilon^\star}{T}\sum_{\tau=1}^{T}\sum_{n=1}^{N} Q^n(\tau). \quad (10.13)$$

The term $\frac{1}{T}\sum_{n=1}^{N}(Q^n(T))^2$ of Eq. (10.13) is positive at the smaller side of the inequal-

ity, therefore ignored. by rearranging Eq. (10.13), we arrive at:

$$\frac{1}{T}\sum_{\tau=1}^{T}\sum_{n=1}^{N}Q^n(\tau) \quad \leq \quad \frac{1}{2\epsilon^\star}[B+\frac{1}{T}\sum_{n=1}^{N}(Q^n(0))^2]. \tag{10.14}$$

If $T \to \infty$, the left hand side (LHS) of (10.14) is the expectation of the sum of the users' queue length, also equivalent to the definition of system delay in Eq. (6.8). This is bounded by the constants $B, \epsilon^\star$ and the initial status $\vec{Q}(0)$ and $\vec{Q}(1)$. If $\vec{Q}(0)$ is not infinity, then the queue lengths will not grow to infinity, thus the stability of MWS is proved.

Published Papers

OFDM BASED ETHERNET TRANSMISSION OVER COPPER CABLES

Beier Li, Alistair Duffy

Electrical Engineering, De Montfort University, UK,
email: p1319654x@myemail.dmu.ac.uk, apd@dmu.ac.uk

ABSTRACT

Following the massive commercial deployment of 10G BaseT and the development of 40GBaseT, twisted pair based copper cable Ethernet is looking towards the next standard of probably 100Gbps.

Intuitively, the straight forward approach for higher data rates is to upgrade the heritage of previous standards. For example, extending frequency spectrum usable, and implement higher order PAM modulation can utilise more frequency resource with higher spectrum efficiency. However, this legacy may not be the best way to extend the throughput, reach or both. This paper looks at whether orthogonal frequency-division multiplexing (OFDM) could be a candidate transmission technology for future Ethernet expansion.

1. NEXT GENERATION ETHERNET OF X-BASET

Ethernet, defined in the protocol set of IEEE 802.3 [1], has been the dominant communication standard in the field of computer networks, including home networks, enterprise networks and data centres. The physical media of Ethernet transmission includes copper based twisted pair cable, optical fibre and the copper backplane. From the 1BASE5, standardised and defined in IEEE 802.3e in 1986, twisted pair cables have been introduced, and since then used as the first choice of copper Ethernet transmission till today. The standard for Ethernet over twisted pair cable has also evolved from the 1BASE5, the 10BASE-T, the 100 BaseT, the 1G-BaseT to 10G-BaseT, and further towards 25G-BaseT, 40G-BaseT and 100G-BaseT.

Powered by their own advantages, the IEEE 802.11 Wireless Lan (WLAN) [2] with the convenience and flexibility and the optical fibre system emerge as the competitors of cable based Ethernet. Ethernet over twisted pair cables still remains as a considerable choice in many application scenarios, by providing high data rate, reliable communication and deployment flexibility simultaneously. With the further development of the Ethernet standard, higher data rate and more reliable transmission are expected for the Ethernet over twisted pair cables, or x-BaseT.

So far, x-BaseT transmission framework has been based on single carrier Pulse-Amplitude Modulation (PAM) modulation, with increasing modulation order and expanding frequency band, so as to achieve higher data rate. The basic structure of four twisted pairs within the cable is kept, with more screening and shielding, so as to improve the electromagnet performance of the cable. The modulation evolution is summarised in Table 1, and the cable specifications are summarised in Table 2.

With the expanding frequency band, the insertion loss and the crosstalk of the cable are much worse. This forms a frequency-selective channel with coloured noise, which is caused by the nature of the copper wire, that the insertion loss degrades with increased frequency range, and can be observed in other copper based technologies. The most seen copper cable applications include the Digital Subscriber Line (xDSL) [3, 4], which provides high speed data service over the existing telephone twisted pair, and the Cable Television system, where both television program and high speed data service over the co-axial television cable, also known as (DOCSIS) [5]. Orthogonal frequency division multiplexing (OFDM) [6–9] is adopted in both xDSL and DOCSIS 3.1, so as to improve the transmission performance over the copper cable. OFDM is a modulation technique, where the wide transmission frequency band is divided into numerous narrow band channels (frequency bins), and the data flow is modulated into corresponding parallel low symbol-rate data streams. In this way, the single carrier high symbol-rate transmission in a frequency selective channel can be decomposed into a set of parallel low symbol-rate transmissions over different flat channels. Priori to the advances of the semiconductor technology development, the implementation of the OFDM was restricted by the capability of the chipset. Nowadays, OFDM has been implemented in many mainstream commercial communication system at a very acceptable cost, like previously mentioned xDSL and DOCSIS, and WLAN in wireless communication and Long Term Evolution (LTE) [10] in mobile communication, and has shown considerable performance in practice.

In Section 2 we will introduce the principle of OFDM transmission and its application in xDSL and DOCSIS 3.1. In Section 3 we will discuss the channel model of Cat7a cable, and propose two transmit power allocation algorithms. In the end we will present the simulated performance, to evaluate the achievable data rate of OFDM transmission over Cat7a cable. In Section 4 we will conclude the research and discuss the future work.

Table 1. PAM Configuration for the Ethernet Standards

Ethernet Standard	10Base-T	100Base-TX	1000Base-T	10GBase-T	40GBase-T
Twisted Pair Used	2	2	4	4	4
Coding	Manchester	4B/5B	PAM5	THP-PAM16	TBD
Transmit Voltage	± 2.5V	$\pm 1, 0$V	$\pm 2, \pm 1, 0$V	N/A	TBD
Symbol Rate	10 MBd	125 MBd	125 MBd	250 MBd	TBD

Table 2. Cable Specifications

	Cat. 3	Cat. 4	Cat. 5	Cat. 5a	Cat. 6	Cat. 6a	Cat.7	Cat.7a
Frequency	16MHz	20MHz	100MHz	100MHz	250MHz	500MHz	600MHz	1600MHz
Data Rate	10Mbit/s	16Mbit/s	100Mbit/s	100Mbit/s	1Gbit/s	10Gbit/s	10Gbit/s	40Gbit/s
Reach	100m	100m	100m	100m	100m	55m	100m	50m
Cable Screening	none	none	none	none	none	none/foil	braiding/foil	braiding/foil
Pair Shielding	none	none	none	none	none	foil/none	foil	foil

2. OFDM TRANSMISSION AND ITS APPLICATIONS IN WIRELINE COMMUNICATION

In this section, the concept of OFDM and its transmission model are introduced, and then the detailed OFDM implementation in xDSL and DOCSIS are described.

2.1. OFDM as an Advanced Transmission Technique

From the perspective of frequency band utilisation, all the communication systems can be divided into two types, single carrier and multiple carrier systems. For early narrow band or voice band communication systems, single carrier transmission has been an attractive option due to its low complexity. As most of wireline communication systems change to broadband systems, the increased channel frequency selectivity caused by the expanding transmission frequency band and the crosstalk become the major bottleneck of performance. The crosstalk includes the near-end crosstalk (NEXT) and the far-end crosstalk (FEXT).The multiple carrier transmission techniques divide the broadband channel into a set of parallel narrow band flat channels (sub-carriers), and transmit over these separate channels simultaneously. as illustrated in Fig. 1.

A very popular multiple carrier technique in recent commercial practice is orthogonal frequency division multiplexing (OFDM), whose sub-subcarriers are orthogonal to each other [8, 9]. At the transmitter side, the transmit data is firstly converted to a set of parallel baseband data streams through a serial-to-parallel converter, where each of these stream corresponds to a sub-carrier, then independently modulated into quadrature amplitude modulation (QAM) symbols. So far, the data signal is still in the time domain. Then the parallel QAM symbols are fed into an inverse Fast Fourier Transformer (iFFT), whose output is serial signal in frequency domain, and then is further converted into analogue signal by a digital-to-analogue converter (DAC). At last this transmit signal will go through the copper wire. This procedure is depicted in Fig. 2.

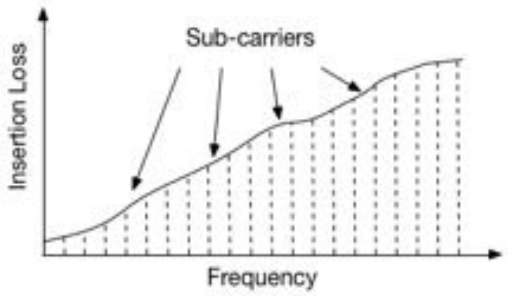

Fig. 1. OFDM Frequency Utilisation

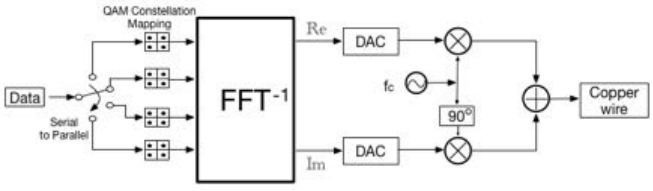

Fig. 2. OFDM Transmitter

At the receiver side, the received signal is converted into digital signal through an analogue-to-digital converter (ADC), and separated into real and imaginary parts for the Fast Fourier Transformer (FFT), which converts the serial time domain signal back into parallel frequency domain QAM symbols. The the QAM symbols will be desolved into data bits, and combined in order into the received data. This procedure is depicted in Fig.3.

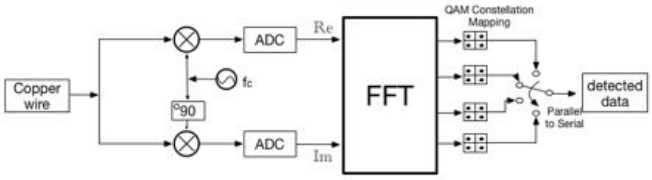

Fig. 3. OFDM Receiver

Mathematically, the frequency band F_{max} is divided into N sub-carriers, which is smaller or equal to the size of FFT/iFFT. Each carrier has a bandwidth of Δf, which is chosen to be narrow enough that the channel condition within it is frequency flat. The symbol rate on each sub-carrier is denoted by f_s, and the corresponding symbol duration is $T = 1/f_s$ second. The transmit power spectrum density, the insertion loss and the return loss on sub-carrier n are denoted by s^n, IL^n and RL^n, respectively. Other interference sources include the background noise and crosstalk, whose sum is denoted here by itf. The bitloading b^n on sub-carrier n, i.e., the information can be carried on sub-carrier n, is calculated as follows,

$$b^n = \log_2\left(1 + \frac{IL^n s^n \Delta f}{RL^n s^n \Delta f + itf}\right) bit, \qquad (1)$$

, and the achievable data rate R of the whole transmission system is calculated as follows,

$$R = f_s \sum_{n=1}^{N} b^n. \qquad (2)$$

Compared with single carrier transmission, the performance degradation caused by the channel selectivity will be improved in OFDM, that only the sub-carriers on the severe frequency will suffer performance degradation. For instance, the severe insertion loss in the high frequency part of the Fig. 1 will not impact the separate transmission in the low frequency part. In the receiver design of the single carrier transmission, usually a time domain filter is adopted for the channel equalisation. Such time domain filter will be a large number of filter taps, which means high complexity, power consumption and processing delay. At the OFDM receiver side, the output of the FFT is parallel QAM symbols, which is low symbol rate frequency domain signal in the form of complex number. The channel equalisation can be easily implemented by multiplication of the QAM symbol with the inverse of the sub-carrier channel estimate.

In the scenario of copper cable based wireline broadband communication systems, the channel condition is frequency selective, but meanwhile time invariant, therefore accurate channel estimation is usually possible. The accurate channel estimate is of great importance for the OFDM sub-carrier partition and channel equalisation. Compared with wireless and mobile communication systems, the stationary nature of the wireline communication terminals allows relaxed power consumption and hardware complexity of the equipment. With large size FFT, the bandwidth of the sub-carrier can be reduced, which is crucial for the frequency flatness of the sub-carrier. Moreover, the transmitter circuit linearity restriction from the high peak-to-average-ratio problem can be easier implemented in stationary hardware.The features above make OFDM a suitable option for the xBaseT Ethernet with 40Gbit/s or higher.

2.2. OFDM in xDSL and DOCSIS

Currently, two major copper cable based broadband communication systems, xDSL [3]and DOCSIS 3.1 [5], have adopted OFDM as the physical layer modulation scheme. The xDSL technology has chosen the OFDM from the beginning of its standardisation, and the DOCSIS 3.1 standard abandoned the single carrier modulation in DOCSIS 3.0 [11] standard and switched to multi carrier OFDM scheme.

xDSL technology provides high speed data service over the existing telephony cables. The customer-premises equipment (CPE) at the end user side is connected to the digital subscriber line access multiplexer (DSLAM), via a single telephony twisted pair cable. The twisted pair can be shielded or unshielded, and even very old paper-wrapped twisted pair can provide acceptable data rate performance. The telephony network and the twisted pair are originally designed for voice band transmission, i.e., up to $8kHz$. Therefore the major bottlenecks in the xDSL systems include the channel attenuation, especially in the high frequency, and the crosstalk, which is the electromagnetic coupling between the twisted pairs in the same cable bundle. The specification of the latest xDSL standard, i.e., Very-high-bit-rate digital subscriber line 2 (VDSL2) [12], will be studied in this paper as a reference.

Another massive existing cable infrastructure is the cable TV (CATV) network, which originally delivered television broadcast signal over the co-axial cables. The CATV network provides data services as well, defined in DOCSIS standard. In the early DOCSIS standards before DOCSIS 3.1, the modulation scheme was single carrier QAM modulation. Facing the strong demand on the faster data service, DOCSIS 3.1 standard switched to OFDM modulation, in order to realise the 10Gbit transmission over the extended frequency band in CATV systems.

These two systems share similarities with xBaseT, while they also have certain differences. The xDSL and the xBaseT both use twisted pair in the cable, however the Ethernet cable consists of four twisted pairs, and can be seen as a mini-bundle of four twisted pairs. The xDSL operates in longer cables and over lower frequency band, Table 3. The DOCSIS and the xBaseT have similar service reach and frequency band, but the DOCSIS cable is another type of co-axial cable, Table 3.

Table 3. VDSL2/DOCSIS/40G BaseT Specifications

	VDSL2 Downstream	DOCSIS 3.1 Downstream	40G BaseT
Cable Structure	single twisted pair	co-axial cable	four twisted pairs
Typical Reach	up to 500m	100m	50m
Maximum Reach	1000m	NA	100m
Data Rate	50 - 100Mbit/s	10Gbit/s	40Gbit/s
Frequency Range	from 8 KHz up to 30 MHz	up to 1218 MHz, total use up to 192 MHz	up to 1600 MHz
Transmit Power	14.5 dBm	65 dBm	3 dBm
Number of Sub-Carrier	3479	7600/3800	NA
Bandwidth of Sub-Carrier	4.3125 kHz	25/50kHz	NA

Another important difference between these systems is the transmission symmetry. The Ethernet transmission is symmetric peer-to-peer transmission, that both transmission directions have similar specification, and both ends of the transmission have similar hardware design. For the xDSL and the DOCSIS systems, the transmission is a central office to terminal modes, where the two transmission directions are distinguished as upstream and downstream services, with different frequency ranges, transmit powers and data rate requirements.

A detailed specification comparison of the three systems are given in Table 3. Note that the transmit power of the xBaseT is the total transmit budget for the four pairs, which will be equally shared by the four pairs.

The next section will present the implementation of OFDM in xBaseT and the simulation result.

3. THE OFDM BASED ETHERNET

This section presents the configuration of OFDM modulation for Cat7a cable with the parameters suggested by ISO/IEC/TR 11801-9901 document [13]. Then the paper will introduce a multi-user power allocation scheme to improve the performance. Finally the simulation result will be presented.

3.1. OFDM Configuration for Cat7a Cable

The Cat7a cable has been specified to support 40 Gbit/s data transmission, at the maximum frequency of 1600 MHz and with a reach of 50 meters. Each pair is foiled, so as to reduce the crosstalk, and the whole cable is foiled and covered with metal braiding, so as to prevent the electromagnetic leakage and external noise.

The parametric channel model, i.e., the insertion loss, the return loss and the crosstalk channel, and the basic transmission parameters are given in [13], e.g., the frequency range is up to $1600MHz$, and the transmit power is $3dBm$. The NEXT cancellation, FEXT cancellation and the return loss cancellation are defined as $28dB$, $14dB$ and $55dB$, respectively. The background noise level is assumed to be $-150dBm/Hz$. The alien crosstalk is either included or not included, as specified in [13].

Consider a simplest OFDM configuration, where the four twisted pairs are seen as four individual channels and they interfere with each other by crosstalk. The transmit power is equally share by the four twisted pairs, and each pair transmits a flat power spectrum density (PSD), i.e., the transmit power on each sub-carrier is identical. By equally distributing the $3dBm$ transmit power over the four twisted pairs and $1600MHz$, the resulting PSD is $-95dBm/Hz$ over the whole frequency band.

Compared with the DOCSIS 3.1 standard, the maximum frequencies are at the same scale, i.e., 1218 MHz and 1600 MHz, but the DOCSIS 3.1 limits the maximum frequency band to $192MHz$. The corresponding 7600/3800 points iFFT can be feasible for hardware implementation in the case of DOCSIS 3.1. In theory, the narrower the sub-carrier is, the more flat that the sub-carrier channel can be. However our choice of sub-carrier bandwidth must be larger than the $25/50kHz$ in DOCSIS 3.1, otherwise a large number of sub-carriers will require a large size iFFT/FFT, which will further cause hardware design difficulty. Here we propose a sub-carrier bandwidth of $200kHz$, and the $1600MHz$ is divided into 8000 sub-carriers. Then an 8192 point FFT processor suffices for our system, which is the same as DOCSIS 3.1, and currently available for mass production and commercial deployment. The sub-carrier bandwidth in xDSL systems is $4.3125kHz$, significantly smaller then our proposed $200kHz$ for Ethernet. Although transmitting over the similar twisted pairs, the channel flatness of the Cat7a cable is more acceptable than the telephone cable, due to the huge difference in cable length. Moreover, the xDSL system has to take into account of all the telephone cables, which are installed at different periods and with different qualities, and the Cat7a cable is designed with the state-of-the-art requirements. Hence our choice of $200kHz$ sub-carrier bandwidth is suitable for the OFDM implementation here.

Our key configuration for OFDM is the $-95dBm/Hz$ transmit power PSD and the $200kHz$ sub-carrier bandwidth.

3.2. Multi-user Power Allocation

The configuration mentioned above is a static configuration scheme, which can be easily implemented by the predefined parameters. In order to improve the performance of the OFDM under the given channel condition, the channel frequency selectivity and the crosstalk between the pairs should be exploited.

In OFDM modulation, the whole frequency range is divided into many sub-carriers. The output QAM symbols of the QAM constellation mapping in Fig. 2 are all normalised in amplitude, then the resulting transmit power on each sub-carrier is the same to each other. If these QAM symbols are differently amplified in amplitude before being fed into iFFT, then the transmit signal on each sub-carrier can have different transmit power. This gives us the freedom to allocate different transmit power to the sub-carriers, subject to the total transmit power constraint.

The OFDM transmission over the four twisted pairs Cat7a cable can be seen as a two-dimensional coupled transmit power allocation problem in information theory. There is a possibility of allocating different amount of transmit power on the same sub-carrier to different users, as depicted in Fig. 4.

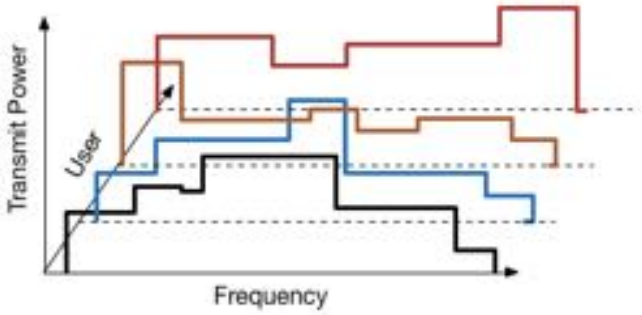

Fig. 4. OFDM Multi-user Power Allocation

Firstly, solely consider one twisted pair, the problem is a frequency selective multiple carrier channel with a transmit power constraint, with static interference of the crosstalk and the background noise [14]. The flat transmit power PSD, i.e., the identical transmit power on all the sub-carriers, does not necessarily reach the maximum spectrum efficiency. The solution is to adaptively allocate different transmit power to the sub-carriers. For instance, on the sub-carrier with low insertion loss and low return loss, it will be more beneficial to allocate more transmit power on such sub-carrier, rather than allocate the same transmit power on the sub-carrier with high insertion loss and high return loss. The water-filling algorithm has been proposed for such problem, and has been theoretically proven to be optimal in [14]. The resulting transmit power allocation of water-filling algorithm is illustrated in Fig. 5. The water-filling algorithm also has a very low complexity, and applied in 3G mobile communication High Speed Packet Access (HSPA) [15].

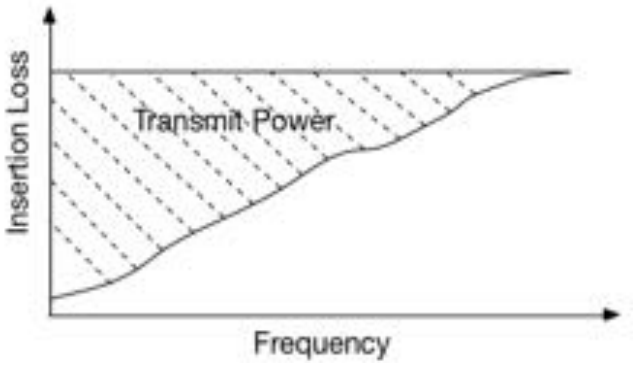

Fig. 5. Water-Filling Power Allocation

Secondly, consider the transmission on each sub-carrier from a multi-user communication point of view, the received signal contains the desired but attenuated signal from the same pair, and the crosstalk from the other three pairs, then this becomes a multi-user interference channel problem in [14]. So far, the interference channel is an open problem, no general or structured algorithm can deliver an optimal solution. Combined with the multi-carrier transmit power allocation over the frequency selective channel for one channel, the optimal transmit power allocation for the four twisted pairs becomes a two-dimensional multi-user multi-carrier transmit power allocation.

Although no existing theoretical solution available for such multi-carrier multi-user problem, similar problem has been addressed in the xDSL research. One simple and effective approach is the iterative water-filling (IWF) algorithm, described in [16]. By treating the crosstalk from other users as static interference, the IWF algorithm performs single user water-filling one after another, and each iteration the updated transmit power generates a new set of crosstalk for other users. When the transmit power allocation converges, a Nash Equilibrium is reached, which is a local optimal solution from a selfish mechanism.

The IWF algorithm has demonstrated considerable performance improvement in xDSL system. The only short coming of the IWF algorithm is the sensitivity to the near-far scenario, which is the case that the different cables in the same cable bundle have different starting and ending locations. Since the Cat7a cable can be seen as a small bundle of four twisted pair with the same length, then the IWF algorithm should be able to improve the data rate performance, as demonstrated later in the simulation result.

Moreover, the multi-user coupling, i.e., the crosstalk channel model, in [13] is simplified to a symmetric channel, which means that the crosstalk channel between any two pairs is identical. In practice, the four twisted pairs are twisted with different twisting rates, and the distance between

the pairs are different, as demonstrated in Fig. 6. Therefore the crosstalk channel is usually not symmetric between the pairs in practice, which is exactly the multi-user technique can significantly improve the performance.

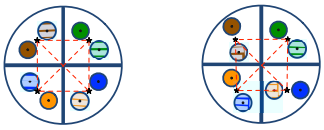

Fig. 6. The distance between the Twisted Pairs

3.3. Simulation Result

After discussing the configuration of OFDM for Cat7a cable and the possibility of further improving the performance by the IWF algorithm, the simulated result is presented in Table 4. The direct channel parameters, e.g., the insertion loss and the return loss, and the crosstalk channel parameters, e.g., the NEXT and the FEXT, are constructed according to the standard document [13]. And the theoretical capacity calculated in [13] is used as a reference metric for the OFDM performance. Both the cases of alien crosstalk ignored or not are simulated, as in the ISO/IEC/TR document [13] .

Two OFDM configurations are simulated, one is the flat transmit power PSD, that the transmit power is $-95dBm/Hz$ over all the sub-carriers, and the other one is the IWF algorithm, where the transmit power on each sub-carrier is optimised according to the direct channel and crosstalk channel conditions. Since the channel coding is not considered in [13], and the coding gain is not in the calculation of the theoretical capacity, hence we also simulate an OFDM system without channel coding. The achievable data rate of the two OFDM configurations and the percentage that they can achieve with respect to the theoretical capacity are listed in Tab.4.

Usually a cyclic prefix is adopted as safeguard in practical OFDM implementation [8,9], so as to eliminate the inter symbol interference. This will cause certainly performance loss in terms of data rate, as part of the transmit signal is repeated. Thus with the consideration of realistic implementation, the simulation result of 10% data rate loss by cyclic prefix is also presented in Tab.4.

From Table 4, we can see that the OFDM modulation can achieve most of the channel capacity, even with the 10% loss of the cyclic prefix. We have three observations:

1. All the simulated result can satisfy the target of 40Gbit/s, with a considerable margin.

2. In the presence of alien crosstalk, the OFDM reaches higher percentage of the theoretical capacity than the scenario without alien crosstalk, which shows the robustness of OFDM in the severe channel condition, including the channel selectivity and coloured interference like alien crosstalk.

3. The data rate performance is improved by IWF algorithm, compared with flat PSD, especially in the scenario with alien crosstalk. The impact of the crosstalk is reduced, and the spectrum efficiency is enhanced.

Table 4. Simulation Result

	Reference	Flat PSD	IWF
No Alien Xtalk			
Data Rate in Gbit/s	85	72.67	76.13
Percentage of Reference	100%	85.5%	89.6%
Cyclic Prefix			
Data Rate in Gbit/s	85	65.40	68.52
Percentage of Referencee	100%	76.9%	80.6%
Alien Xtalk			
Data Rate in Gbit/s	73	67.20	72.09
Percentage of Reference	100%	92.1%	98.8%
Cyclic Prefix			
Data Rate in Gbit/s	73	60.48	64.88
Percentage of Reference	100%	82.8%	88.9%

4. CONCLUSION AND FUTURE WORK

In this paper, we have discussed the possibility of OFDM scheme for the future copper cable based Ethernet. We have introduced the concept of OFDM modulation, and its copper cable applications of xDSL and DOCSIS. Then we studied the configuration of OFDM for Cat7a cable, and the IWF algorithm to improve the performance from the multi-user communication point of view. In the end we have presented simulation result, where OFDM shows great data rate performance and can be seen as a very potential candidate for the future Ethernet.

The work of this paper can be seen as a starting point for the OFDM implementation for the Ethernet. In the future, the simulation can be carried out on more realistic channel model. With the help of hardware based experiment, the performance of OFDM transmission can be investigated on the real cables. Also, more sophisticated static and multi-user OFDM power allocation scheme should be developed, so as to optimise the transmit power and improve the spectrum efficiency.

5. REFERENCES

[1] "IEEE Standard 802.3," *IEEE Standard For Ethernet*, 2012.

[2] "IEEE Standard 802.11," *IEEE Standard For Wireless Lan*, 2012.

[3] Thomas Starr, John M Cioffi, and Peter J Silverman, *Understanding digital subscriber line technology*, Prentice Hall PTR, 1999.

[4] Bin Lee, J.M. Cioffi, S. Jagannathan, and M. Mohseni, "Gigabit DSL," *Communications, IEEE Transactions on*, vol. 55, no. 9, pp. 1689–1692, Sept 2007.

[5] "Data-Over-Cable Service Interface Specifications DOC- SIS 3.1 MAC and Upper Layer Protocols Interface Specification CM-SP-MULPIv3.1-I03-140610," 2014.

[6] Stephen B Weinstein, "The history of orthogonal frequency-division multiplexing [history of communications]," *Communications Magazine, IEEE*, vol. 47, no. 11, pp. 26–35, 2009.

[7] Cheong Yui Wong, Roger S Cheng, K Ben Lataief, and Ross D Murch, "Multiuser OFDM with adaptive subcarrier, bit, and power allocation," *Selected Areas in Communications, IEEE Journal on*, vol. 17, no. 10, pp. 1747–1758, 1999.

[8] Lajos L Hanzo, Matthias Münster, Byungcho Choi, and Thomas Keller, *OFDM and MC-CDMA for broadband multi-user communications, WLANs and broadcasting*, John Wiley & Sons, 2005.

[9] Richard van Nee and Ramjee Prasad, *OFDM for wireless multimedia communications*, Artech House, Inc., 2000.

[10] Basic Transmission Scheme, "LTE: the evolution of mobile broadband," *IEEE Communications magazine*, vol. 45, 2009.

[11] "Data-Over-Cable Service Interface Specifications DOC- SIS 3.0 MAC and Upper Layer Protocols Interface Specification CM-SP-MULPIv3.1-I03-140610," 2012.

[12] G ITU-T, "993.2: Very high speed digital subscriber line transceivers 2 (VDSL2)," 2011.

[13] ISO/IEC/TR 11801-9901 Ed. 1.0, Information Technology, "Guidance for balanced cabling in support of at least 40 Gbit/s data transmission ," *ISO/IEC JTC 1/SC 25 BPUB 2014-10*, 2014.

[14] Thomas M Cover and Joy A Thomas, *Elements of information theory*, John Wiley & Sons, 2012.

[15] Erik Dahlman, Stefan Parkvall, Johan Skold, and Per Beming, *3G evolution: HSPA and LTE for mobile broadband*, Academic press, 2010.

[16] Wei Yu, Wonjong Rhee, Stephen Boyd, and John M Cioffi, "Iterative water-filling for gaussian vector multiple-access channels," *Information Theory, IEEE Transactions on*, vol. 50, no. 1, pp. 145–152, 2004.

UNBALANCED TRANSMISSION CHANNEL MODEL SIMULATION FOR CAT7A ETHERNET CABLE

Beier Li, Alistair Duffy

Electrical Engineering, De Montfort University, UK,
email: p1319654x@myemail.dmu.ac.uk, apd@dmu.ac.uk

ABSTRACT

Aiming at high speed data transmission beyond the standard of 10G Base-T, 40G Base-T and 100G Base-T have been proposed and researched. With improved physical characteristics, the structure of the copper based Ethernet cable remains unchanged, which is composed of four twisted pairs. Each pair transmits a balanced signal, so as to reduce the crosstalk leakage into other pairs. The scenario of unbalanced transmission is investigated in this study, where each wire is individually excited, with the metal shield as the common ground. In this case, the number of transmission channels is doubled to eight channels, with a trade-off of higher crosstalk. However, with advanced transmission techniques, the unbalanced transmission mode has a great potential for better data rate performance. The simulated unbalanced transmission channel model is presented and analysed in the study.

1. INTRODUCTION

Ethernet, defined as the standard of IEEE 802.3 [1], is the most seen network in the field of computer networks, including home networks, enterprise networks and data centres. The original signal carrier of Ethernet was coaxial cable, and later more options are introduced, including twisted pair cable, single mode and multi mode optical fibre, and backplane. Each of these physical media has specific application scenario with own advantage, while the twisted pair based cable has been most widely used.

The structured twisted pair cable consists of four twisted pairs, which can be seen as four parallel communication channels. Each twisted pair is a balanced transmission system, where the two wires are excited in differential mode. The two wires are twisted with the same twisting rate, therefore they have same actual wire length and and same impedance to the ground at any point along the cable. Such balanced lines receive identical common mode interference from the same interference source. With the differential mode excitation, the two wires are fed with the same signal with opposite signs, and their difference between the two received signals. In this way, the same interference component in both received signal will be cancelled. Meanwhile, the signal leakage from the two wires are of the same amplitude, but opposite signs as well, thus the resulting interference outside the twisted pair is minimised. Behind the cable jackets, the signal is in the form of pulse-amplitude modulation (PAM), from the early standard of 1BASE5 for 1 Mbit/s to the 10G-BaseT for 10 Gbit/s now, with increasing modulation order and bandwidth.

The upcoming challenge of the Ethernet over twisted pair (EoTP) is to transmit 40 Gigabit per second over the structured cable, especially for the data centre applications. The step from 10 Gbit/s to 40 Gbit/s is bigger than any other steps in the evolution of the EoTP history.

However, the previous approach, higher quality cable can provide better channel characteristics, wider frequency band can provide more bandwidth and higher order modulation can increase the frequency spectrum efficiency, have very limited room to further enhance the data rate performance. Although the new cable standard will adopt new measures to improve the physical, or namely the electro magnetic properties of the cable, originally designed for telephony service, the channel characteristics of the twisted pair is only ideal for lower frequencies. Operating at radio frequency, e.g., over 1 GHz, the insertion loss degrades significantly compared with the lower frequency, and the crosstalk increases rapidly along the frequency. As a result, the channel characteristics show a strong frequency selectivity.

Other wireline and wireless communication systems have adopted variety of communication/signal processing techniques, in order to cope the severe channel conditions. In communication theory, the EoTP system can be viewed as a communication system with four parallel channel, which interfere each other through the electro magnetic coupling as the major performance degradation, i.e., crosstalk. With the state of the art signal processing technology and well developed chipset, the channel frequency selectivity is practically handled by multi-carrier modulation, e.g., orthogonal frequency division multiplexing (OFDM) [2], and the impact of crosstalk is minimised through different crosstalk cancellation techniques. In other words, the approach is to transmit over "nice and clean" channel, efficiently. EoTP has already made a step in 10G-BaseT, by introducing Tomlinson-Harashima precoding in order to reduce the far-end crosstalk (FEXT), while the single carrier PAM modulation is inher-

ited.

In this paper, we propose an alternative channel model, where the restriction of the balanced transmission is removed, each twisted pair is split into two wires and all connected to the metal shield as the common ground. And each wire is excited with individual signal and excitation source. In this way, there will be eight paths of conductors for eight communication channels, instead of four. The available resource for the EoTP system is expanded in the dimension of channel numbers. As we can foresee, the trade-off here is the increased crosstalk for the increased number of channels. With the help of the crosstalk cancellation techniques, there will be eight "not so bad" channels instead of four "nice and clean" channels.

In Section 2 we will briefly study the circuitry of of the Ethernet cable under our proposed channel model. In Section 3 we will introduce the specifics of the channel model simulation and present the simulation results, with the ISO standard specified Cat7a cable as a reference. In Section 4 we will conclude the research and discuss the future work.

2. THE CIRCUIT OF ETHERNET CABLE

In this section, the concept of balanced and unbalanced transmission model of EoTP are discussed, and then the RLGC circuit model of EoTP cable unbalanced transmission is described.

2.1. The Balanced and Unbalanced Transmission

The balanced transmission model of EoTP cable is depicted in Fig. 1. Each of the four channels contains two wires, which are twisted together with the same twisting rate. The input signals fed into the two wires of the same pair carry the same amplitude but opposite signs. In this differential mode excitation, the difference between the received signal of the two wires in each pair is taken as the output, therefore there are four communication channels of the four pairs. Each communication channel, i.e., each pair, is a balanced transmission.

In the balanced transmission, each pair is an interference source to other pairs, and they are not balanced pairwise. Since each pair is excited in differential mode, the crosstalk to the same end of the transmission, i.e., the near-end crosstalk (NEXT), and the FEXT from pair 1 to wire 2 to 4 is demonstrated, while the same applies to other pairs.

Alternatively, the unbalanced transmission model of EoTP cable is shown in Fig. 3. There are eight channels with individual excitation sources, which are independent from each other. This single-ended mode excitation generate eight individual outputs, therefore in this unbalanced transmission there are eight communication channels. The NEXT and FEXT from wire 1 to other wires are demonstrated, and the same applies to other wires.

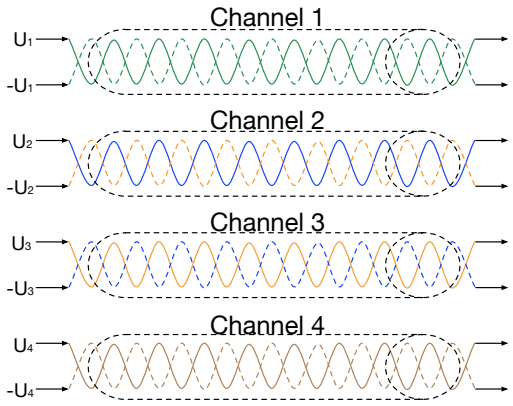

Fig. 1. Balanced Transmission of EoTP Cable

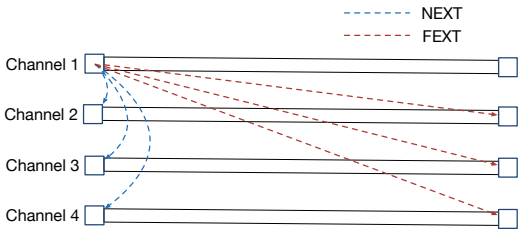

Fig. 2. The Crosstalk of Balanced Transmission

When given the same transmit power to balanced and unbalanced transmission models, the proposed unbalanced transmission does not feed the two wires of the same pair with symmetric signal, obviously the output signal contains only half of the energy of that of the balanced transmission. This means that the single communication channel of the unbalanced transmission model is more sensitive to interference. Moreover, without the self-cancellation of the symmetric signal leakage, the crosstalk between the channels in the unbalanced model will be stronger.

2.2. RLGC Circuit Model

Here we continue the discussion from the macro wire/pair level down to the micro circuit level. In the transmission line theory, the EoTP cable can be studied as a multiple transmission line (MTL) circuit [3]. The EoTP cable can be divided into many small cable segment, which are detailed described by a Resistance-Inductance-Conductance-Capacitance (RLGC) circuit model. And the S-parameters of each segment can be computed accurately.

The RLGC model of the unbalanced transmission is illustrated in Fig. 4. The conductor in the bottom, indexed with 0, is the metal shield of the cable, which is used as the common ground for wire 1 to wire 8. Although provided as a powerful tool, the EoTP cable is not a suitable application for MTL theory. Most of the variables for RLGC model can be obtained

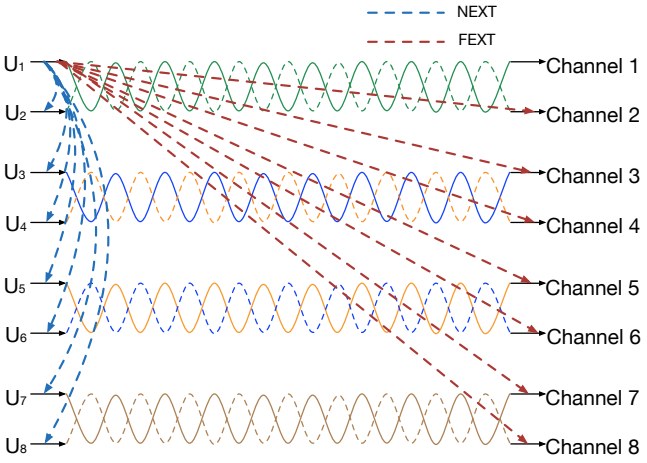

Fig. 3. Unbalanced Transmission of EoTP Cable

from the physical properties of the material used in the cable modelling. However, the twisting nature of the EoTP wires leads to a continuous changing geometry, plus the different twisting rate of the four pairs, which needs a theoretically infinite segmentation for the RLGC model. And this prohibits a feasible theoretical analysis.

However with the help of the computer aided design CAD software, we can still model a realistic cable and obtain its S-parameters from simulation, as introduced in the next section.

3. THE CHANNEL MODEL SIMULATION RESULT

This section presents the specification of the Cat7a cable modelled in the software, and its S-parameter simulation result.

3.1. The Cable Specification

In order to investigate the S-parameter performance of the unbalanced transmission model, a Cat7a screened S/FTP cable is modelled in CAD software, whose specific parameters are provided from our industry partner.

The conductor, i.e., the wires, is of 22 AWG, with a diameter of 0.64 ± 0.008mm, and the material is pure copper. The conductor is covered by a layer of foam as insulation, the thickness of which is 0.4 mm. And the total diameter of the insulated wire is 1.45 ± 0.1mm.

Then eight wires are twisted into four twisted pairs, with different twisting rate, as listed in Fig. 5. Each pair is wrapped with aluminium foil, to provide an individual screen against the electro magnetic leakage between the pairs. The foil has a thickness of $65\mu m$

As the outer layer of the cable, firstly there is a metal braiding covering the four pairs, for the purpose of external interference rejection. The braiding is waived by tinned copper wire with a diameter of 0.12 mm, and covers 40% of the

	Pair color	[cm] per turn	Turns per [m]
	Green	1.53	65.2
	Blue	1.54	64.8
	Orange	1.78	56.2
	Brown	1.94	51.7

Fig. 5. The Twisting Rate of the Pairs

cylinder outside the four pairs. In the end, there is a layer of non-conductive Low Smoke Zero Halogen (LSOH) jacket, as the protection of the cable.

This cable is designed to work up to 1200 MHz, however the maximum frequency for the next EoTP standard is still pending. In this paper we choose 1600 MHz as the maximum frequency, and simulate the cable up to 1700 MHz.

The total cable length is limited to 1 meter, due to the restriction of the CAD software. In practice, 1 meter cable suffices the scenario of top of rack (TOR) or other short reach connections in the data centre.

3.2. The Simulation Platform

The simulation platform consists of a Windows workstation and the CAD software on it. The desktop workstation is powered with a quad-core Intel i5-2400 CPU at 3.1GHz, and 12 Gbit RAM. The CAD software is the Computer Simulation Technology (CST) Microwave Studio.

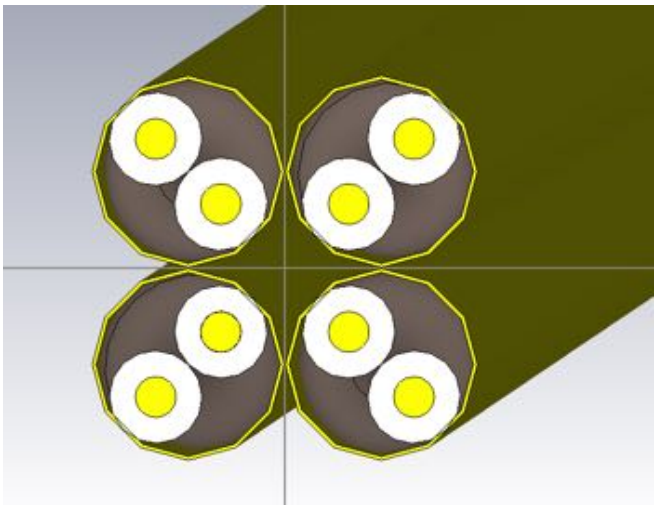

Fig. 6. The Cable Modelling in CST

In the CST software, firstly the cable is modelled through a 3D modelling procedure, with the corresponding physical properties for the material mentioned previously, as demonstrated in Fig. 6. Then this realistic 3D model is meshed into

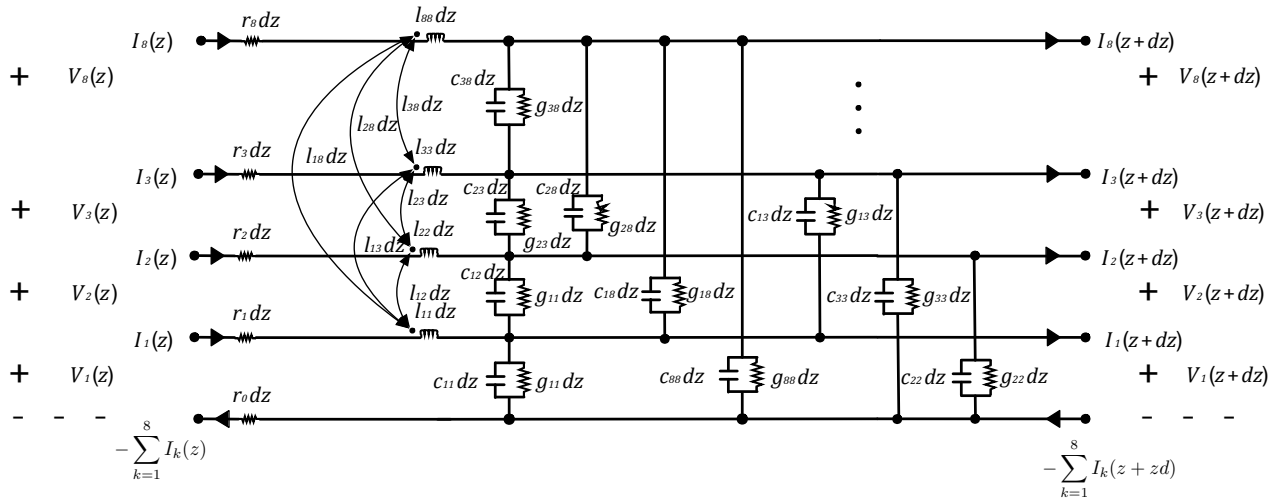

Fig. 4. RLGC Model of Unbalanced Transmission

small mesh cells Fig. 7. In our simulation, the 1 meter cable is meshed into approximately 2.58 million mesh cells.

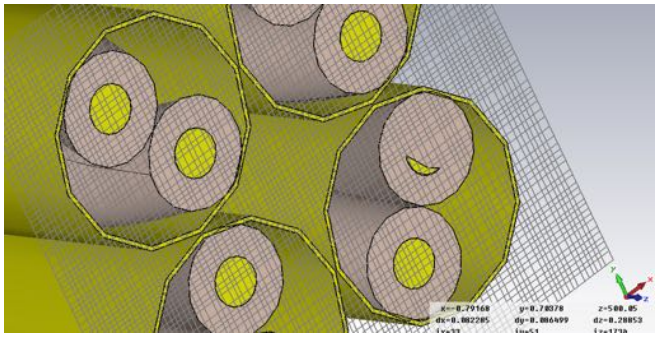

Fig. 7. The Meshing of the Cable Model

Each end of the channel is defined by a port, with 50Ω impedance. When each of the ports is excited with a signal, the electro magnetic wave travels through each mesh cell, which is then processed in physics, and generates an output signal at other ports. In the end the S-parameters is calculated by the inputs and outputs.

3.3. The Simulation Result: Insertion Loss

The simulation is conducted for both unbalanced and balanced transmission mode. For the unbalanced transmission mode, first we examine the insertion loss of the eight wires, which is channel characteristic of the direct channel. The simulation result is shown in Fig. 8. The insertion loss of the eight wires shows general similarity, only differs from each other slightly.

All the eight wires have a rapid growing insertion loss as the frequency increases, as a typical frequency selectivity for twisted pairs. Moreover, all the eight wires also have a fluctuation in their curves with a similar period. The explanation for the similar period is the wave reflection over the very similar wire length, not identical due to the different twisting rates.

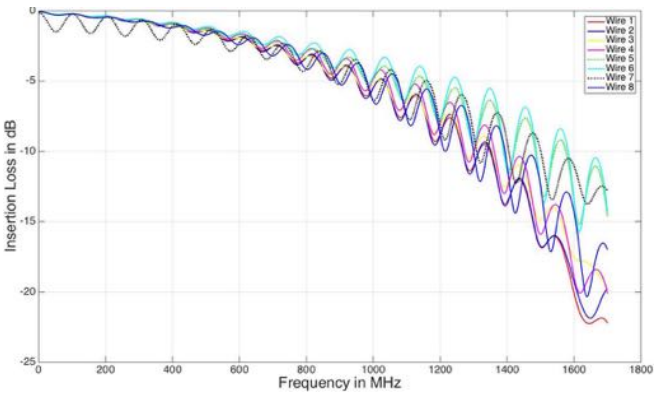

Fig. 8. The Insertion Loss of Unbalanced Transmission

As a duplex communication system, the EoTP requires symmetric transmission between the two ends of the cable over the same frequency band. The insertion loss of a selection of the wires in two transmission directions is shown in Fig. 9, where the direction of the previous insertion loss result is considered as downstream (DS) and the other direction is considered as upstream (US). We can see that, for the same wire, the insertion loss is symmetric over the two directions.

As a comparison, the cable is simulated in balanced transmission as well, where the two wires of each pair are short circuited to form a balanced pair. The insertion loss of the four pairs in two directions are demonstrated in Fig. 10. The insertion loss shows a very similar performance to each other, and symmetric in two directions. The fluctuation is also seen

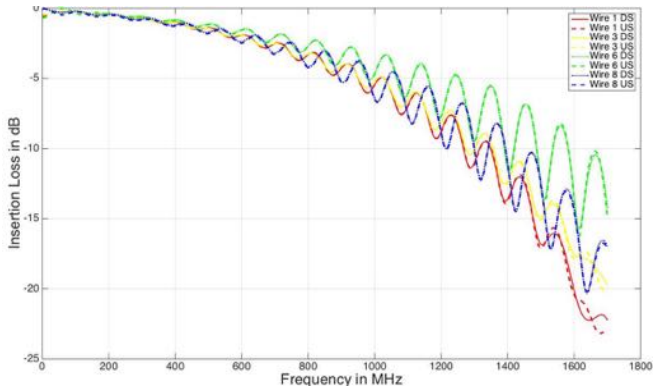

Fig. 9. The Insertion Loss Symmetry of Duplex Mode

here. However the frequency selectivity is very minor for this balanced transmission, at the highest frequency the insertion loss is lower only no more than 5 dB in low frequency, due to low energy loss of the short cable length and the concentrated power of the two wires. Therefore the insertion loss of the balanced transmission is also better than that of unbalanced transmission.

Moreover, the insertion loss of a 30 meter Cat7 cable specified in ISO/IEC/TR 11801-9901 document [4] is also plotted in Fig. 10 as a reference, labelled as Case0. The insertion loss of the 30 meter cable is much worse than that of the 1 meter cable. Also, there is a 10 to 15 dB insertion loss gap between the 30 meter cable and the unbalanced transmission cable. Since the 30 meter cable has shown a theoretical capacity of over 70 Gbit/s in [4], with the doubled number in channel numbers, we can see a spectacular potential of the unbalanced transmission cable.

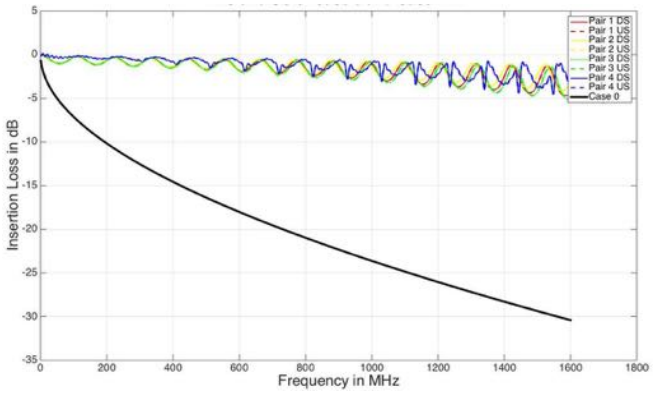

Fig. 10. The Insertion Loss of Balanced Transmission

3.4. The Simulation Result: The Return Loss

Similar simulation procedure is conducted for the investigation of the return loss, which is a major performance degradation for the EoTP transmission. The return loss of the unbalanced transmission mode in one direction is shown in Fig. 11, basically all the eight wires have similar return loss performance.

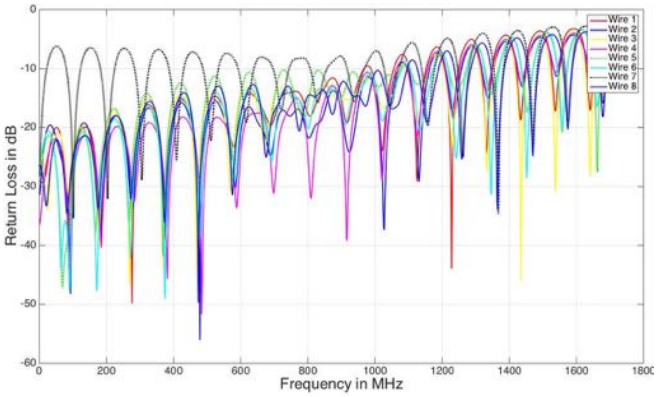

Fig. 11. The Return Loss of Unbalanced Transmission

For the duplex mode symmetry study, the return loss of the two directions of the unbalanced transmission is demonstrated in Fig. 12. There are different ripple amplitude in the fluctuations, however the upper bounds of the return loss generally conform with each other in two directions.

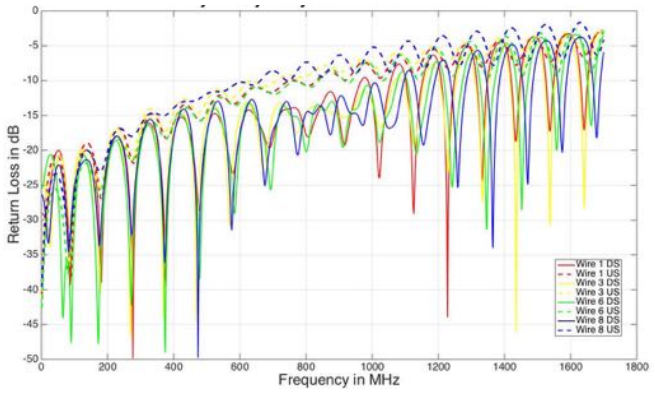

Fig. 12. The Return Loss Symmetry of Duplex Mode

The return loss of the balanced transmission mode and the ISO standard cable is demonstrated in Fig.13. From Fig.13, we can see a similar performance of the 1 meter cable and the 30 meter cable, which means that the return loss is basically not dependent to the cable length. Compared with the unbalanced transmission mode, the return loss of the unbalanced transmission is lower than that of the balanced transmission, especially much lower in the low frequency part. Therefore we can conclude that the unbalanced transmission mode will not suffer more performance degradation from return loss than the balanced transmission.

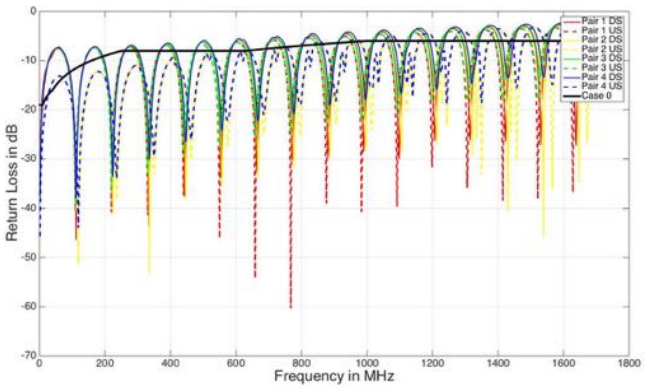

Fig. 13. The Return Loss of Balanced Transmission

4. CONCLUSION AND FUTURE WORK

In this paper, we have introduced the concept of unbalanced transmission mode of EoTP cable, where the eight wires are connected to the metal shield as a common ground and excited individually by single-ended excitation. We have compared the balanced and unbalanced transmission models and discussed the RLGC Circuit Model of unbalanced transmission mode. In the end we have presented S-parameter simulation result of the unbalanced transmission, where the unbalanced transmission channel model shows a considerable insertion loss performance and better return loss performance with respect to the balanced transmission model in the same cable.

The future work of this research will focus on the crosstalk channel investigation of the unbalanced transmission and the further study the achievable capacity of the unbalanced transmission with PAM or other multi-carrier modulation schemes.

5. SPECIAL THANK

Here we would like to thank our industry partner, Mr. Paul Cave from Mayflex, who kindly helped us with the cable specification and helpful discussions.

6. REFERENCES

[1] "IEEE Standard 802.3," *IEEE Standard For Ethernet*, 2012.

[2] Lajos L Hanzo, Matthias Münster, Byungcho Choi, and Thomas Keller, *OFDM and MC-CDMA for broadband multi-user communications, WLANs and broadcasting*, John Wiley & Sons, 2005.

[3] Clayton R Paul, *Analysis of multiconductor transmission lines*, John Wiley & Sons, 2008.

[4] ISO/IEC/TR 11801-9901 Ed. 1.0, Information Technology, "Guidance for balanced cabling in support of at least 40 Gbit/s data transmission ," *ISO/IEC JTC 1/SC 25 BPUB 2014-10*, 2014.

UNBALANCED TRANSMISSION CHANNEL MODEL SIMULATION FOR CAT7A ETHERNET CABLE

Beier Li, Alistair Duffy

Electrical Engineering, De Montfort University, UK,
email: p1319654x@myemail.dmu.ac.uk, apd@dmu.ac.uk

ABSTRACT

For the ongoing evolution of Ethernet over twisted pair standard, from 10G BASE-T to 40G BASE-T and future 100G BASE-T or beyond, expanding the transmission spectrum and increasing PAM modulation order are considered as the straight-forward approaches. However, the twisted pair is originally invented for low frequency voice band analog signal transmission, and the straight-forward approaches are limited by the physical nature of the conductor. Therefore the inherited transmission configurations become the bottleneck for higher performance, due to the lack of adaptability to the non-ideal frequency-selective channel with crosstalk between the pairs. Before introducing the new transmission technologies to enhance the performance under such channel condition, like OFDM and MIMO, the channel model of the structured Ethernet twisted pair cable should be revisited, and to be exploited for the new technology. In this paper we present both balanced and unbalanced transmission channel model for the Ethernet cable, which can realise four pair-wise transmission channels or eight wire-wise transmission channels. Considering the trend of using short cables for high speed links in the datacenter scenario, an one meter long CAT7A cable is simulated for balanced and unbalanced transmission, with detailed direct channel and crosstalk channel parameters for the MIMO channel model.

1. INTRODUCTION

Ethernet, defined as the standard of IEEE 802.3 [1], is the most seen network in the field of computer networks, including home networks, enterprise networks and data centres. The original signal carrier of Ethernet was coaxial cable, and later more options are introduced, including twisted pair cable, single mode and multi mode optical fibre, and backplane. Each of these physical media has specific application scenario with own advantage, while the twisted pair based cable has been most widely used.

The structured twisted pair cable consists of four twisted pairs, which can be seen as four parallel communication channels. Each twisted pair is a balanced transmission system, where the two wires are excited in differential mode. The two wires are twisted with the same twisting rate, therefore they have same actual wire length and and same impedance to the ground at any point along the cable. Such balanced lines receive identical common mode interference from the same interference source. With the differential mode excitation, the two wires are fed with the same signal with opposite signs, and their difference between the two received signals. In this way, the same interference component in both received signal will be cancelled. Meanwhile, the signal leakage from the two wires are of the same amplitude, but opposite signs as well, thus the resulting interference outside the twisted pair is minimised. Behind the cable jackets, the signal is in the form of pulse-amplitude modulation (PAM), from the early standard of 1BASE5 for 1 Mbit/s to the 10G-BaseT for 10 Gbit/s now, with increasing modulation order and bandwidth.

The upcoming challenge of the Ethernet over twisted pair (EoTP) is to transmit 40 Gigabit per second over the structured cable, especially for the data centre applications. The step from 10 Gbit/s to 40 Gbit/s is bigger than any other steps in the evolution of the EoTP history.

However, the previous approach, higher quality cable can provide better channel characteristics, wider frequency band can provide more bandwidth and higher order modulation can increase the frequency spectrum efficiency, have very limited room to further enhance the data rate performance. Although the new cable standard will adopt new measures to improve the physical, or namely the electro magnetic properties of the cable, originally designed for telephony service, the channel characteristics of the twisted pair is only ideal for lower frequencies. Operating at radio frequency, e.g., over 1 GHz, the insertion loss degrades significantly compared with the lower frequency, and the crosstalk increases rapidly along the frequency. As a result, the channel characteristics show a strong frequency selectivity.

Other wireline and wireless communication systems have adopted variety of communication/signal processing techniques, in order to cope the severe channel conditions. In communication theory, the EoTP system can be viewed as a communication system with four parallel channel, which interfere each other through the electro magnetic coupling as the major performance degradation, i.e., crosstalk. Aiming at higher data rate, the frequency diversity is exploited by adopting multi-carrier modulation technique, where the or-

thogonal frequency division multiplexing (OFDM) has shown considerable performance improvement over EoTP cable [2]. The multi-user diversity is also exploited inn 10G-BaseT, by introducing Tomlinson-Harashima precoding in order to reduce the far-end crosstalk (FEXT), while the single carrier PAM modulation is inherited. In this paper, we propose an alternative channel model, where the restriction of the balanced transmission is removed, each twisted pair is split into two wires and all connected to the metal shield as the common ground. And each wire is excited with individual signal and excitation source. In this way, there will be eight paths of conductors for eight communication channels, instead of four. The available resource for the EoTP system is expanded in the dimension of channel numbers. As we can foresee, the trade-off here is the increased crosstalk for the increased number of channels. With the help of the crosstalk cancellation techniques, there will be eight "not so bad" channels instead of four "nice and clean" channels.

In Section 2 we will briefly study the circuitry of of the Ethernet cable under our proposed channel model. In Section 3 we will introduce the specifics of the channel model simulation and present the simulation results, with the ISO standard specified Cat7a cable as a reference. In Section 4 we will conclude the research and discuss the future work.

2. THE CIRCUIT OF ETHERNET CABLE

In this section, the balanced and unbalanced transmission models of EoTP are discussed, and then the RLGC circuit model of EoTP cable unbalanced transmission is described.

2.1. The Balanced and Unbalanced Transmission

The balanced transmission model of EoTP cable is depicted in Fig. 1. Each of the four channels contains two wires, which are twisted together with the same twisting rate. The input signals fed into the two wires of the same pair carry the same amplitude but opposite signs. In this differential mode excitation, the difference between the received signal of the two wires in each pair is taken as the output, therefore there are four communication channels of the four pairs. Each communication channel, i.e., each pair, is a balanced transmission.

In the balanced transmission, each pair is an interference source to other pairs, and they are not balanced pairwise. Since each pair is excited in differential mode, the crosstalk to the same end of the transmission, i.e., the near-end crosstalk (NEXT), and the FEXT from pair 1 to wire 2 to 4 is demonstrated, while the same applies to other pairs.

Alternatively, the unbalanced transmission model of EoTP cable is shown in Fig. 3. There are eight channels with individual excitation sources, which are independent from each other. This single-ended mode excitation generate eight individual outputs, therefore in this unbalanced transmission there are eight communication channels. The NEXT and FEXT from wire 1 to other wires are demonstrated, and the same applies to other wires.

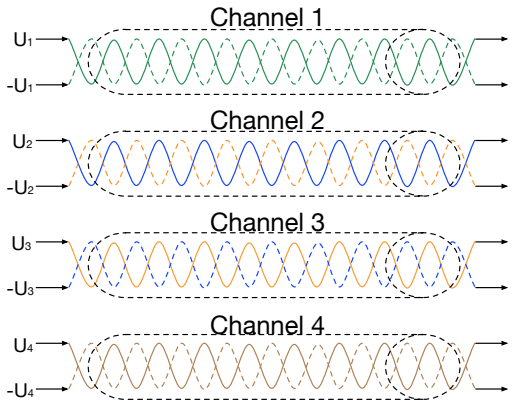

Fig. 1. Balanced Transmission of EoTP Cable

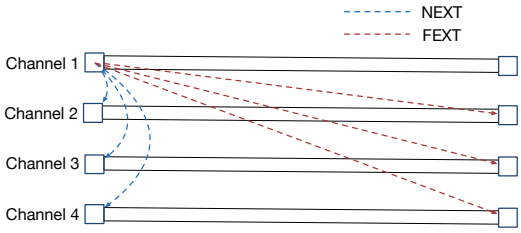

Fig. 2. The Crosstalk of Balanced Transmission

When given the same transmit power to balanced and unbalanced transmission models, the proposed unbalanced transmission does not feed the two wires of the same pair with symmetric signal, obviously the output signal contains only half of the energy of that of the balanced transmission. This means that the single communication channel of the unbalanced transmission model is more sensitive to interference. Moreover, without the self-cancellation of the symmetric signal leakage, the crosstalk between the channels in the unbalanced model will be stronger.

2.2. RLGC Circuit Model

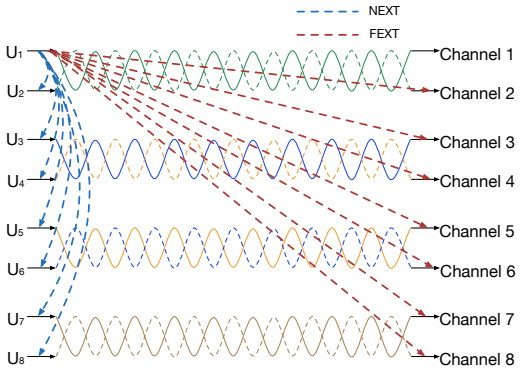

Fig. 3. Unbalanced Transmission of EoTP Cable

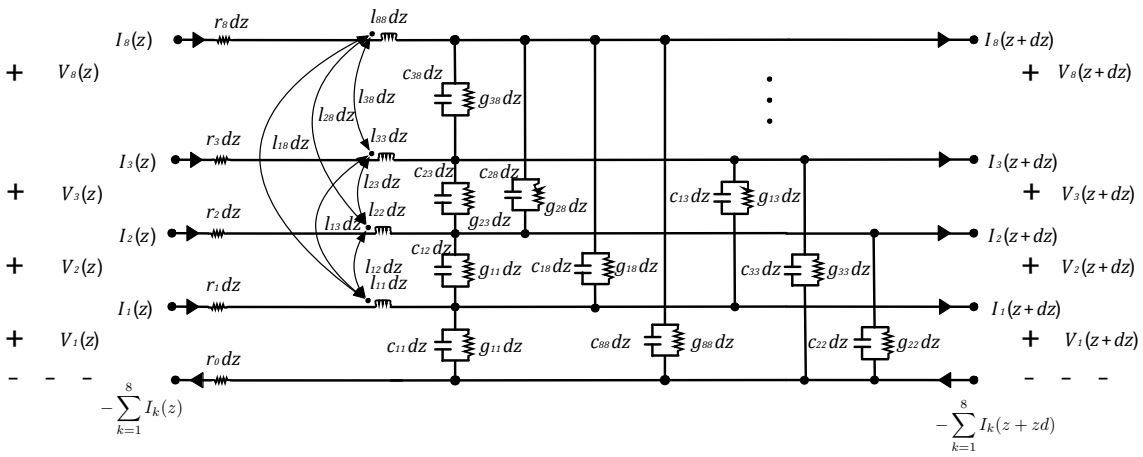

Fig. 4. RLGC Model of Unbalanced Transmission

Here we continue the discussion from the macro wire/pair level down to the micro circuit level. In the transmission line theory, the EoTP cable can be studied as a multiple transmission line (MTL) circuit [3]. The EoTP cable can be divided into many small cable segment, which are detailed described by a Resistance-Inductance-Conductance-Capacitance (RLGC) circuit model. And the S-parameters of each segment can be computed accurately. Similar approach has been applied to single twisted pair cable [4].

The RLGC model of the unbalanced transmission is illustrated in Fig. 4. The conductor in the bottom, indexed with 0, is the metal shield of the cable, which is used as the common ground for wire 1 to wire 8. Although provided as a powerful tool, the EoTP cable is not a suitable application for MTL theory. Most of the variables for RLGC model can be obtained from the physical properties of the material used in the cable modelling. However, the twisting nature of the EoTP wires leads to a continuous changing geometry, plus the different twisting rate of the four pairs, which needs a theoretically infinite segmentation for the RLGC model. And this prohibits a feasible theoretical analysis. However with the help of the computer aided design CAD software, we can still model a realistic cable and obtain its S-parameters from simulation, as introduced in the next section.

3. THE CHANNEL MODEL SIMULATION RESULT

This section presents the simulation detail of the Cat7a cable, and its S-parameter simulation result.

3.1. The Cable Specification

In order to investigate the S-parameter performance of the unbalanced transmission model, a Cat7a screened S/FTP cable is modelled in CAD software, whose specific parameters are provided from our industry partner.

The conductor, i.e., the wires, is of 22 AWG, with a diameter of 0.64 ± 0.008mm, and the material is pure copper. The conductor is covered by a layer of foam as insulation, the thickness of which is 0.4 mm. And the total diameter of the insulated wire is 1.45 ± 0.1mm.

Then eight wires are twisted into four twisted pairs, with different twisting rate, as listed in Fig. 5. Each pair is wrapped with aluminium foil, to provide an individual screen against the electro magnetic leakage between the pairs. The foil has a thickness of $65\mu m$. As the outer layer of the cable, firstly

	Pair color	[cm] per turn	Turns per [m]
	Green	1.53	65.2
	Blue	1.54	64.8
	Orange	1.78	56.2
	Brown	1.94	51.7

Fig. 5. The Twisting Rate of the Pairs

there is a metal braiding covering the four pairs, for the purpose of external interference rejection. The braiding is waived by tinned copper wire with a diameter of 0.12 mm, and covers 40% of the cylinder outside the four pairs. In the end, there is a layer of non-conductive Low Smoke Zero Halogen (LSOH) jacket, as the protection of the cable.

This cable is designed to work up to 1200 MHz, however the maximum frequency for the next EoTP standard is still pending. In this paper we choose 1600 MHz as the maximum frequency, and simulate the cable up to 1700 MHz.

The total cable length is limited to 1 meter, due to the restriction of the CAD software. In practice, 1 meter cable suffices the scenario of top of rack (TOR) or other short reach connections in the data centre [5].

3.2. The Simulation Platform

The simulation is performed on a Windows workstation, which is powered with a quad-core Intel i5-2400 CPU at 3.1GHz, and 12 Gbit RAM. The full wavelength simulation software is the Computer Simulation Technology (CST) Microwave Studio.

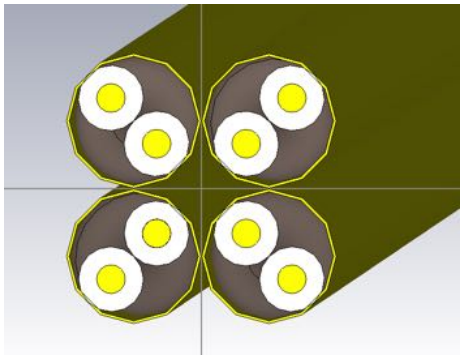

Fig. 6. The Cable Modelling in CST

In the CST software, firstly the cable is modelled through a 3D modelling procedure, with the corresponding physical properties for the material mentioned previously, as demonstrated in Fig. 6. Then this realistic 3D model is meshed into small mesh cells Fig. 7. In our simulation, the 1 meter cable is meshed into approximately 2.58 million mesh cells.

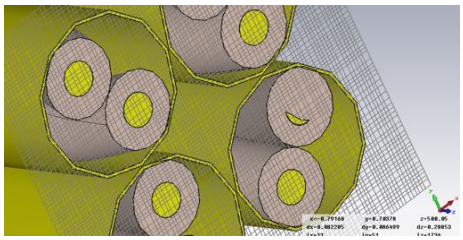

Fig. 7. The Meshing of the Cable Model

Each end of the channel is defined by a port, with 50Ω impedance. When each of the ports is excited with a signal, the electro magnetic wave travels through each mesh cell, which is then processed in physics, and generates an output signal at other ports. In the end the S-parameters is calculated by the inputs and outputs.

3.3. The Simulation Result: Insertion Loss

The simulation is conducted for both unbalanced and balanced transmission mode. For the unbalanced transmission mode, first we examine the insertion loss of the eight wires, which is channel characteristic of the direct channel. The simulation result is shown in Fig. 8. The insertion loss of the eight wires shows general similarity, only differs from each other slightly. All the eight wires have a rapid growing insertion loss as the frequency increases, as a typical frequency selectivity for twisted pairs. Moreover, all the eight wires also have a fluctuation in their curves with a similar period. The explanation for the similar period is the wave reflection over the very similar wire length, not identical due to the different twisting rates. As a duplex communication system, the EoTP

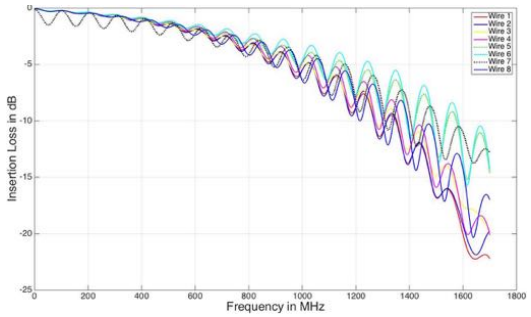

Fig. 8. The Insertion Loss of Unbalanced Transmission

requires symmetric transmission between the two ends of the cable over the same frequency band. The insertion loss of a selection of the wires in two transmission directions is shown in Fig. 9, where the direction of the previous insertion loss result is considered as downstream (DS) and the other direction is considered as upstream (US). We can see that, for the same wire, the insertion loss is symmetric over the two directions.

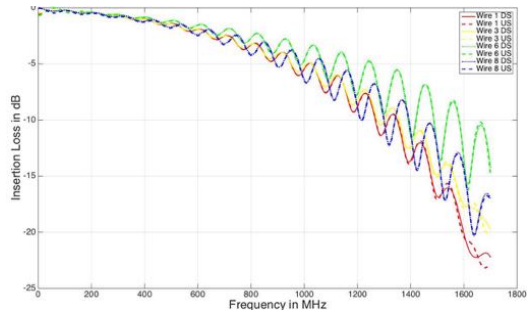

Fig. 9. The Insertion Loss Symmetry of Duplex Mode

As a comparison, the cable is simulated in balanced transmission as well, where the two wires of each pair are short circuited to form a balanced pair. The insertion loss of the four pairs in two directions are demonstrated in Fig. 10. The insertion loss shows a very similar performance to each other, and symmetric in two directions. The fluctuation is also seen here. However the frequency selectivity is very minor for this balanced transmission, at the highest frequency the insertion loss is lower only no more than 5 dB in low frequency, due to low energy loss of the short cable length and the concentrated power of the two wires. Therefore the insertion loss of the balanced transmission is also better than that of unbalanced transmission.

Moreover, the insertion loss of a 30 meter Cat7 cable specified in ISO/IEC/TR 11801-9901 document [6] is also plotted in Fig. 10 as a reference, labelled as Case0. The

insertion loss of the 30 meter cable is much worse than that of the 1 meter cable. Also, there is a 10 to 15 dB insertion loss gap between the 30 meter cable and the unbalanced transmission cable. Since the 30 meter cable has shown a theoretical capacity of over 70 Gbit/s in [6], with the doubled number in channel numbers, we can see a spectacular potential of the unbalanced transmission cable.

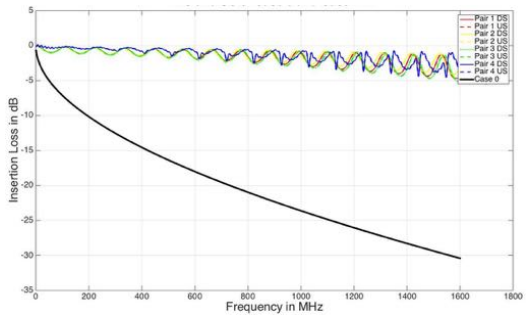

Fig. 10. The Insertion Loss of Balanced Transmission

3.4. The Simulation Result: The Return Loss

Similar simulation procedure is conducted for the return loss, which is a major performance degradation for the EoTP transmission. The return loss of the unbalanced transmission mode in one direction is shown in Fig. 11, basically all the eight wires have similar return loss performance.

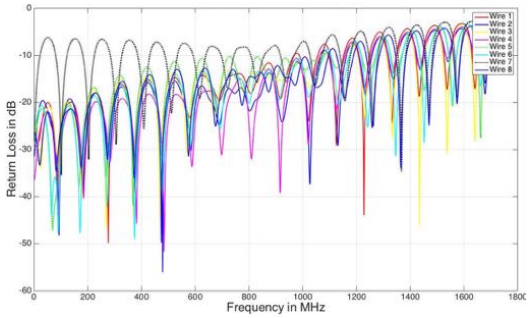

Fig. 11. The Return Loss of Unbalanced Transmission

For the duplex mode symmetry study, the return loss of the two directions of the unbalanced transmission is demonstrated in Fig. 12. There are different ripple amplitude in the fluctuations, however the upper bounds of the return loss generally conform with each other in two directions.

The return loss of the balanced transmission mode and the ISO standard cable is demonstrated in Fig.13. From Fig.13, we can see a similar performance of the 1 meter cable and the 30 meter cable, which means that the return loss is basically not dependent to the cable length. Compared with the unbalanced transmission mode, the return loss of the unbalanced transmission is lower than that of the balanced transmission, especially much lower in the low frequency part.

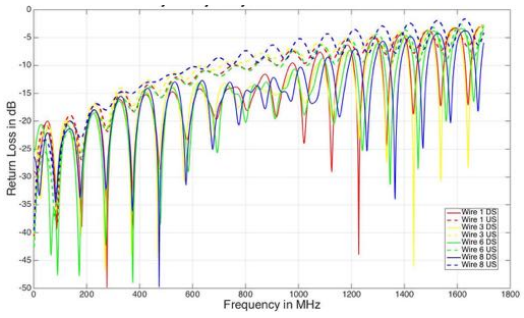

Fig. 12. The Return Loss Symmetry of Duplex Mode

Therefore we can conclude that the unbalanced transmission mode will not suffer more performance degradation from return loss than the balanced transmission.

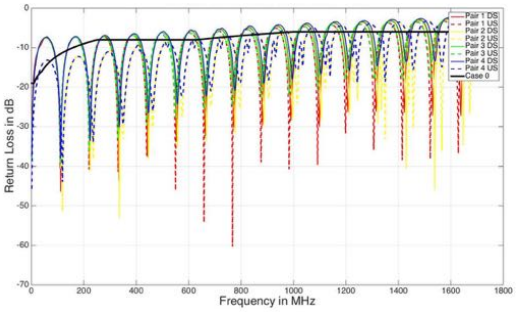

Fig. 13. The Return Loss of Balanced Transmission

3.5. Crosstalk Performance

In Fig.14, the FEXT channel of unbalanced transmission, i.e., the simulation result of wire 1 and wire 2 is shown. The two curves on the top are the intra-pair FEXT of pair 1, between wire 1 and wire 2, and clearly these intra-pair FEXT is higher than other inter-pair FEXT received by wire 1.

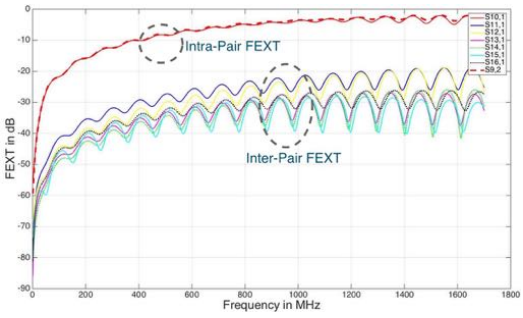

Fig. 14. The FEXT of the Unbalanced Transmission

In Fig.15, we present a comprehensive comparison between the intra-pair, inter-pair FEXT and the FEXT in balanced transmission. Here we can see that the 30 meter cable has the best FEXT performance, and short cable has higher

FEXT due to the short distance between the two ends. This implies that a shorter cable does not necessarily provide the best channel, and this will have an impact on the short cable performance in TOR scenario. Another very interesting observation is that for the same cable, the FEXT of the balanced transmission is between the the intra-pair FEXT and the inter-pair FEXT of the unbalanced transmission.

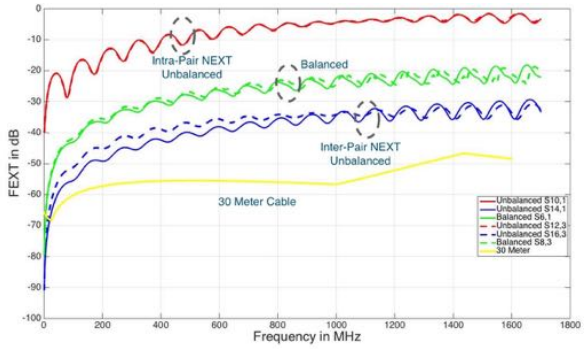

Fig. 15. The FEXT Performance Comparison

Like FEXT, similar simulation results of NEXT performance are formulated and demonstrated in Fig.16 and Fig.17. And we have the same observations: stronger intra-pair NEXT than inter-pair NEXT, 30 meter cable with the best NEXT performance, and the NEXT of the balanced transmission is between the the intra-pair and the inter-pair NEXT of the unbalanced transmission for the one meter cable.

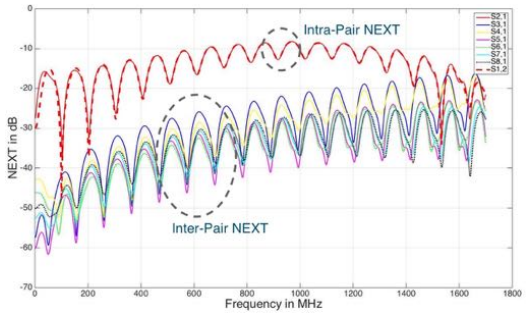

Fig. 16. The NEXT of the Unbalanced Transmission

For the one meter cable, the balanced transmission shows slightly better channel condition than the unbalanced transmission, channel-wise. With proper MIMO realisation, especially in FEXT cancellation, the unbalanced transmission has a huge potential from the doubled number of the channels. Compared with the 30 meter cable, the one meter cable shows both better direct channel performance and higher crosstalk performance. This interesting observation should be further studied, so as to improve the data rate for the general short reach cabling systems.

4. CONCLUSION AND FUTURE WORK

In this paper, we have introduced the concept of unbalanced transmission mode of EoTP cable, where the eight wires are

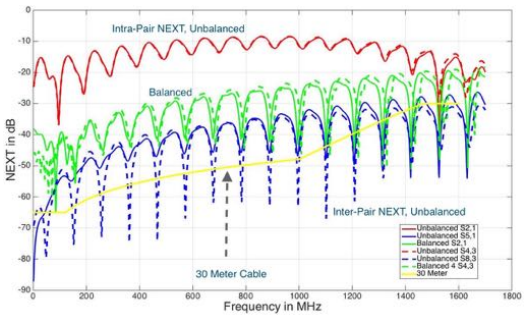

Fig. 17. The NEXT Performance Comparison

connected to the metal shield as a common ground and excited individually by single-ended excitation. We have compared the balanced and unbalanced transmission models and discussed the RLGC Circuit Model of unbalanced transmission mode. In the end we have presented S-parameter simulation result of the unbalanced transmission, where the unbalanced transmission channel model shows a considerable insertion loss performance and better return loss performance with respect to the balanced transmission model. The data rate performance will be investigated in the future research.

5. REFERENCES

[1] "IEEE Standard 802.3," *IEEE Standard For Ethernet*, 2012.

[2] Beier Li and Alistair Duffy, "OFDM Based Ethernet Transmission over Copper Cables," in *the Proceeding of International Wire & Cable Symposium (IWCS) 2015*, 2015.

[3] Clayton R Paul, *Analysis of multiconductor transmission lines*, John Wiley & Sons, 2008.

[4] M. Yamamura, Y. Kami, K. Murano, and F. Xiao, "Analysis of transmission characteristics for twisted pair cables using the rlgc parameters of the cable," in *2015 Asia-Pacific Symposium on Electromagnetic Compatibility (APEMC)*, May 2015, pp. 720–723.

[5] Nikolaos Bamiedakis, Jian Chen, Petter Westbergh, Johan S Gustavsson, Anders Larsson, Richard V Penty, and Ian H White, "40 Gb/s Data Transmission Over a 1-m-Long Multimode Polymer Spiral Waveguide for Board-Level Optical Interconnects," *Journal of Lightwave Technology*, vol. 33, no. 4, pp. 882–888, 2015.

[6] ISO/IEC/TR 11801-9901 Ed. 1.0, Information Technology, "Guidance for balanced cabling in support of at least 40 Gbit/s data transmission ," *ISO/IEC JTC 1/SC 25 BPUB 2014-10*, 2014.